PRELIMINARY INVESTIGATION OF THE NATURE OF HYDROCARBON MIGRATION AND ENTRAPMENT IN FAULTED STRUCTURES

A Dissertation

by

JIANYONG BAI

Submitted to the Office of Graduate Studies of
Texas A&M University
in partial fulfillment of the requirements for the degree of

DOCTOR OF PHILOSOPHY

May 2003

Major Subject: Geophysics

PRELIMINARY INVESTIGATION OF THE NATURE OF HYDROCARBON MIGRATION AND ENTRAPMENT IN FAULTED STRUCTURES

A Dissertation

by

JIANYONG BAI

Submitted to Texas A&M University
in partial fulfillment of the requirements
for the degree of

DOCTOR OF PHILOSOPHY

Approved as to style and content by:

Joel S. Watkins (Chair of Committee)	Brann Johnson (Member)
Richard Gibson (Member)	Luc T. Ikelle (Member)
Thomas A. Blasingame (Member)	Andrew Hajash (Head of Department)

May 2003

Major Subject: Geophysics

ABSTRACT

Preliminary Investigation of the Nature of Hydrocarbon Migration and Entrapment

in Faulted Structures. (May 2003)

Jianyong Bai, B.E., Xi'an Jiaotong University;

M.S., Tsinghua University

Chair of Advisory Committee: Dr. Joel S. Watkins

Numerical simulations indicate that hydrocarbon migration and entrapment in stacked fault-bounded reservoirs are mainly affected by the following factors: charge time, faults, pressure and geological structures. The charge time for commercial hydrocarbon accumulation is much longer in oil-water systems than in oil-gas-water systems.

Faults are classified into charging faults and "back doors" – faults other than charging faults in stacked fault-bounded reservoirs. The lower the displacement pressure of a fault, the higher its updip oil transportation ability. The downdip oil transportation ability of a fault is usually low and cannot cause commercial downdip oil accumulation.

Back doors affect both hydrocarbon percent charge and hydrocarbon migration pathways. Updip back doors improve updip oil charge. The lower the displacement pressure of an updip back door, the more efficient the updip oil charge before 3,000 years. Back doors whose displacement pressure is equal to or higher than 28.76 psi are effective in sealing faults in oil-water systems. On the contrary, only sealing faults result in commercial gas accumulations in stacked fault-compartmentalized reservoirs. Otherwise gas is found over oil. Downdip back doors generally have few effects on downdip hydrocarbon charge.

Geopressure enhances the updip oil transportation of a fault and improves the positive effects of updip back doors during updip oil charge. Geopressure and updip back doors result in more efficient updip oil charge. A physical barrier is not necessarily a barrier to oil migration with the aid of geopressure and updip back doors.

The chance for hydrocarbon charge into reservoirs along growth faults is not equal. Any one of the above controlling factors can change the patterns of hydrocarbon charge and distribution in such complex geological structures. Generally, lower reservoirs and updip reservoirs are favored. Reservoirs along low-

permeability charging faults may be bypassed. Gas can only charge the updip reservoirs. Both updip and downdip back doors can facilitate oil penetrating a barrier fault to charge reservoirs offset by the barrier fault.

Interreservoir migration among stacked fault-compartmentalized reservoirs is an important mechanism for hydrocarbon accumulation and trap identification. The interreservoir migration is a very slow process, even though the displacement pressures of bounding faults may be very low.

DEDICATION

To my family

ACKNOWLEDGEMENTS

I would like to especially thank Dr. Joel S. Watkins, the chair of my advisory committee, for his patience, guidance, mentorship and interest in the research. His insights and encouragement made the research a truly rewarding and exciting experience. I also would like to extend sincere thanks to my committee members, Dr. Brann Johnson, Dr. Thomas A. Blasingame, Dr. Richard Gibson and Dr. Luc T. Ikelle, for their constructive criticism and helpful advice. Thanks also go to Dr. Charles J. Glover, who served as the Graduate Council Representative.

The research is a part of the Integrated Reservoir Investigations Group (IRIG) at Texas A&M University and was financially supported by the IRIG. I would like to thank every member in the IRIG for sharing valuable information and cooperation. Among them, Dr. Carrie L. Decker was a valuable resource for questions on field development and geological structures.

Dr. Bryan Maggard and Dr. Daulat D. Mamora in the Department of Petroleum Engineering provided invaluable advice during the research.

I acknowledge Dr. Fuping Zhu and her family, Dr. Wenwu He, Yuqian Li and all the other Chinese graduate students for their help and advice in various forms.

I also would like to thank my parents and parents-in-law, my sisters and my brother for their support and understanding. Finally, I want to thank my lovely wife for her support during my graduate study.

TABLE OF CONTENTS

CHAPTER Page

LIST OF FIGURES

FIGURE Page

FIGURE Page

FIGURE Page

FIGURE Page

FIGURE Page

LIST OF TABLES

CHAPTER I

INTRODUCTION

PURPOSE

Although geoscientists recognized that oil and gas migrate upward under the force of buoyancy into anticlinal traps over 60 years ago, much of the process whereby oil and gas migrate and become traps remains poorly understood. This is especially true in the case of multiple, stacked fault-compartmentalized reservoirs. This is also true where multiple near-vertical faults further divide the stack into additional compartments. It is found that some of these compartments are saturated with oil, some with gas, some with water, and some with a mix of oil and gas.

For this study numerical simulations were applied in order to investigate how faults affect hydrocarbon migration and entrapment in faulted structures. With so little known about the process of migration in complexly faulted reservoirs, it was necessary to first investigate simple migration models. This was essential in order to determine what could reasonably be considered to learn possible in terms of the details regarding the migration of oil and gas through stacked fault-bounded reservoirs. In this investigation the following problems were specifically investigated:

a. How do charging faults and "back door" faults – faults other than charging faults in stacked fault-bounded reservoirs – affect oil percent charge, oil distribution and oil migration pathways during active charge? Bounding faults in stacked fault-bounded reservoirs provide routes through which fluid (oil, gas and/or water) enters into and escapes from reservoirs. Understanding the roles of charging faults and back door faults is fundamental to a comprehension of their effects on oil distribution and oil migration pathways in complex stacked fault-bounded reservoirs such as stacked reservoirs along growth faults. Back door faults may facilitate water escape from reservoirs in order to improve oil charge efficiency. Otherwise, water escaping from charging faults might causes a slow charge, or even no charge. This function is crucial to the understanding of hydrocarbon migration and entrapment in normal faults.

This dissertation follows the style and format of the AAPG Bulletin.

b. How does interreservoir migration happen once an oil supply stops in an oil-water system? Interreservoir migration is hydrocarbon migration from lower reservoirs to upper reservoirs through bounding faults in faulted structures. This migration, driven only by buoyancy, is an important mechanism for establishing oil accumulation and trap identification, since it is mainly affected by the properties of bounding faults in faulted structures. For this study interreservoir migration was investigated only in an oil-water system.

c. What is the role of back doors in hydrocarbon migration and distribution when hydrocarbons charge through growth faults in an oil-gas-water system? The role of back doors in the migration and distribution of hydrocarbons in oil-gas-water systems is different from their role in oil-water systems. Moreover, the influence of back doors on gas migration and entrapment is different from their influence on oil migration and entrapment, even in the same three-phase systems. Therefore, a better understanding of the role of back doors on hydrocarbon migration and distribution in an oil-gas-water system is essential to identifying possible migration pathways along faults in stacked fault-bounded reservoirs, as well as to identifying different traps related to growth faults.

SCOPE OF INVESTIGATION

This investigation mainly focuses on how the properties of faults affect hydrocarbon migration and entrapment, as well as those same faults affect hydrocarbon migration pathways in stacked fault-bounded reservoirs. Consequently, the properties of reservoirs were fixed in order to exclude their influences on hydrocarbon migration and entrapment and the width of faults are fixed in order to exclude their influences on fluid flow rate. Excluding the influences of fault width and the properties of the reservoir would mean that hydrocarbon migration and entrapment were affected only by the properties of faults.

Reservoir simulations were applied and numerical models were built in order to investigate the roles of faults on hydrocarbon migration and entrapment in various faulted structures in this investigation. In these numerical models stacked reservoirs were bounded by faults. By changing the properties of bounding faults, the role of faults under hydrostatic pressure and geopressure during active charges play, as well as that of interreservoir migration once an oil supply stops under hydrostatic pressure, was investigated.

This investigation was first conducted in oil-water systems. The simplest models are ones with a single stacked reservoir bounded by two faults. Using this kind of models, the oil transportation ability of a charging fault was first assessed by an oil charge efficiency through which the oil charges the single stacked reservoir through a charging fault, and fluid (oil and/or water) is allowed to escape from the reservoir only through the same charging fault. Once an understanding of the role of charging faults was accomplished, the role of back door faults was investigated by fixing the properties of a charging fault by using this same kind of models. Because an updip back door could improve oil charge efficiency, an attempt to demonstrate that an updip back door might make two reservoirs separated by a central barrier in communication was then made. In more complicated models with two stacked reservoirs bounded by two faults: one a charging fault and the other a back door fault, how the back door fault affect oil migration pathways was investigated. How faults affect oil migration pathways was also being investigated in numerical models with four stacked reservoirs bounded by three faults: the central fault being a charging fault and other faults an updip and a downdip back door fault, respectively. In complicated growth-fault models, oil charge in stacked fault-bounded reservoirs along growth faults was investigated under hydrostatic pressure and geopressure. Finally, interreservoir migration was investigated under hydrostatic pressure in models with two stacked reservoirs bounded by two faults.

In oil-gas-water systems, constant fluid flow rates were specified and GOR (gas/oil ratio) was constantly kept at 3,000 during numerical simulations. The fundamental influence of a back door fault was first investigated in models with a single stacked reservoir bounded by two faults: one a charging fault and the other a back door fault. Then, how back doors affect a hydrocarbon charge was investigated when both a downdip and an updip back door fault existed in numerical models where hydrocarbons charge stacked reservoirs through a central charging fault. Finally, hydrocarbon migration along growth faults was simulated in order to investigate how back door faults might affect hydrocarbon migration and entrapment in stacked reservoirs along a growth fault during an active charge.

SIGNIFICANCE OF THIS STUDY

Faults may act as routes or seals to hydrocarbon migration. Since faults may demonstrate different types of seal behavior, faults can control (1) the presence or absence of hydrocarbons; (2) the percent charge; (3)

the lateral and vertical distribution of hydrocarbons; (4) the migration pathways; and (5) the distribution and remigration of hydrocarbons during field development. As a result, the understanding of the role of faults on hydrocarbon migration and entrapment is crucial to the explanation and prediction of commercial traps, especially for stacked fault-compartmentalized reservoirs.

However, it is complex and non-intuitive to explain and predict fault seals due to the following reasons. First, fault zones are usually chaotic. Second, the data about the properties of faults are sparse. Third, the role of faults in hydrocarbon migration and entrapment is practically complex, and a fault cannot simply be classified as a leaking or a sealing fault. A fault may leak gas but seal oil, or it might leak on one side but seal on the other. A fault could leak at one point but seal another. A fault could even juxtapose independent individual sands with different seal capacities. In addition, the seal behavior of a fault is time-dependent. Forth, the seal behavior of a fault is time-dependent. Finally, hydrocarbon migration and entrapment along a fault are dynamic, either under hydrostatic pressure or under geopressure.

In this investigation faults are simply classified into charging faults and back door faults – non-charging faults – in faulted structures. The role of back door faults is primarily concerned, either under hydrostatic pressure or under geopressure. In general, back door faults have two contrasting effects on hydrocarbon migration and entrapment. On the one hand, back door faults may improve hydrocarbon charge efficiency by providing routes for water to escape from stacked fault-bounded reservoirs in order to make room for a hydrocarbon charge, since formation water is essentially impressible. On the other hand, back door faults may reduce the hydrocarbon charge efficiency for hydrocarbon escape from stacked fault-bounded reservoirs through them. As a result, better understanding of the role of back door faults is necessary and crucial in order to explain and predict hydrocarbon migration and entrapment in faulted structures.

This investigation was conducted in a quantitative and integrated fashion in order to address the roles of back door faults on hydrocarbon migration and entrapment in faulted structures. Sensitive study provides insight into the local-scale role of back door faults in faulted structures.

CHAPTER II

BACKGROUND

This chapter briefly reviews previous work regarding hydrocarbon migration and entrapment. First, the concepts of hydrocarbon migration and the role of capillary pressure on hydrocarbon migration are introduced. Second, how faults affect hydrocarbon migration and entrapment is reviewed. Third, the influence of geopressure on hydrocarbon migration and entrapment is considered, especially in the northern Gulf of Mexico. Finally, the identification and mapping of hydrocarbon migration pathways in oil fields is discussed.

HYDROCARBON MIGRATION AND ENTRAPMENT

Rock pores constitute a network through which hydrocarbons can migrate. The expulsion of hydrocarbons from source rocks is known as primary migration. This is the movement of hydrocarbons to an escape point where oil and gas collect as droplets and stringers of continuous-phase liquid hydrocarbon and secondary migration can occur (Schowalter, 1979). Secondary migration is the movement of hydrocarbons as a single continuous-phase fluid through water-wetted rocks, faults, or fractures and the concentration of that fluid into traps (Schowalter, 1979). Only secondary migration can carry hydrocarbons toward the traps where hydrocarbons can then be commercially extracted.

Hydrocarbon migration and entrapment is determined by both driving and resistance forces. Main driving forces include buoyancy, geopressure and hydrodynamics. Main resistance forces include capillary pressure and hydrodynamics. Hydrodynamics can either assist or inhibit hydrocarbon migration, depending on the hydrodynamic forces acting with or against the driving forces (Berg, 1975; and Schowalter, 1979). The seal capacity of a rock is determined by its displacement pressure (Smith, 1966 and 1980; Berg, 1975; and Watts, 1987). Hydrocarbon migration requires that the pressure of continuous-phase hydrocarbons exceed the displacement pressure of a rock acting as a barrier to hydrocarbon migration under hydrostatic conditions. Hydrocarbons displace formation water from the pore throats of the rock and initiate the migration as a continuous phase. Hydrocarbons continuously migrate through a rock as long as the driving force of any continuous-phase hydrocarbons is greater than the resistance force. As hydrocarbons migrate,

snap-off will occur wherever water can flow into a pore throat and the barrier is resealed in order to cease hydrocarbon migration (Schowalter, 1979).

The understanding of hydrocarbon migration and entrapment has come a long way. Gussow (1954) presented the first migration model and explained the anomalous occurrences of oil and gas in a single, dipping, and continuous reservoir. Hydrocarbons migrate continuously updip, due to the buoyancy. They are then trapped in local anticlines within the reservoir. Gas can be found downdip from oil (Figure 1). In contrast to the spill differential entrapment model, the leak differential entrapment principle shown in Figure 2, proposed by Petroleum Research Corp. in 1960, could explain why gas fills higher traps while oil fills lower traps because of a series of displacement-pressure barriers (Schowalter, 1979).

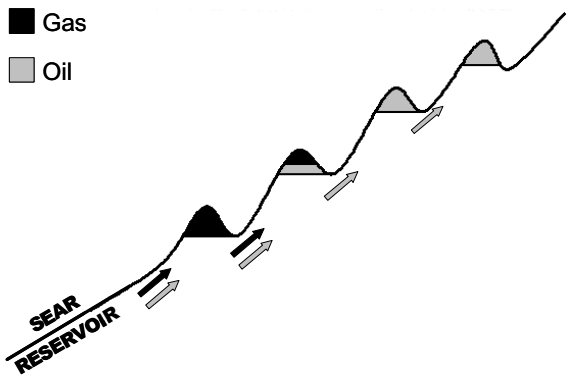

Figure 1. Structural differential entrapment of oil and gas (after Schowalter, 1979).

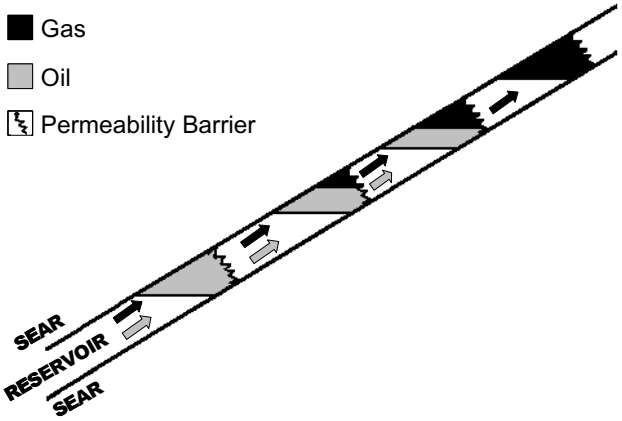

Figure 2. Stratigraphic differential entrapment of oil and gas (after Schowalter, 1979).

Berg (1975) pointed out the role of capillary pressure in stratigraphic traps. He modified the Hobson equation in order to calculate the capillary pressure between oil and water in rock pores, and concluded that porous and permeable, very fine-grained sandstone and siltstone were effective barriers against oil migration.

Schowalter (1979) systematically reviewed the variations of the interfacial tension of oil and gas and discussed the importance of the capillary pressures of a seal in migration and entrapment. He defined primary migration as a conversion of kerogen to liquid hydrocarbons and an expulsion from source rocks, and defined secondary migration as a migration occurring after the expulsion of hydrocarbons from a source rock.

Watts (1987) pointed out the difference between membrane and hydraulic seals, and discussed their importance to fault-related seals. He also discussed variations in interfacial tension regarding the depth and temperature of oil and gas, partial seals and their effects on the migration of oil and gas, the effects of hydraulic seals, and the differential leakage of oil and gas across membrane seals. Membrane seals are caused by capillary leakage while hydraulic seals are caused by capillary entry pressure great enough to cause seal by fractures and/or the wedging open of faults. He concluded that since displacement pressure was a function of the membrane seal and the coefficient of the interfacial tension of the hydrocarbon phase beneath that seal, a two-phase hydrocarbon column thicker than oil or gas alone was probably trapped. The gas in contact with the base of a seal determined the displacement pressure of that seal. The buoyancy effect of an oil column was less than that of a pure gas column, and therefore a greater total hydrocarbon column can be concluded to be trapped. Since with depth, the interfacial tension of gas increased at a different rate from that of oil, more gas can probably be concluded to be trapped than oil.

Berg (1996) and Skerlec (1999) pointed out that a seal fault generally permits the migration of water (possibly at a very low rate) but usually blocks the migration of hydrocarbons. I call such seals “back doors” in this investigation. They are key to understanding migration and entrapment in normal faults.

Kulander et al. (1998) has observed that the Ship Shoal 274 reservoirs in the Gulf of Mexico comprise over 40 compartments. About half the compartments leaked during production while another half sealed among them. The Ship Shoal 274 reservoirs have exhibited a complex history of migration and entrapment. An early stage of oil and gas charge was followed and disturbed by late stage gas migration, mainly

through growth faults. The Ship Shoal 274 antithetic faults tended to operate as the principal migration pathways.

Berg and Gangi (1999) have shown that pressures generated during the maturation process can exceed the fracture gradient of source rocks, thereby creating cracks to allow for the escape of liquid hydrocarbons. An electron microscopic investigation of the variation of shales as it is associated with depth (Kim et al., 1998) has indicated that a similar process occurs when water is expelled from geopressured shales and muds during compaction.

FAULTS AND HYDROCARBON MIGRATION AND ENTRAPMENT

A fault may either act as a conduit or a seal during hydrocarbon migration. There are two basic types of fault seal behavior: (1) cross sealing or leaking, which refers to a lateral communication across a fault between juxtaposed sands; and (2) dip sealing or leaking, which refers to a vertical communication along a fault between sacked sands (Skerlec, 1999). A cross-leaking fault can be identified using the following criteria: (1) common hydrocarbon contacts, Figure 3(a); (2) common free water level, Figure 3(b); (3) juxtaposed lithology leak points, Figure 3(c); or (4) common pressures in juxtaposed sands. A cross-sealing fault can be identified using the following criteria: (1) hydrocarbon-bearing sands juxtaposed with water-wet sands, Figure 3(d); (2) different hydrocarbon contacts, Figure 3(e); or (3) different pressures in juxtaposed sands. Because shale is usually impermeable, faults with sands juxtaposed with shale will be cross-sealing. A typical dip leak fault is a fault with a dip-leaking point in which the hydrocarbon-water contact coincides with an intersection between the fault plane and the top of the sand, Figure 4(a). Otherwise the fault is dip-sealing, Figure 4(b).

The critical factor to form a fault trap is the capillary pressure difference between juxtaposed sands or fault-zone materials (Smith, 1966 and 1980; Watts, 1987; Allan, 1989; Berg and Avery, 1995; Matthai and Roberts, 1996; and Alexander and Handschy, 1998). The following procedures could result in the capillary pressure difference:

(1) Grain crushing, which significantly reduces the permeability within a fault zone by producing a fine-grained gouge during fault movement (Watts, 1987; Antonellini and Aydin, 1994; and Alexander and Handschy, 1998);

(2) Clay smear in which clay becomes incorporated into the fault planes (Watts, 1987; Bouvier et al., 1989; Jev et al., 1993; Antonellini and Aydin, 1994; and Alexander and Handschy, 1998);

(3) Cementation along an original permeability fault plane, which significantly increases the displacement pressure of the fault (Watts, 1987; and Alexander and Handschy, 1998).

The seal capacity of a fault is expressed in terms of the vertical hydrocarbon column entrapped by the fault. Smith (1966 and 1980) provided equations to calculate the maximum height of a hydrocarbon column by the differential of displacement pressures between juxtaposed sands or fault zone materials. Watts (1987) discussed in detail the varying effectiveness of faults as barriers to hydrocarbon migration on the basis of the capillary properties of sands juxtaposed along those faults. Allan (1989) proposed the analytical technique of fault-plane-section analysis in order to identify fault traps such as sand-on-sand and sand-on-shale traps. A fault-plane section is a vertical across section that shows the structure and stratigraphy against the fault. Bouvier et al. (1989), and Jev et al. (1993) used fault-slicing techniques on 3D seismic surveys, and focused on the clay-smear potential (CSP) as a sealing mechanism for the Niger Delta fault traps. The CSP is the relative amount of clay smeared from individual shale source beds at a certain point along a fault surface. The CSP is a viable, fault-seal prediction tool that can be used to distinguish clay smears in fault material zones that might form barriers to fluid flow. Yielding (1997) predicted this fault-seal potential by using shale-gouge ratio (SGR), which is defined as the percentage of shale or clay in a slipped interval.

Berg and Avery (1995) indicated that growth faults seal in sealing sheared zones and leak along nonsealing fault surfaces. The sheared zones result from the ductile deformation of soft sediments during mass movement, and are effective seals because their ductile deformation homogenizes the original sediments and results in a uniform distribution of small pores. In contrast, a fault surface is a region with high permeability and low displacement pressure.

In this investigation the sealing capacity of a fault (also called the leaking or spill point of a fault), which includes both the cross seal and dip seal capacity, is determined simply by the difference between the displacement capillary pressure of the fault and the reservoir.

$$h = 0.433 \frac{P_{df} - P_{ds}}{\rho_w - \rho_h} \tag{1}$$

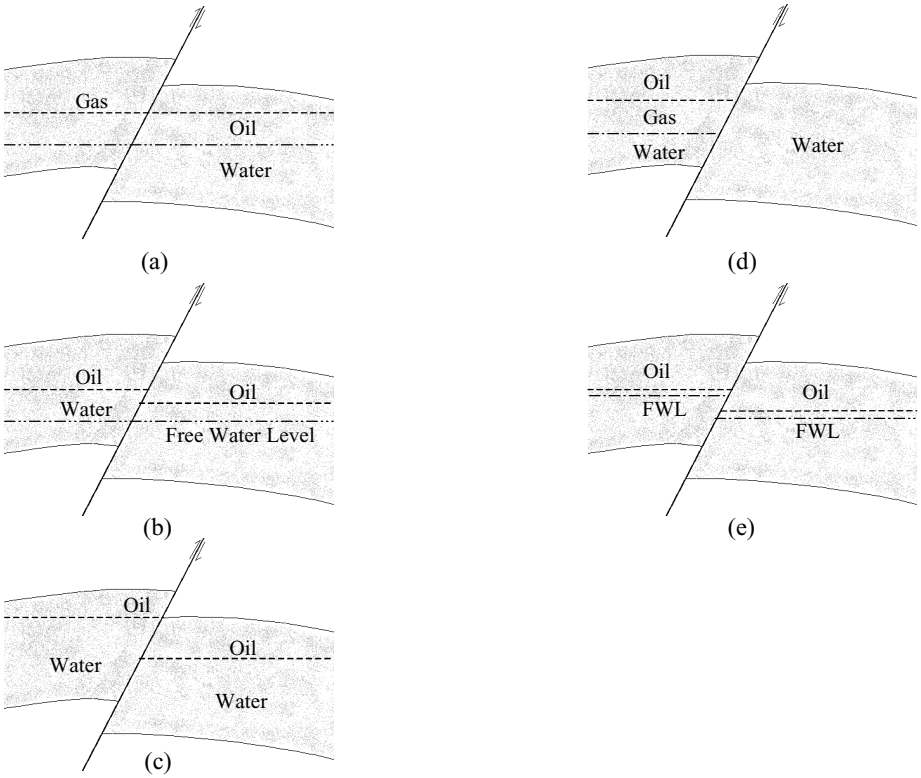

Figure 3. Cross-leaking faults: (a) common hydrocarbon contacts; (b) common free water levels (FWL) and (c) juxtaposed lithology leak points and leakages, and cross sealing faults: (d) hydrocarbon against water and (e) different hydrocarbon contacts (after Skerlec, 1999).

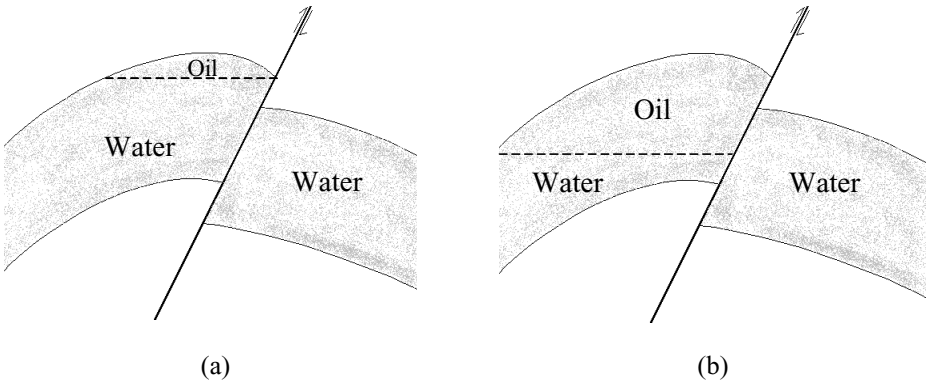

Figure 4. (a) A dip-leaking fault with a leaking point in which oil contact coincides with the intersection of a fault plane and the top of a reservoir and (b) a dip-sealing fault that traps oil (after Skerlec, 1999).

where h is the maximum hydrocarbon column height in ft that a fault can trap. P_{df} and P_{ds} are the displacement pressures in psi of a fault and sand, respectively. ρ_w and ρ_h are water and hydrocarbon densities in g/cm^3, respectively.

GEOPRESSURE AND HYDROCARBON MIGRATION

Geopressure has a significant influence on hydrocarbon migration and entrapment, especially involving faults. Faults often divide reservoirs into individual compartments. Each compartment may have different pressures and different geopressure gradients.

Causes of geopressure formation include cementation, mature gases, aquathermal pressuring, the expansion of pore fluids, rapid loading and disequilibrium compaction, the dehydration of clay minerals, paleohydrology and paleo-pressure histories, the generation of gas from source rocks, petroleum accumulation and charging, or oil cracking to gas (Roberts et al., 1996; Kuo, 1997; and Berg and Gangi, 1999). For example, in the Ship Shoal 274/293 and South Eugene Island 330 fields, shallow sediments

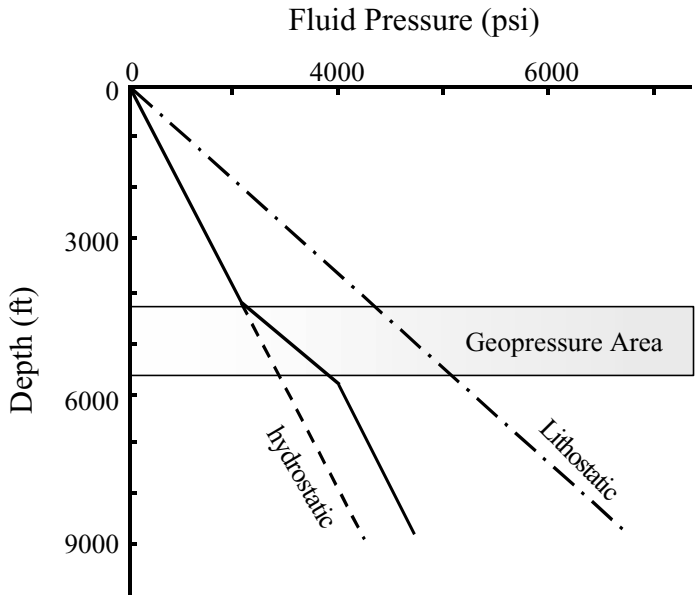

Figure 5. A typical pressure profile in the northern Gulf of Mexico. The hydrostatic pressure gradient is 0.46 psi/ft. The lithostatic pressure gradient is 1.08 psi/ft. The fluid pressure gradient is greater than the lithostatic pressure gradient in the geopressure area (after Nunn, 1996; and Kim, 1998).

contain pore fluids at hydrostatic pressure and deeper sediments contain geopressured pore fluids (Nunn, 1996; and Kim, 1998). This geopressure was mainly created by the action disequilibrium of low-permeability sediments in these fields (Nunn, 1996; Roberts et al., 1996; Kuo, 1997; and Kim, 1998). A typical pressure profile of these fields is shown in Figure 5 (Nunn, 1996; and Kim, 1998).

The effects of geopressure on hydrocarbon migration were early discussed by Meyers (1968), who used examples from the Gulf Coast where hydrostatically pressured blocks were faulted down against geopressured fault blocks, thus creating traps. The effects are paid more attention with the recent increase of exploration activities in the northern Gulf of Mexico since hydrocarbon source rocks are usually located deep within the geopressured zones in the northern Gulf of Mexico (Nunn, 1996; Roberts and Nunn, 1996; Kim, 1998; and Kulander, 1998). A low-permeability (with high displacement pressure) barrier along the upper boundary of a geopressured region is essential in order to generate and maintain its geopressure (Roberts and Nunn, 1996; Kim, 1998; and Kulander, 1998). The barrier separating the hydrostatic and geopressured zones is always mechanically weak, and a fracture network is usually quite easily formed. Here, the formation of a fracture network has resulted in the expulsion of geopressured hydrocarbons from its geopressured regions, and into the hydrostatic zones. Evidence, including temperature, pressure, salinity anomalies, mud volcanoes, biotic communities and active venting sites, has all supported expulsion of hydrocarbons from some geopressured zones mainly focused along fault zones (Nunn, 1996; Roberts and Nunn, 1996; Kim, 1998; and Kulander, 1998). The studies conducted in the South Eugene Island 330 area by Holland (1990), Schumacher (1993) and Whelan (1994) indicated that some hydrocarbon migration into hydrostatic zones along nearly vertical growth faults occurred due to geopressure. Roberts and Nunn (1996) also studied temperature and pressure anomalies resulting from geopressure in the South Eugene Island block 330 field, and demonstrated that the permeability of a fault zone, the permeability of shales and the depth of faults all determined the magnitude and shape of anomalies.

IDENTIFICATION AND MAPPING OF MIGRATION PATHWAYS

Since hydrocarbon migration is kinematic and typically occurs over a geological time scale, it is no simple task to reconstruct a migration pathway. According to Skerlec (1999), migration pathway maps are useful tools. In these migration pathway maps, structure-depth contours define buoyant vectors for

hydrocarbon migration and arrows are drawn perpendicular to the structural contours. Fault plane profiles in migration pathway maps define sand/sand and sand/shale juxtaposition and any potentially juxtaposed lithology leaking points. Other forms of evidence are also valid to use when constructing migration pathways. These include hydrocarbon saturation, biomarkers, whole-oil carbon isotopes, the chemical composition of hydrocarbons, and pressure and temperature anomalies. The residual hydrocarbon saturation of migration pathways usually ranges from 1 to 10 percent (Schowalter, 1979). Since source rocks are usually deep and both temperature and pressure can change along migration pathways, it can be expected that the chemical composition of hydrocarbons significantly change while traveling along the migration pathways. These pathways in Ship Shoal 274/293 were successfully constructed based on available salinity, biomarkers and whole-oil carbon isotope data. Hydrocarbon migration along growth faults caused both geopressure and temperature anomalies in the South Eugene Island 330 field (Roberts and Nunn, 1996).

CHAPTER III

METHODOLOGY

This chapter is principally concerned with constructing numerical models. In the study numerical simulations are extended in order to investigate the effect of faults on hydrocarbon migration and distribution in stacked, fault-bounded reservoirs. However, this is not to say that numerical simulations can always easily solve migration problems. In fact, they cannot unless appropriate simulation models are designed. In this chapter, the procedure followed during this numerical simulation study is first summarized, and this is followed by a review of the basic equations that has been used to describe fluid flow in porous media. Finally, the model design is discussed in detail.

SIMULATION PROCESS

Reservoir simulators are very powerful tools, and are now widely used for evaluating reservoir behavior under various conditions. The reservoir simulator Eclipse® was used for this investigation. Eclipse® offers multiple numerical techniques and its excellent convergence controls ensure reliable and accurate solutions to full field-scale and coning studies, as well as minimal material balance errors. Flexible grid blocks can be used to model complex geological features in one, two or three-dimension. IMPES (implicit pressure, explicit saturation) and other fully implicit solvers are available in Eclipse®. A typical procedure for this study is illustrated in Figure 6.

Reservoir study and migration problems

Geological structure and migration history in interested fields are fundamental to construct both conceptual and numerical models to solve migration problems. Geological structure provides overall reservoir geometry, as well as a definition of the internal structure of reservoirs (the position of faults, reservoirs and shale, and their properties and relationships) necessary for conceptual models. Once this information was obtained, numerical models were then designed. Well logs, structural and stratigraphic interpretation of 3D seismic data, engineering analyses, as well as the analysis of available paleo, sedimentological, and tectonic data provide information about lithology, reservoir zones, reservoir and non-reservoir rocks, thickness trends, permeability and porosity, faults, fluids, etc. What is especially important

to numerical simulations is the distribution of lithology, and the petrophysical and fluid dynamic properties of reservoir and fault rocks. Any numerical models should consist of a deterministic description of these terms. However, a high degree of uncertainty regarding in inter-well zones practically exists in the spatial distribution of porosity and permeability.

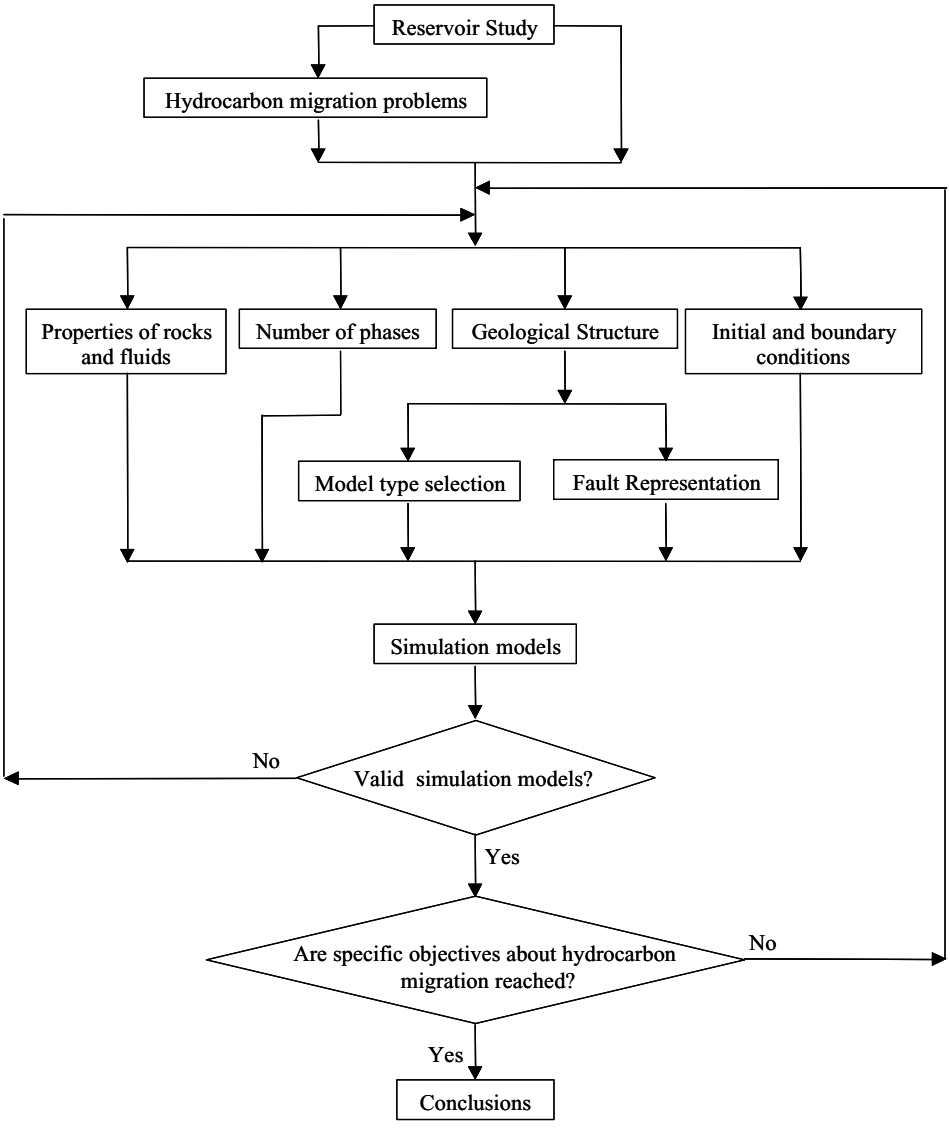

Figure 6. Flow chart for numerical simulations.

Numerical simulations

Simulation models must be carefully designed to answer specific migration problems. Since this investigation is mainly concerned with the effects of faults on stacked, fault-bounded fields experiencing hydrocarbon migration and distribution, two basic issues need to be handled based on typical reservoir simulation techniques. The first issue was how to represent these faults in the numerical models. The second issue was how to construct the pseudo-properties of rocks and fluids in the numerical models. Both issues are discussed in the following sections. Since data on the properties of rocks and fluids are sparse, a sensitivity analysis, which provided insight into how faults affect hydrocarbon migration and distribution, was conducted for this investigation.

RESERVOIR FLOW

A fundamental understanding of physical and mathematical principles is essential for the wise and efficient use of numerical simulations.

Darcy's law

The flow of fluids to a reservoir is described by Darcy's law, which states that Darcy velocity vector is proportional to the potential gradient of any phase.

$$\mathbf{u} = -\frac{\mathbf{k}}{B\mu}\nabla \mathrm{F} \tag{2}$$

Here, $\mathbf{u}$ is Darcy velocity vector. Formation volume factor (FVF) B reflects the volume that a unit volume of fluid occupies under reservoir conditions. μ is the viscosity. $\mathbf{k}$ is a permeability tensor. $\nabla\mathbf{F}$ is the gradient of flow potential. For a single-phase flow, Darcy's law is expressed as:

$$\mathbf{u} = -\frac{\mathbf{k}}{B\mu}(\nabla p + \gamma\nabla d) \tag{3}$$

where, p is the pressure of the phase at an arbitrary level d. γ is the pressure per unit distance. $\gamma\nabla d$ is related to potential energy.

Single-phase flow

The diffusivity equation for a liquid system in a porous medium is derived from the following relationships:

Continuity equation:

$$\nabla \bullet \rho \, \mathbf{u} \pm q = -\frac{\partial(\phi\rho)}{\partial t} \tag{4}$$

Darcy's law:

$$\mathbf{u} = -\frac{\mathbf{k}}{\mu}(\nabla p + \gamma \nabla d) \tag{5}$$

Equation of state:

$$\rho = \rho(p) \tag{6}$$

Combining equations (4) and (5) results in the diffusivity equation

$$\nabla \bullet \rho \, [-\frac{\mathbf{k}}{\mu}(\nabla p + \gamma \nabla d)] \pm q = -\frac{\partial(\phi\rho)}{\partial t} \tag{7}$$

Various technologies, including both theoretical analyses and numerical methods, were developed and employed in order to simplify and solve equation (7). These technologies are outside the scope of this research and hence are not discussed in detail in this dissertation. Only the minimum amount of necessary knowledge regarding finite-difference methods as they are used by in Eclipse® software is introduced in the following sections.

Multi-phase flow

If capillary effects are included, assuming that no solution occurs between any two phases, Darcy's law is easily extended to a multi-phase flow.

$$\mathbf{u}_o = -\frac{\mathbf{k}_o}{\mu_o}(\nabla p + \gamma_o \nabla d) \tag{8}$$

$$\mathbf{u}_g = -\frac{\mathbf{k}_g}{\mu_g}(\nabla p + \gamma_g \nabla d + \nabla p_{cog}) \tag{9}$$

and

$$\mathbf{u}_w = -\frac{\mathbf{k}_w}{\mu_w}(\nabla p + \gamma_w \nabla d - \nabla p_{cow}) \tag{10}$$

Here, oil pressure p is used in equations (8), (9) and (10). $\mathbf{k}_v$ is an effective permeability tensor for phase v ($v =$ w, o or g for water, oil or gas, respectively). $\mathbf{k}_v = k_{rv}\mathbf{k}$, where k_{rv} is the relative permeability of

phase v. p_{cog} is the capillary pressure between oil and gas and p_{cow} is the capillary pressure between oil and water.

MODEL DESIGN

Model design mainly depends upon the following factors: (a) geological structures; (b) the type and complexity of migration problems; (b) economics; and (c) available data. In a word, migration problems should be solved by those models that are both the simplest and the most cost efficient, yet still yielding adequate answers. The section, then, especially addresses design issues: the representing of faults and the constructing of the pseudo-properties of rocks and fluids.

Representing faults

Cross-sectional models were used in this investigation since they are capable of handling both vertical and horizontal variations. The results obtained in any cross-sectional model can be applied to 3D cases. A part of one cross-sectional model, including a fault, is shown in Figure 7. Blocks, which simulate fluid flow in two directions, are essential elements representing fault and reservoir rocks.

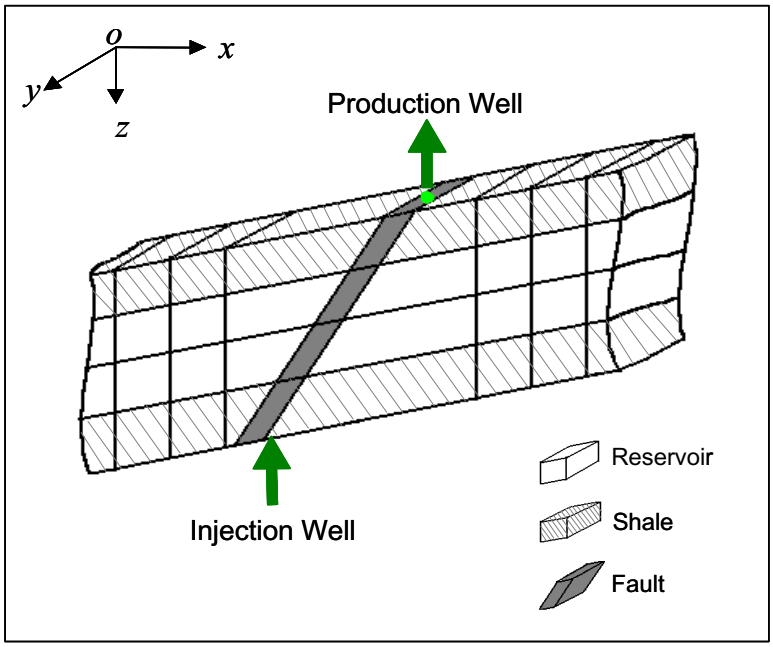

Figure 7. Cross-sectional model.

In order to simulate fluid flow through faults in numerical models, faults may be connected to one or more injection wells, or even a production well (Figure 7). Oil and/or gas can be injected into reservoirs through injection wells. Water, oil and/or gas can escape from reservoirs through production wells. There are two types of boundary conditions: Dirichlet condition — specified pressure (constant or varying with time); or Neumann condition — specific flow rates (constant or varying with time). Constant gas/oil ratios (GOR) or constant bottom-hole pressure in an injection or production well was specified by the boundary conditions in this investigation.

Once the blocks in a model were constructed, initial conditions were assigned to each block and the data required representing the reservoir and rocks, and the fluids were also assigned to individual blocks and fluids, respectively. The initial conditions included initial pressures and an initial fluid saturation of each fluid. This investigation dealt with both oil-water and oil-gas-water systems. The input data for 2-phase and 3-phase systems in Eclipse® software are listed in Tables 1 and 2, respectively. Because the required data are sparse, necessary assumptions were made to simplify numerical simulations and pseudo-properties of rocks and fluids were built in this investigation.

Assumptions

Numerical models were kept as simple as possible to reveal the role of faults on hydrocarbon migration and entrapment in faulted structures. The following assumptions were necessary to make models as simple as possible.

- No phase behavior.
- No dissolution between any two phases.
- Ignore convection and any other thermal effects. Thus, only the buoyant force and/or fluid-pressure gradients drove fluid flow.
- Shale is impermeable. Shale has a high displacement pressure and can trap large columns of oil, as compared to sands. Good shale can trap oil columns of thousands of feet, while good sands can only trap oil columns of 50 ft or less (Smith, 1966; Schowalter, 1979). Therefore, shale is reasonably considered impermeable. Because shale is impermeable, any cells related to shale in numerical models are treated simply as inactive cells.
- Reservoirs and faults are homogeneous and water-wetted.

- The irreducible water saturation is considered to be 22% for both reservoirs and faults.
- Hydrocarbons continuously charge reservoirs during active charge.
- Hydrocarbons simultaneously migrate along faults in oil-gas-water systems.

Pseudo-properties of rocks and fluids

At standard temperature and pressure, oil density is 45 lb/ft^3, gas density 0.0702 lb/ft^3, and water density 66.314 lb/ft^3, causing the hydrostatic pressure gradient to be 0.46 psi/ft. Oil viscosity and formation volume factors are shown in Figure 8 (Eclipse® manual, 1998). Gas viscosity and FVF are shown in Figure 9 (Eclipse® manual, 1998). Water compressibility is 3×10^{-6} /psi. Water formation volume factors and viscosity at reference pressure (3,600 psi) are 1.00341 lb/STB and 0.52341 cP, respectively. Water viscosity is assumed to be constant. The method used here to calculate the water formation volume factor is described in Appendix A. Rock compressibility at reference pressure is 4×10^{-3} /psi. The calculation method to calculate the rock compressibility in Eclipse® software is described in Appendix B.

The properties of faults are poorly understood. Laboratory experiments and field measurements indicate that the permeabilities of faults could be either larger or smaller than the permeabilities of formation rocks (Hintz, 2001). The Coates equation (Ahmed et al., 1989) was applied to calculate porosities, which were then compared to data obtained from field measurements and published papers (Thomeer, 1960 and 1983; Hawkins et al., 1993; and Hintz, 2001):

$$\phi = \sqrt{\frac{S_{iw}}{1-S_{iw}}\frac{\sqrt{k}}{100}} \tag{11}$$

where S_{iw} is the irreducible water saturation, fraction; k is the permeability, md; and ϕ is the porosity, fraction.

Displacement pressure is theoretically estimated from laboratory measurements (mercury injection measurements, log analysis, sedimentary faces, or pore-size distribution). Empirical equations are also available based on field and laboratory measurements. Thomeer (1983) indicated that the pore geometrical factor F_g reflects the distribution of pore throats and their corresponding pore volumes. Larger values of F_g indicate poor reservoirs and more poorly sorted pore throats, while smaller values of F_g indicate good

Table 1. Input data in oil-water systems

	Rock	Fluid
Data to Describe Initial Condition	• Formation top (structure) • Gross formation thickness • Porosity at initial pressure • Water/oil capillary pressure function	• Oil formation volume factor (FVF) • Water FVF • Oil density at standard conditions • Water density at standard conditions
Data to describe oil displacement	• Absolute permeability • Oil relative permeability vs. water saturation • Rock compressibility	• Oil FVF vs. pressure • Oil viscosity vs. pressure • Oil compressibility • Water compressibility
Data to describe water/oil displacement	• Oil and water relative-permeability functions • Water/oil capillary pressure function	• Water FVF vs. pressure • Water viscosity vs. pressure

Table 2. Input data in oil-gas-water systems

	Rock	Fluid
Data to Describe Initial Condition	• Formation top (structure) • Gross formation thickness • Porosity at initial pressure • Water/oil capillary pressure function • Gas/oil capillary pressure function	• Oil formation volume factor (FVF) • Water FVF • Gas FVF • Oil density at standard conditions • Water density at standard conditions • Gas density at standard conditions
Data to describe gas/oil displacement	• Absolute permeability • Gas and oil relative permeability vs. water saturation • Rock compressibility	• Gas in solution vs. pressure • Oil FVF vs. pressure • Gas FVF vs. pressure • Oil viscosity vs. pressure • Gas viscosity vs. pressure • Oil compressibility • Water compressibility
Data to describe water/oil displacement	• Oil and water relative-permeability functions • Water/oil capillary pressure function	• Water FVF vs. pressure • Water viscosity vs. pressure
Data to describe three-phase flow	• Three-phase relative permeability functions	

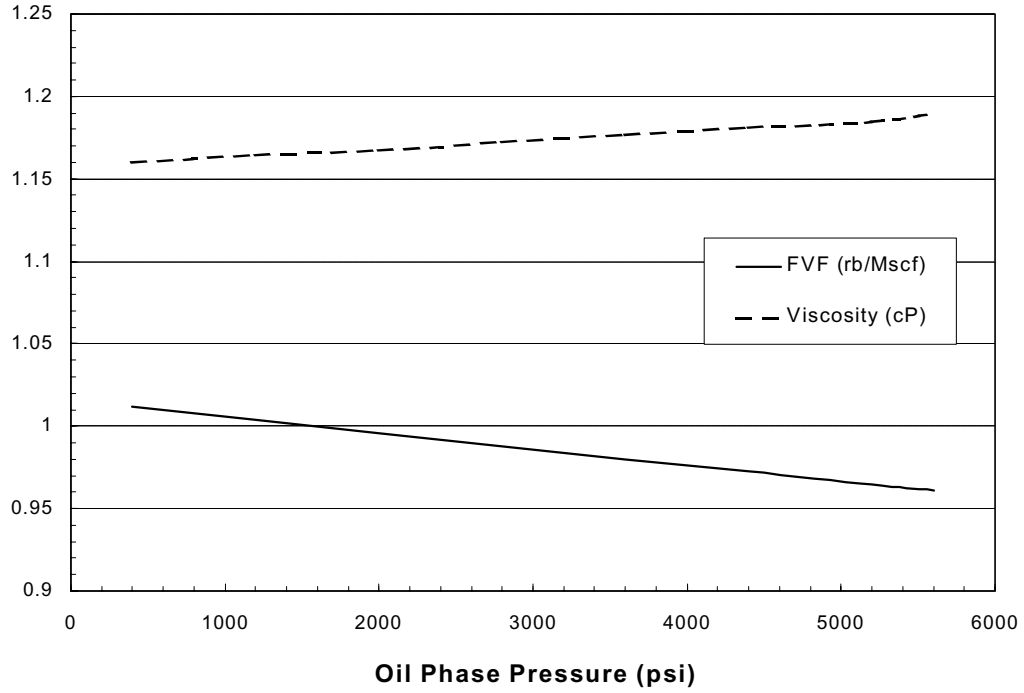

Figure 8. Oil formation volume factor and viscosity versus oil phase pressure (Eclipse manual, 1998).

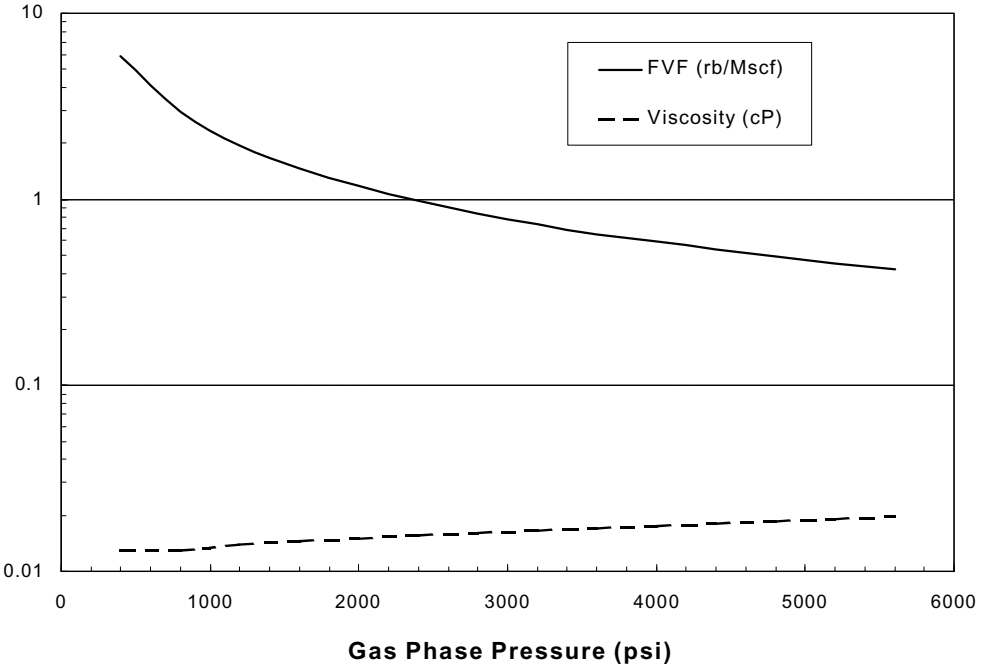

Figure 9. Gas formation volume factor and viscosity versus gas phase pressure (Eclipse manual, 1998).

reservoirs and well-sorted pore throats. F_g usually ranges from 0.1 to 0.4 for reservoirs. Hawkins et al. (1993) used multiple regressions on data from 202 samples taken from 14 formations ranging in age from Ordovician to Tertiary. The porosity and permeabilities ranged from 3.3 to 28% and 0.05 to 998 md, respectively. Hawkins et al. (1993) provided methods for calculating the pore geometrical factor F_g, the mercury/air displacement pressure P_{dma}, and the mercury/air capillary pressure P_{cma} based on the permeability *k* and porosity ϕ:

$$F_g = \left[\ln\left(3.1 \frac{k^{0.1254}}{\phi} \right) \right]^2 \Big/ 2.303 \tag{12}$$

$$P_{dma} = 177 \Big/ (k^{0.3406} \phi) \tag{13}$$

$$P_{cma} = 10^{\left[-F_g / \ln(1 - S_w) + \log P_{dma} \right]} \tag{14}$$

S_w in equation (14) is water saturation, fraction.

The following equations have been applied in oil-water systems in order to convert mercury/air displacement pressure P_{dma} and mercury/air capillary pressure P_{cma} to oil/water displacement pressure P_d and oil/water capillary pressure P_c, respectively.

$$P_d = \frac{\sigma_{ow} \cos\theta_{ow}}{\sigma_{ma} \cos\theta_{ma}} P_{dma} \tag{15}$$

$$P_c = \frac{\sigma_{ow} \cos\theta_{ow}}{\sigma_{ma} \cos\theta_{ma}} P_{cma} \tag{16}$$

where σ_{ow} is the interfacial tension of oil and water, σ_{ma} is the interfacial tension of mercury and air, and θ_{ow} and θ_{ma} are the oil/water contact angle and the mercury/air contact angle, respectively. In this study σ_{ow} is 30 mN/m, σ_{ma} is 480 mN/m, and θ_{ow} is 0° because water represents the wetted phase of an oil-water system. θ_{ma} is 140°. These values were provided by Berg (1996).

In order to apply Darcy's law to calculation regarding fluid flow, one must have effective permeability values. The effective permeability measures the permeability of the fluid flowing under saturation conditions. Effective permeability values can be calculated from the absolute permeability and the relative permeability. Standing (1975) defined the pore size distribution index λ in order to calculate relative

permeability values and capillary pressures. Small pore size distribution indexes indicate that rocks have a wide range of pore sizes.

$$P_c = P_d \left(\frac{S_w - S_{iw}}{1 - S_{iw}} \right)^{-\frac{1}{\lambda}} \tag{17}$$

$$k_{rw} = \left(\frac{S_w - S_{iw}}{1 - S_{iw}} \right)^{\frac{2+3\lambda}{\lambda}} \tag{18}$$

$$k_{ro} = k_r^o \left(1 - \frac{S_w - S_{iw}}{1 - S_{iw}} \right)^2 \left[1 - \left(\frac{S_w - S_{iw}}{1 - S_{iw}} \right)^{\frac{2+\lambda}{\lambda}} \right] \tag{19}$$

$$k_r^o = 1.31 - 2.62 S_{iw} + 1.1 (S_{iw})^2 \tag{20}$$

where S_{iw} is the irreducible water saturation, and k_{rw} and k_{ro} are the relative permeabilities of water and oil, respectively. Combining equations (12), (13), (15), (16) and (17) relates λ and F_g as

$$\lambda = \log \left(\frac{S_w - S_{iw}}{1 - S_{iw}} \right) \ln(1 - S_w) / F_g \tag{21}$$

The calculated porosity, pore geometrical factors, displacement pressures of both sand and faults, capillary pressures, and both the oil and water relative permeabilities in oil-water systems are shown in Figures 10, 11, 12, 13, 14 and 15, respectively.

In calculations concerning oil-gas-water systems, additional data about both oil and gas are required. First, gas/oil capillary pressure P_{cog} must be converted from the mercury/air capillary pressure P_{cma}.

$$P_{cog} = \frac{\sigma_{og} \cos\theta_{og}}{\sigma_{ma} \cos\theta_{ma}} P_{cma} \tag{22}$$

where σ_{og} is the interfacial tension between gas and oil, and θ_{og} is the gas/oil contact angle. According to Berg (1996), σ_{og} is 46 mN/m and θ_{og} is 0° because oil represents the wetted phase in the gas-oil system. Calculated gas/oil capillary pressures are shown in Figure 16.

Second, water, oil and gas relative permeabilities must always be calculated for oil-gas-water system calculations. Water relative permeability can be calculated by equation (18). According to Standing (1975),

oil relative permeability k_{rog} in three-phase systems and gas relative permeability k_{rg} in oil-gas systems can be computed according to the following equations:

$$k_{rog} = k_r^o \left(\frac{S_o}{1 - S_{iw}} \right)^2 \left[\left(\frac{1 - S_g - S_{iw}}{1 - S_{iw}} \right)^{\frac{2+\lambda}{\lambda}} - \left(\frac{S_w - S_{iw}}{1 - S_{iw}} \right)^{\frac{2+\lambda}{\lambda}} \right] \tag{23}$$

$$k_{rg} = k_r^o \left(\frac{S_g}{1 - S_{iw}} \right)^2 \left[1 - \left(\frac{1 - S_g - S_{iw}}{1 - S_{iw}} \right)^{\frac{2+\lambda}{\lambda}} \right] \tag{24}$$

where S_g is the gas saturation.

Gas relative permeability can be calculated according to equation (24), since gas saturation S_g is the only variable. Calculated gas relative permeabilities are shown in Figure 17. However, oil saturation S_o, gas saturation S_g and water saturation S_w are simultaneously required to calculate oil relative permeability k_{rog} in oil-gas-water systems according to equation (23). Since the data about the three variables are unknown, the oil relative permeability k_{rog} versus oil saturation S_o simply adapts the data listed in Table 3 for all rocks in the investigation.

Table 3. Oil relative permeability in three-phase systems (Eclipse® manual, 1998)

So	krog
0.00	0.00
0.50	0.02
0.60	0.10
0.70	0.33
0.74	0.60
0.78	0.78

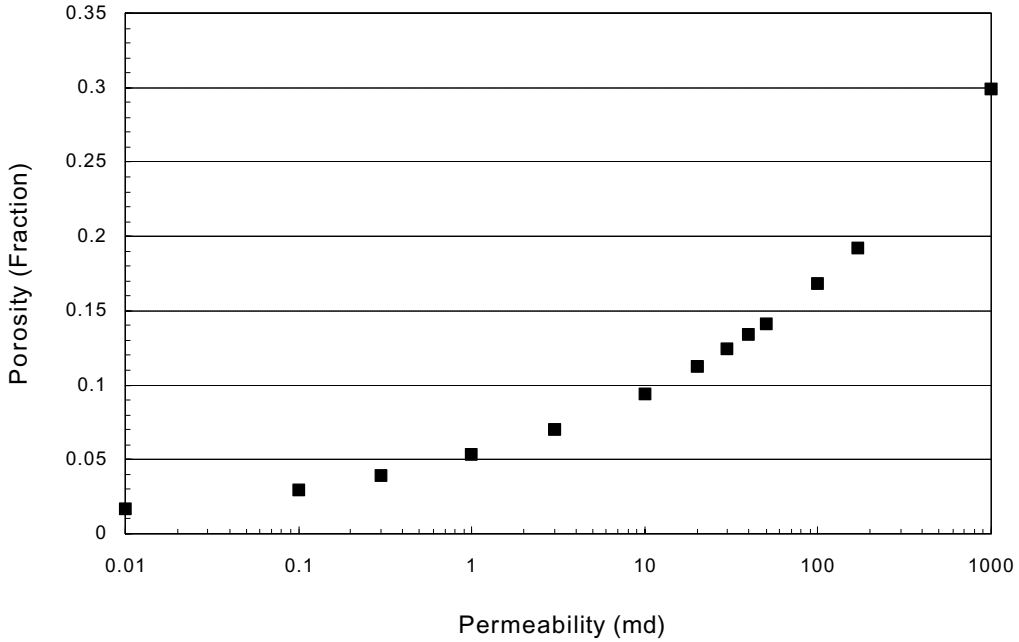

Figure 10. Porosity versus permeability. The permeability of reservoir sand is 100 md. The permeabilities of faults are 0.01, 0.1, 0.3, 1, 3, 10, 50, 170 and 1000 md (Functions after Ahmed and Coates, 1989).

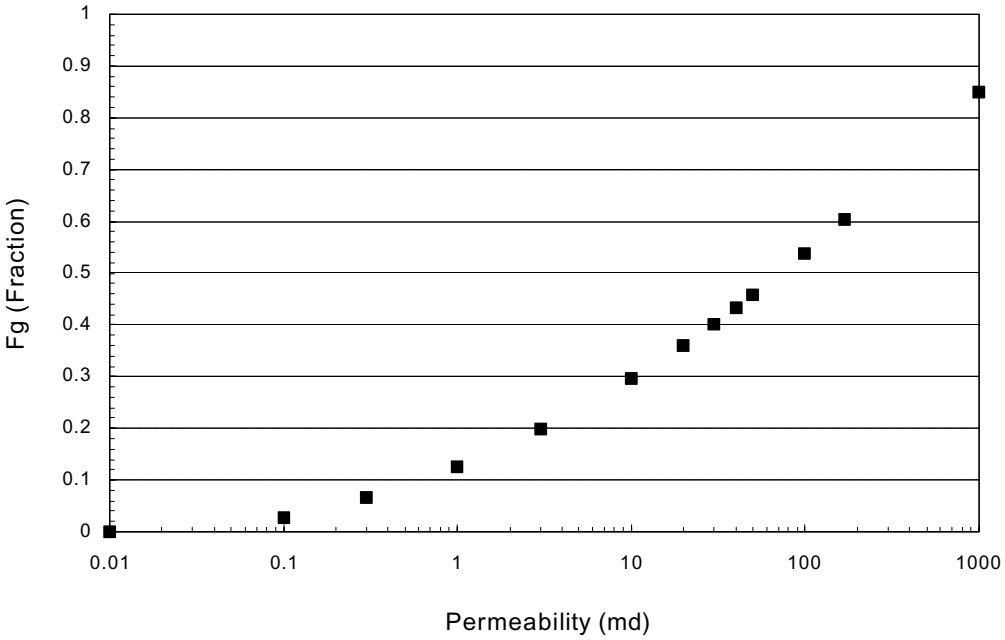

Figure 11. Pore geometrical factor Fg versus permeability. The permeability of reservoir sand is 100md. The permeabilities of faults are 0.01, 0.1, 0.3, 1, 3, 10, 50, 170 and 1000 md (Functions after Hawkins et al., 1993).

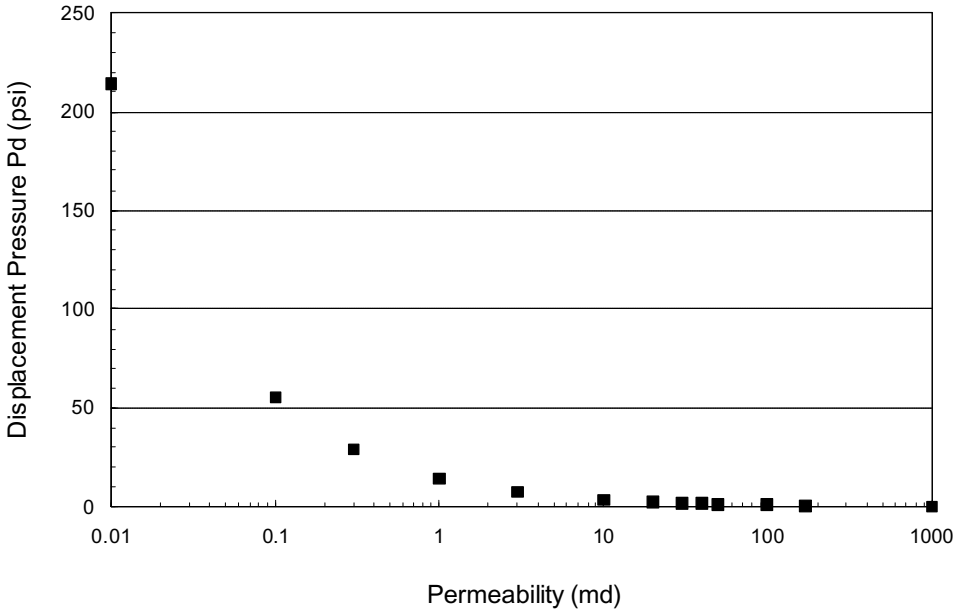

Figure 12. Displacement pressure versus permeabilities. The permeability of reservoir sand is 100md. The permeabilities of faults are 0.01, 0.1, 0.3, 1, 3, 10, 50, 170 and 1000 md (Functions after Hawkins et al., 1993 and Berg, 1996).

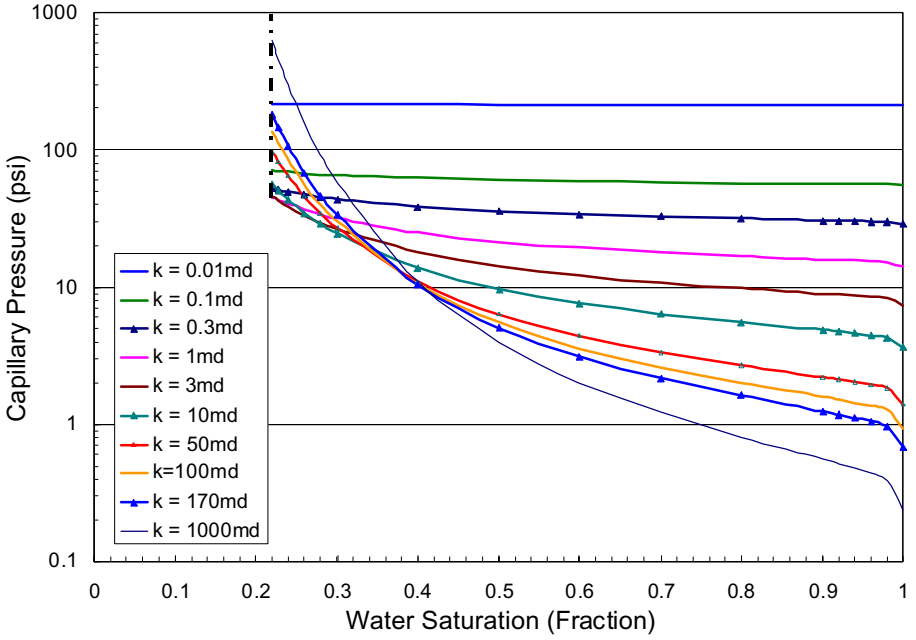

Figure 13. Oil-water capillary pressures versus water saturation. The capillary pressure curve of reservoir corresponds to 100 md. Other curves are the capillary pressures of faults. The reservoir sand and all faults are water-wetted and their irreducible water saturation is 0.22 (Functions after Hawkins et al., 1993 and Berg, 1996).

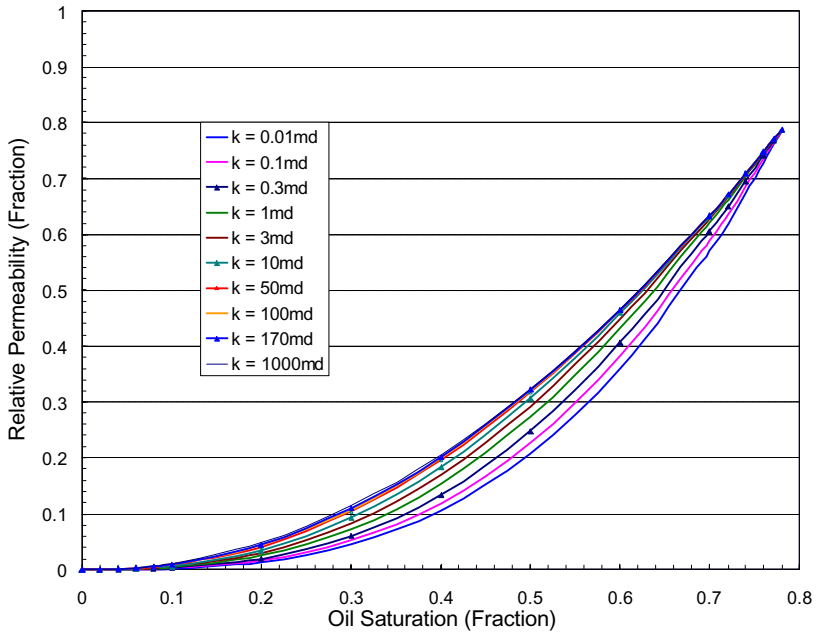

Figure 14. Relative oil permeabilities versus oil saturation in oil-water systems. The relative oil permeability curve of reservoir corresponds to 100 md. Other curves are the oil relative permeabilities of faults. The reservoir sand and all faults are water-wetted and their irreducible water saturation is 0.22 (Function after Standing, 1975).

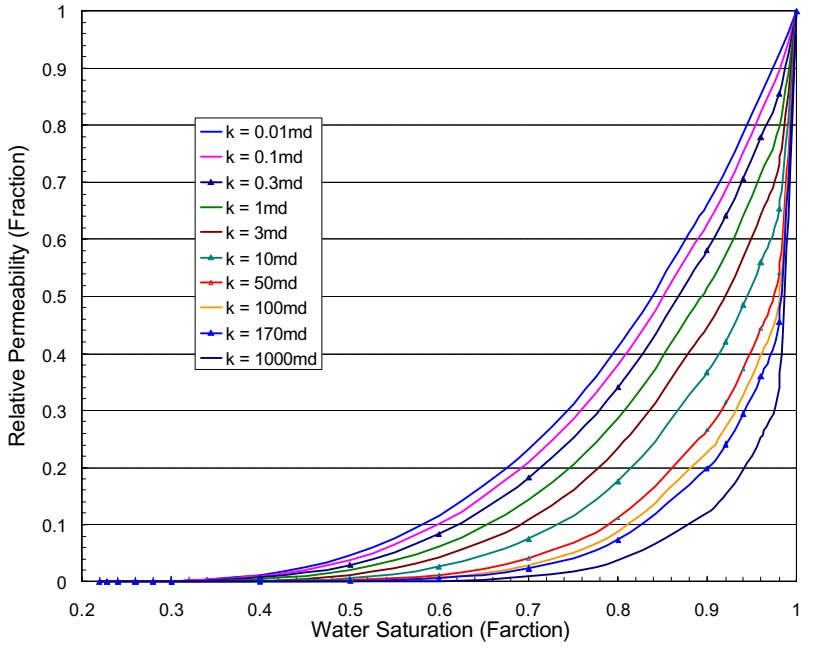

Figure 15. Relative water permeabilities versus water saturation in oil-water systems. The relative water permeability curve of reservoir corresponds to 100 md. Other curves are the relative water permeabilities of faults. The reservoir sand and all faults are water-wetted and their irreducible water saturation is 0.22 (Function after Standing, 1975).

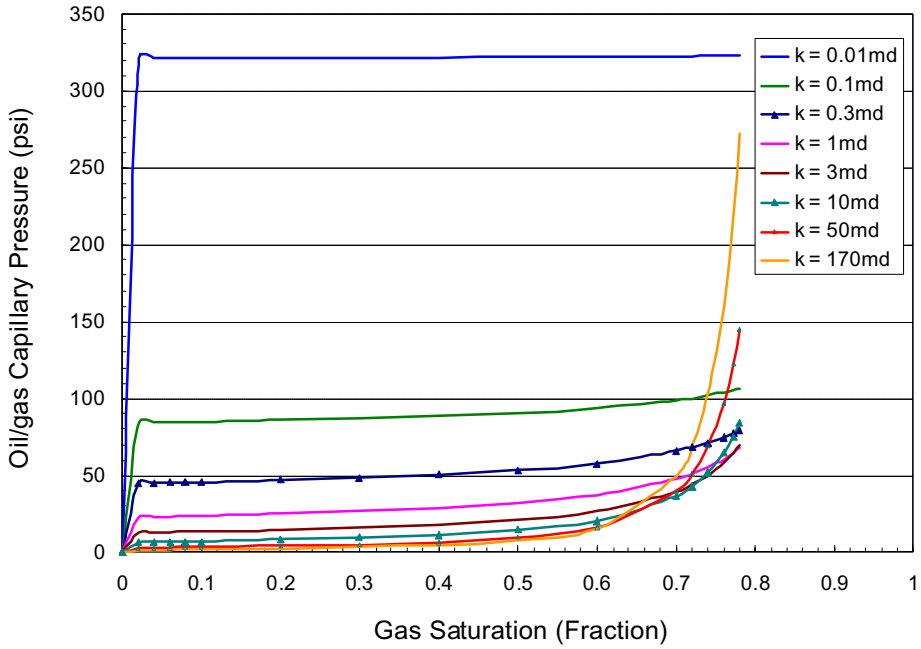

Figure 16. Oil/gas capillary pressures versus gas saturation. The capillary pressure curve of reservoir corresponds to 100 md. Other curves are the capillary pressures of faults. Irreducible water saturation is 0.22 (Function after Standing, 1975).

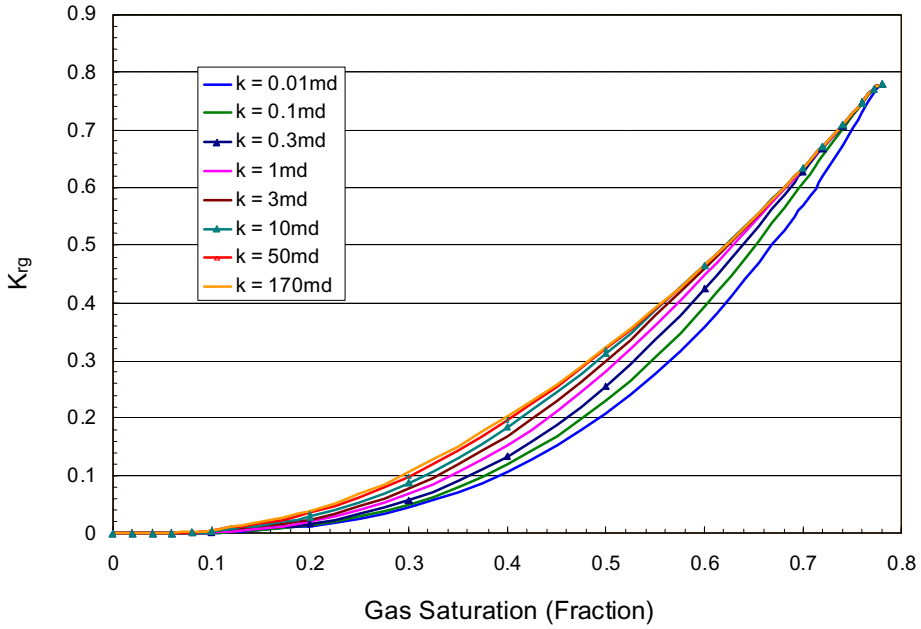

Figure 17. Relative gas permeabilities versus gas saturation in oil-gas systems. The relative gas permeability curve of reservoir corresponds to 100 md. Other curves are the relative gas permeabilities of faults. Irreducible water saturation is 0.22 (Function after Standing, 1975).

CHAPTER IV

THE ROLE OF "BACK DOORS" DURING AN OIL CHARGE

This chapter focuses primarily on the effects of back door faults during active oil charges in fault-compartmentalized reservoirs, under either hydrostatic pressure or geopressure. The simplest simulations were conducted in a single reservoir bounded by two faults in order to assess the oil transportation ability of a charging fault, as well as to study how back doors might improve oil charge efficiency by comparing oil percent charges. An attempt was then made to demonstrate how back doors could make two reservoirs separated by a barrier fault be in communication was made.

INTRODUCTION

This chapter mainly demonstrates that back door faults may improve hydrocarbon charge efficiency in stacked fault-bounded reservoirs. The role of back door faults in oil-water systems during an active oil charge was first investigated. The role of back door faults in oil-gas-water systems will be discussed in Chapter V. This chapter has three specific goals.

The first concern is to investigate the oil transportation ability of a fault under hydrostatic pressure and geopressure. In order to investigate the ability of a fault, oil is allowed to charge a single stacked reservoir through a charging fault and any fluids (oil and water) are allowed to escape only through that same charging fault. It is shown that water escaping only through the charging fault may cause a slow charge, or even no charge. The oil transportation ability of a fault is assessed by oil charge efficiency.

The second goal is to investigate the effects of back door faults on oil migration and entrapment under hydrostatic pressure and under geopressure, after excluding the effects of charging faults. It is shown that back door faults could facilitate water escape from stacked fault-bounded reservoirs, and could then improve hydrocarbon charge efficiency. This goal is of critical interest and is fundamental to understanding reservoir communication through a barrier.

The third mission is to identify whether or not an updip back door fault could facilitate oil penetration through a central barrier, when oil is charging two dipping stacked reservoirs separated by the barrier, through a downdip charging fault under hydrostatic pressure and geopressure. A barrier with a high

displacement pressure usually seals hydrocarbon migration. Barriers are very common. For example, among 41 compartments separated by faults in the Ship Shoal 274/293 field, 20 were tight. Conclusions from this mission can explain and predict whether two sands separated by a barrier are in communication.

SIMULATION MODELS

The properties of sands are considered to be fixed but the properties of bounding faults are considered variable for all models in this chapter. Since the permeability of sand is constantly 100 md, oil migration and entrapment are affected only by the properties of bounded faults. The permeabilities of faults can be either larger or smaller than the permeability of the reservoir. Although the permeabilities of faults in the Ship Shoal 274/293 fields mainly range from 0.1 md to 10 md, practically speaking, the permeabilities of faults can range from 0.01 md to 1000 md (Hintz, 2001). In this study the possible permeabilities of faults are assigned as 0.01, 0.1, 1, 0.3, 1, 3, 10, 50, 170, and 1000 md.

Besides various fault properties, other factors that affect oil migration and entrapment such as the dip angle and the width of a fault should be properly considered. The seal capacity of a fault is determined by its displacement pressure, but the dip angle of a fault can affect the level of hydrocarbon volume it traps. Although dip angle of a fault can widely vary (by up to nearly 90° in the Ship Shoal 274/294 field and the South Eugene Island 330 field), the angles between 15° and 75° are fairly common. The width of a fault can affect the rate at which fluid flows through it. In this study faults are considered to be constantly 0.3 ft wide so that only those properties of faults that affect fluid flow will be focused upon.

Updip Back Door (UDBD) model

A geological cross section and the corresponding numerical model represented by the UDBD models are shown in Figure 18(a). Here, a dipping reservoir is bounded by two faults. The downdip fault is a charging fault, antithetic to the dipping sand, and the updip fault is a back door, synthetic to the dipping sand. Oil charges the sand through the charging fault under either hydrostatic pressure or geopressure. Both oil and water could escape from the charging fault and the back door, depending on the back door's property. This conceptual model, then, is constructed to simulate an updip oil charge into typical sand juxtaposition geometry along a fault.

The corresponding numerical model has total 378 cells, Figure 18(b). The dip angle of the sand is 5° in this numerical model. The dip angle of the downdip charging fault is 70°, antithetic to the dipping sand, and the updip back door dips 60°, synthetic to the dipping sand. To simulate fluid flow into and out of this system, three wells were connected: an injection well for oil injection and two production wells in order to allow water and oil to escape. Constant well bottom hole pressures, $P_{injector}$, P_d and P_u, are specified as boundary conditions in this numerical model. $P_{injector}$ is the bottom hole pressure of the injection well at the point at which oil is injected into the system. P_d and P_u are the bottom hole pressures at which water and oil escape from the charging fault and from the back door, respectively. In order to guarantee oil injection and fluid escape through the charging fault or the back door, $P_{injector}$ is made 5 psi higher than the pressure of the cell where the injection well is connected, and P_d and P_u are kept at 10 psi lower than the corresponding pressures of the cells where they are connected.

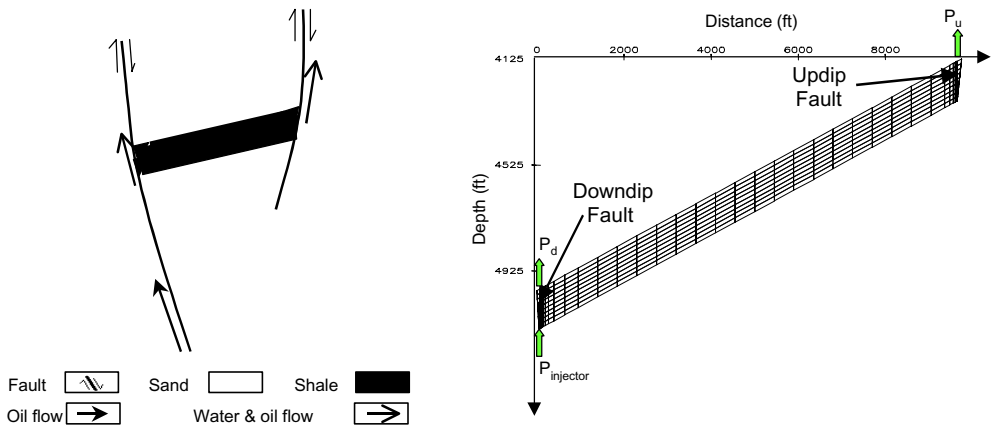

(a) (b)

Figure 18. UDBD model: (a) conceptual model and (b) numerical model. The downdip fault is a charging fault. The updip fault is a back door. Oil charges along the charging fault. Both water and oil may escape from the charging fault or the back door. Constant pressures P_d, P_u and $P_{injector}$ are specified as boundary conditions in this numerical model.

Downdip Back Door (DDBD) model

Figure 19 shows a geological cross section and a corresponding numerical model that represents the UDBD model. The geological structure of the DDBD model is the same as the structure of the UDBD model, except that in the DDBD model the downdip fault is a back door and the updip fault is a charging fault. Constant well bottom hole pressures, $P_{injector}$, P_d and P_u, are also specified as boundary conditions in the numerical model, as well as in UDBD model.

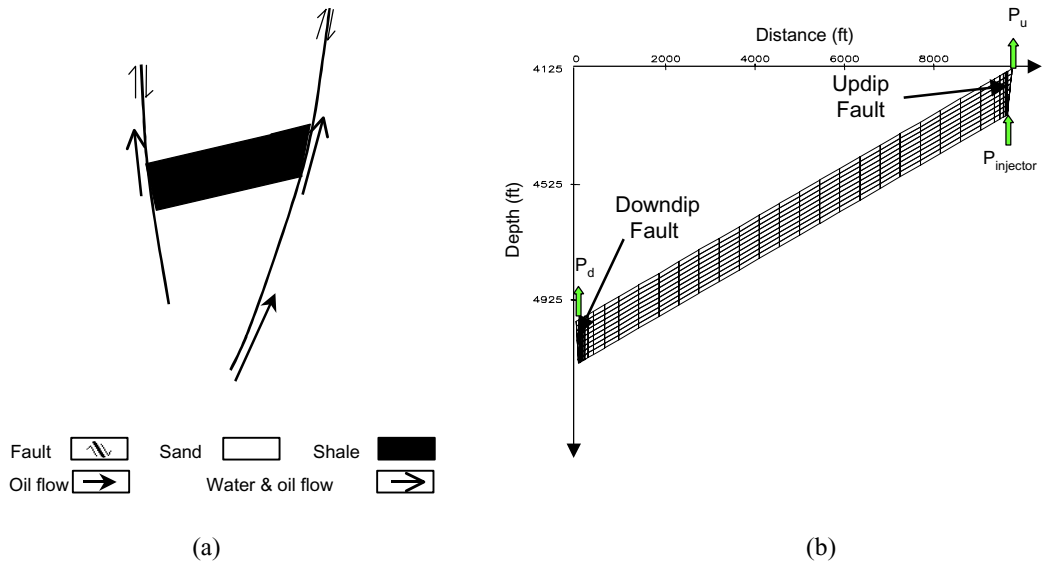

Figure 19. DDBD model: (a) conceptual model and (b) numerical model. The updip fault is a charging fault. The downdip fault is a back door. Oil charges trough the charging fault. Both water and oil can escape from the charging fault and the back door. Constant pressures P_d, P_u and $P_{injector}$ are specified as boundary conditions in the numerical model.

Communication model

In the communication model two sands are bounded by two faults and separated by a central barrier, as shown in Figure 20. The dip angles of these two sands are 5°. The charging fault is the downdip fault, antithetic to the sands and dipping at 70°. The back door is the updip fault, synthetic to the sands and dipping at 60°. The properties of the central barrier are variable with the different displacement pressures. No fluids flow into these sands through the central barrier, nor can any fluids flow out of the system

through the central barrier. Constant well bottom hole pressures, $P_{injector}$, P_d and P_u, are applied in the numerical model as in the UDBD model.

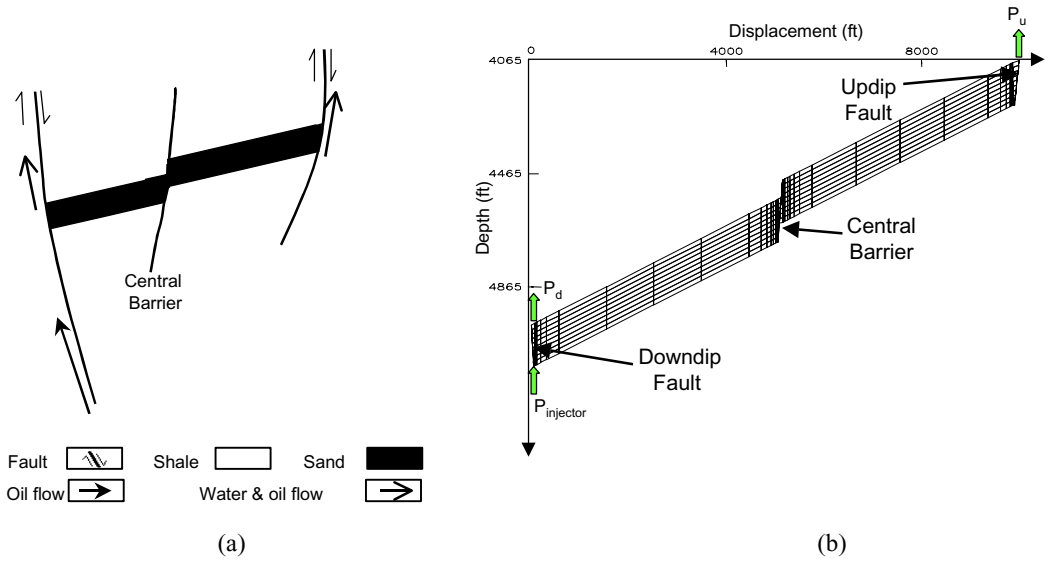

Figure 20. Communication model: (a) conceptual model and (b) numerical model. Two sands are separated by a central barrier. The downdip fault is a charging fault. The updip fault is a back door. Oil charges through the charging fault. Both water and oil can escape from the charging fault and the back door. Constant pressures P_d, P_u and $P_{injector}$ are specified as boundary conditions in the numerical model.

SIMULATION RESULTS

In this chapter, simulations with or without a back door, under hydrostatic pressure or geopressure, were conducted in order to simulate updip and downdip oil charges. The purpose of constructing these models without any back doors was to investigate the oil transportation ability of a fault that is mainly determined by the properties of a charging fault, while the purpose of constructing these models with a back door was to investigate how the back door could facilitate water escape from a reservoir, and hence improve oil charge efficiency. After the fundamentals were achieved from the above investigations, the communication models were then constructed to investigate whether or not an updip back door could facilitate oil penetration of a central barrier to charge an updip reservoir.

UDBD models: The updip oil transportation ability of a fault

The updip oil transportation ability of a downdip fault is determined by a percent charge through which oil charges an updip sand. Oil charges the sand through a downdip charging fault. No back door exists in this kind of models. Both oil and water can flow out of the sand only through the downdip charging fault. The properties of charging faults are variable. Two pressure distributions are possible: one is hydrostatic pressure with the pressure gradient being 0.46 psi/ft; another is geopressure with 1901.78 psi at 4133.9 ft and 3082.12 psi at 5137.28 ft. The geopressure gradient within the geopressure zone is 1.176 psi/ft. Although the geopressure gradient within the geopressure zone is higher than the lithostatic pressure gradient, the geopressure is still much less than the corresponding lithostatic pressures at the same depth as shown in Figure 3, thus preventing rocks from fracturing in this zone. Oil saturation at 300 years, 5,200 years, 51,000 years and 381,400 years under hydrostatic pressure is shown in Figure 21 with the charging fault permeabilities at 0.01 md, 1 md and 170 md. Oil saturation under geopressure is shown in Figure 22. Because oil is less dense than water, oil occupies the upper part of the sand. The percent charges under both hydrostatic pressure and geopressure are shown in Figures 23 and 24, respectively, when the charging fault permeabilities are 0.01, 0.1, 0.3, 1, 3, 10, 50, 170 and 1000 md.

Under hydrostatic pressure, the percent charge for all models is less than 10 percent within 1,100 years. The percent charge is about 50 percent at 108,000 years when the charging fault permeability is 0.1 md, while the percent charge reaches 50 percent at 6,800 years when the charging fault permeability is 170 md. At 381,400 years, the percent charge is consistently at about 70 percent, except for the model whose charging fault permeability is 0.01 md. The percent charge at 381,400 years is only at about 20 percent when the permeability of the charging fault is 0.01 md.

Constructing numerical models under geopressure simulates fluid flow from a geopressure zone into a hydrostatic pressure zone. Compared to the results generated from the hydrostatic pressure model, simulation results under geopressure demonstrate that geopressure facilitates an oil updip charge because geopressure acts in conjunction with the buoyant pressure. The percent charge reaches about 50 percent at 18,600 years when the permeability of the charging fault is 0.1 md, while the percent charge is about 50

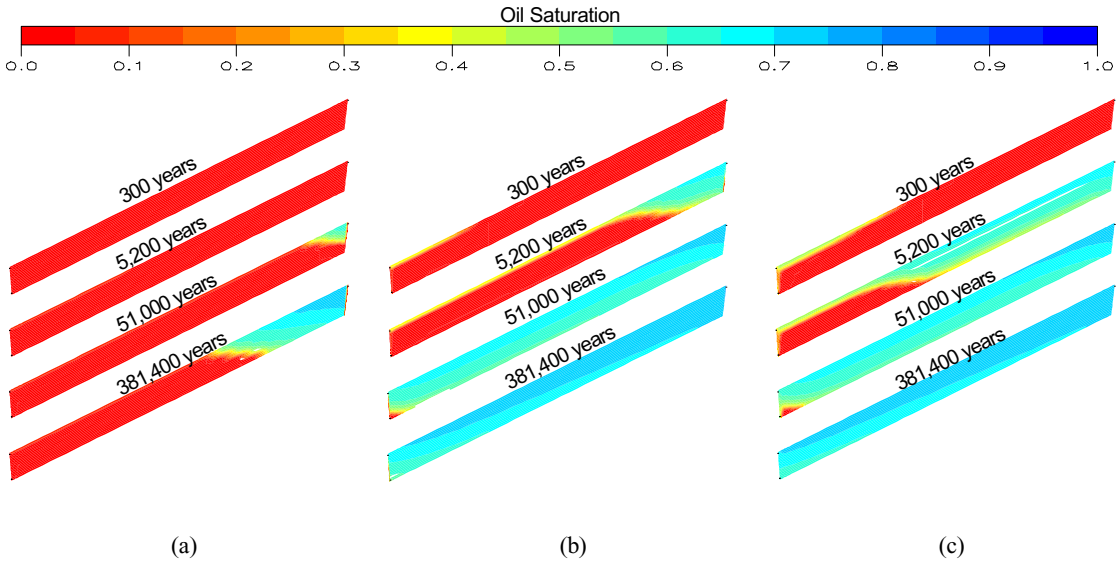

(a) (b) (c)

Figure 21. Oil saturation under hydrostatic pressure in UDBD models without any updip back door when the permeability of the charging fault is (a) 0.01 md, (b) 1 md and (c) 170 md (Eclipse® figures).

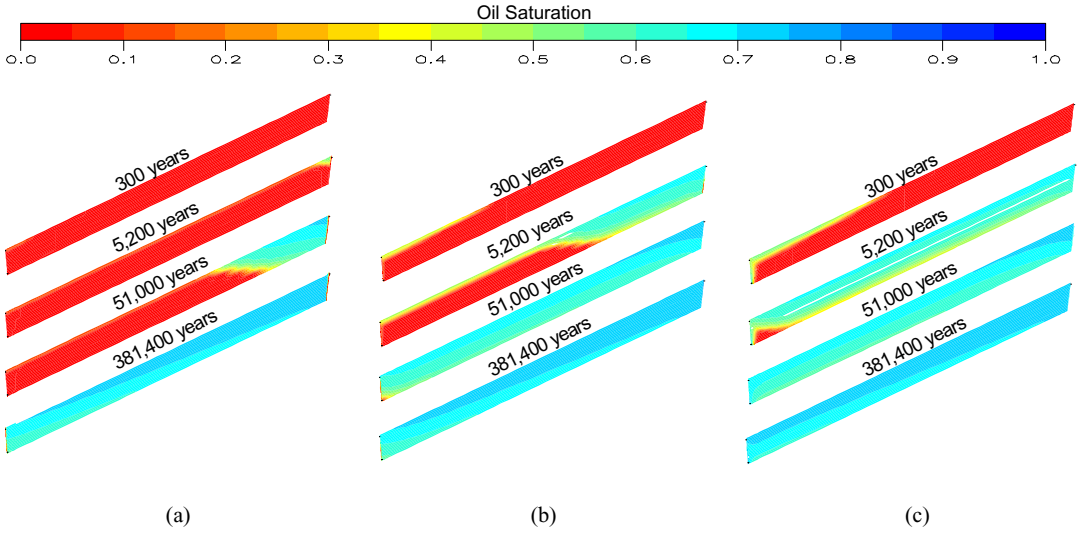

(a) (b) (c)

Figure 22. Oil saturation under geopressure in UDBD models without any updip back door when the permeability of the charging fault is (a) 0.01 md, (b) 1 md and (c) 170 md (Eclipse® figures).

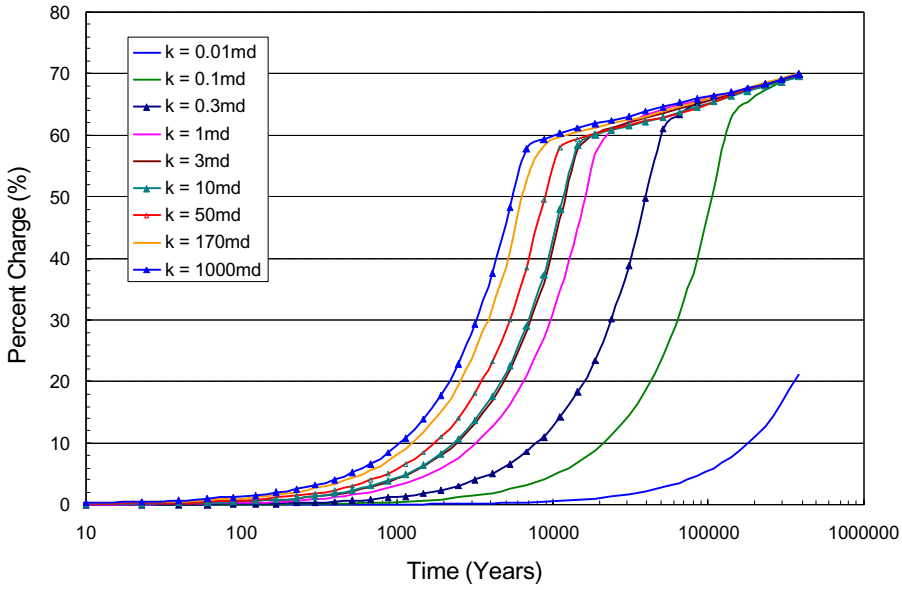

Figure 23. Percent charge under hydrostatic pressure in UDBD models without any updip back door. In the model, oil charges through a downdip charging fault. The permeability of the sand is constantly 100 md. The shown permeabilities are the permeabilities of the charging fault (Data from Eclipse®).

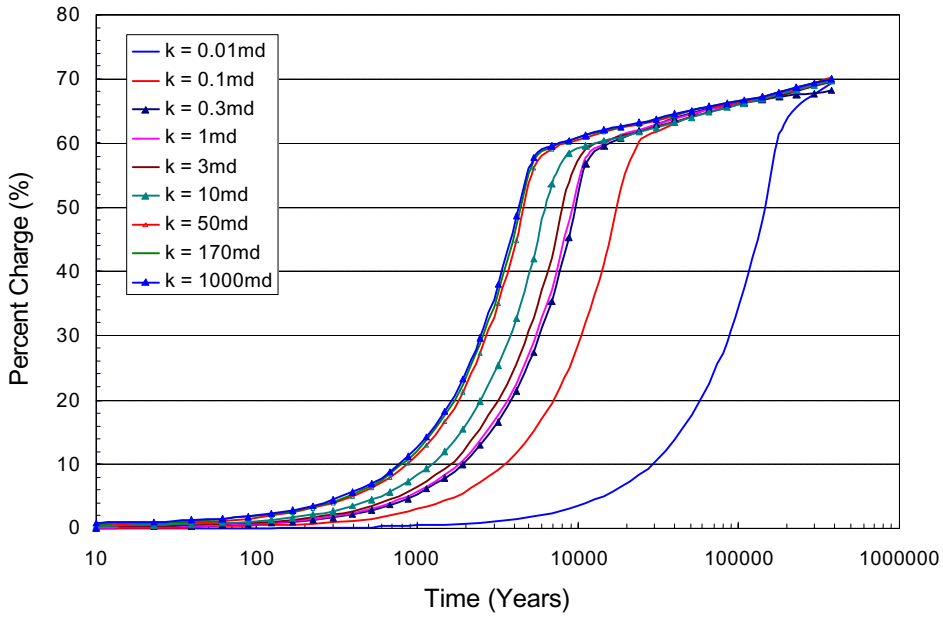

Figure 24. Percent charge under geopressure in UDBD models without any updip back doors. In the models, oil charges through a downdip charging fault. The permeability of the sand is constantly 100 md. The shown permeabilities are the permeabilities of the charging fault (Data from Eclipse®).

percent at 4,200 years when the permeability of the charging fault is 170 md. The percent charge at 381,400 years is about 70 percent for the other models.

Obviously, if no back door exists, the updip oil charge efficiency is determined by the properties of the charging fault. The lower the displacement pressure of the charging fault, the higher the charge efficiency. Geopressure, which acts with the buoyant pressure, facilitates an updip oil charge.

UDBD models: Updip oil charge efficiency with the aid of updip back doors

Oil charges sand through a downdip charging fault. The properties of a charging fault are constant, with the value of permeability considered to be 170 md. Both oil and water can escape through the charging fault, and the updip fault acts as a back door. The properties of this back door are variable. Oil saturation under hydrostatic pressure at different times is shown in Figure 25 when back door permeabilities are 0.3 md and 1,000 md. The percent charges under hydrostatic pressure and geopressure are shown in Figures 26 and 27, respectively.

Before 3,000 years and under hydrostatic pressure, the lower the displacement pressure of an updip back door, the more efficient the oil charge. At 2,000 years, the percent charges are over 20 percent when the permeability of the back door is higher than 10 md. If there is no back door, the percent charge is only about 15 percent at 2,000 years. Oil continuously charges the sand. A back door with higher displacement pressures impedes oil flow and oil finally accumulates in the sand, causing the oil accumulation rate to be faster than the oil escape rate. Oil mainly flows out of the sand through a back door with a lower displacement pressure because a back door with a higher displacement pressure has a higher entrapment capacity than a back door with a lower displacement pressure. Oil quickly accumulates from 1,000 years to 7,000 years when the permeability of a back door is 0.01 md, 0.1 md and 0.3 md, or when no back door exists. Hence, the percent charge of models with no back door or whose back door permeability ranges from 0.01 md to 0.3 md is higher than models at 381,400 years. The results shown in Figure 26 indicate that a back door whose permeability is between 0.01 md and 0.3 md actually acts as a seal to oil hydrocarbon migration.

No back door causes a downdip water flow into the sand under hydrostatic pressure, and water finally escapes from the sand through a charging fault (Figure 28(a)). A back door causes an updip water flow into the sand and that water finally exits through a back door (Figure 28(b)). Within 3,000 years, no back door

causes less water to exit from the sand in the UDBD model than from the sand in the UDBD model with a back door (Figure 29). Oil charges continue in both cases. In the UDBD models without a back door, oil accumulates at the upper part of the sand and forces water to escape the sand from the downdip charging fault. In contrast, oil accumulates at the upper part of the sand in the UDBD model with an updip back door but that oil only partly escapes from the back door if the oil accumulation exceeds the seal capacity of the back door. Therefore, the total escape water in the UDBD model without a back door is greater than the total escape water in the UDBD with a back door after 3,000 years (Figure 29). This also explains why under hydrostatic pressure the percent charge in the UDBD model without a back door is higher than that of the other model with a back door, after 3,000 years have passed (Figure 26). Figure 29 also shows that water mainly escapes the sand from the back door if the back door has low displacement pressure.

Oil charges much faster under geopressure than under hydrostatic pressure. The oil percent charge under geopressure reaches over 40 percent within 3,000 years for all models, even if there is no back door. When the permeability of a back door is 1,000 md, it takes about 60 years to reach a 40 percent charge under geopressure, but 10,000 years to reach a 40 percent charge under hydrostatic pressure. The percent charge is over 65 percent for all models at 381,400 years because of geopressure.

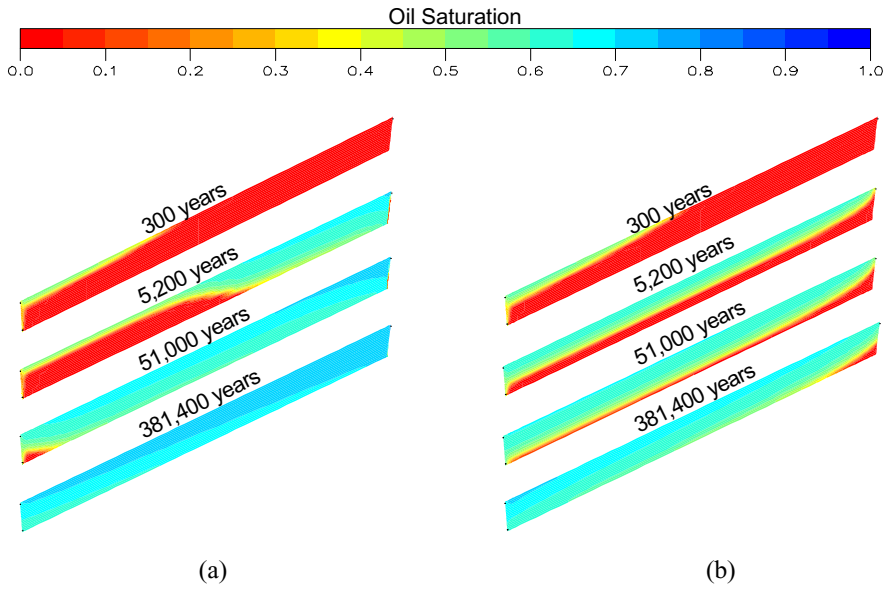

Figure 25. Oil saturation under hydrostatic pressure in UDBD models with an updip back door whose permeability is (a) 0.3 and (b) 1000 md. The permeability of a downdip charging fault is 170 md (Eclipse® figures).

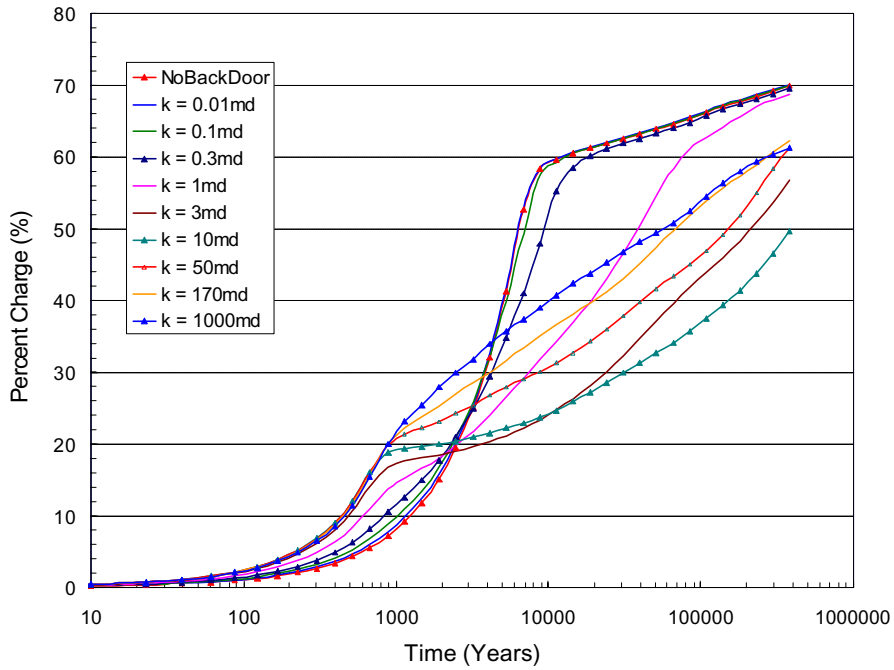

Figure 26. Percent charge under hydrostatic pressure in UDBD models with back doors. Oil charges through a downdip charging fault. The permeability of the charging fault is 170 md. The sand permeability is constantly 100 md. The shown permeabilities are the permeabilities of updip back doors (Data from Eclipse®).

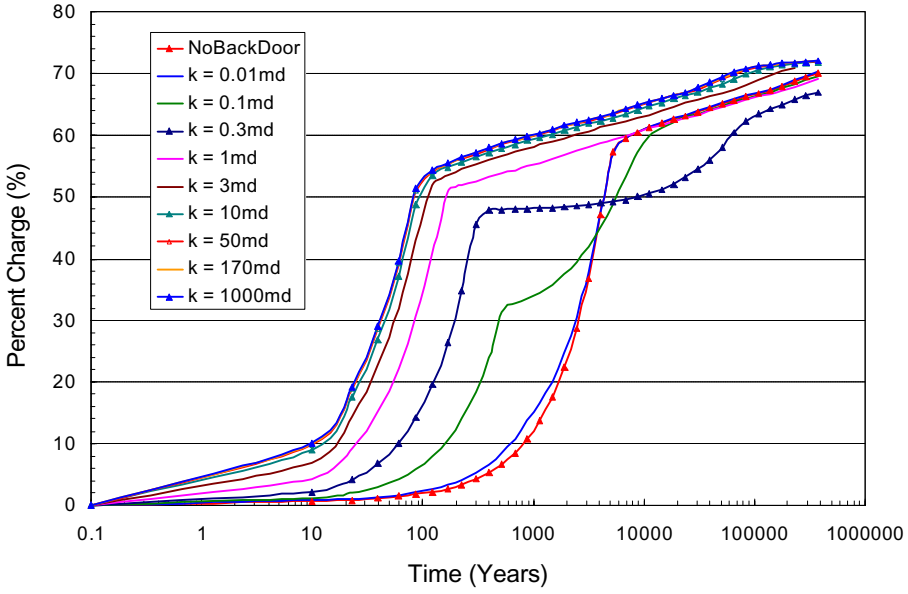

Figure 27. Percent charge under geopressure in UDBD models with back doors. Oil charges through a downdip charging fault. The permeability of the charging fault is 170 md. The sand permeability is constantly 100 md. The shown permeabilities are the permeabilities of updip back doors (Data from Eclipse®).

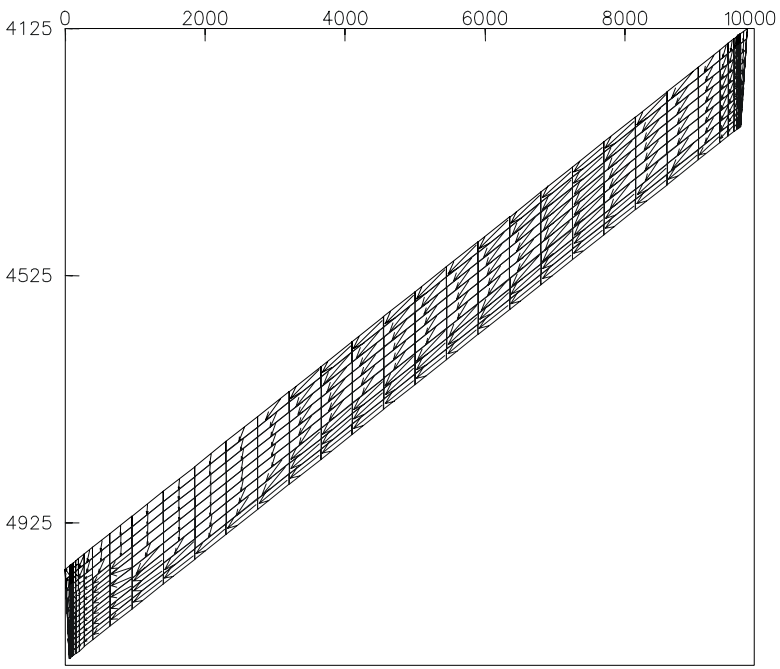

(a) No Back door

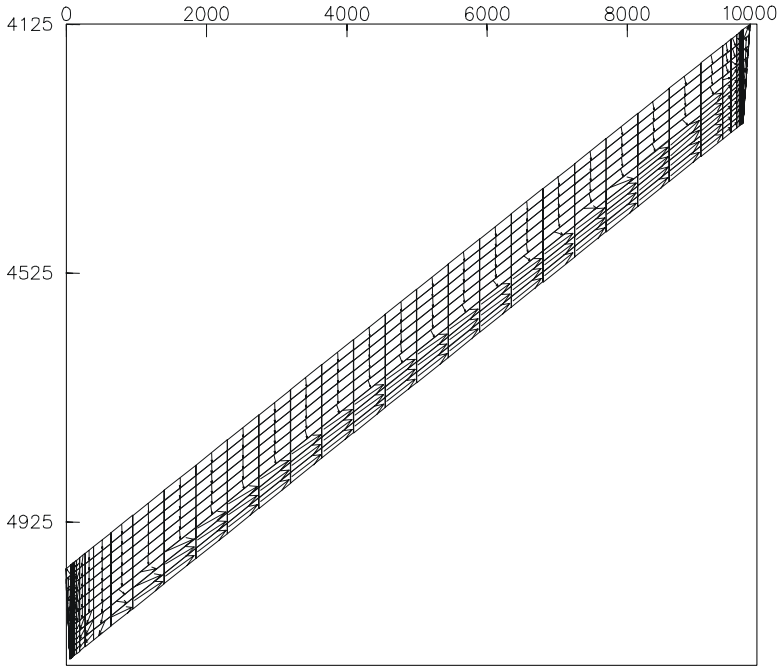

(b) Back Door

Figure 28. Water flow at 6,800 years under hydrostatic pressure in the UDBD model without (a) any updip back door and (b) with an updip back door. The downdip fault is the charging fault. The permeability of the charging fault is 170 md. The permeability of the sand is constantly 100 md. The permeability of the back door is 170 md. The length of arrays is proportional to water flow (Eclipse® figures).

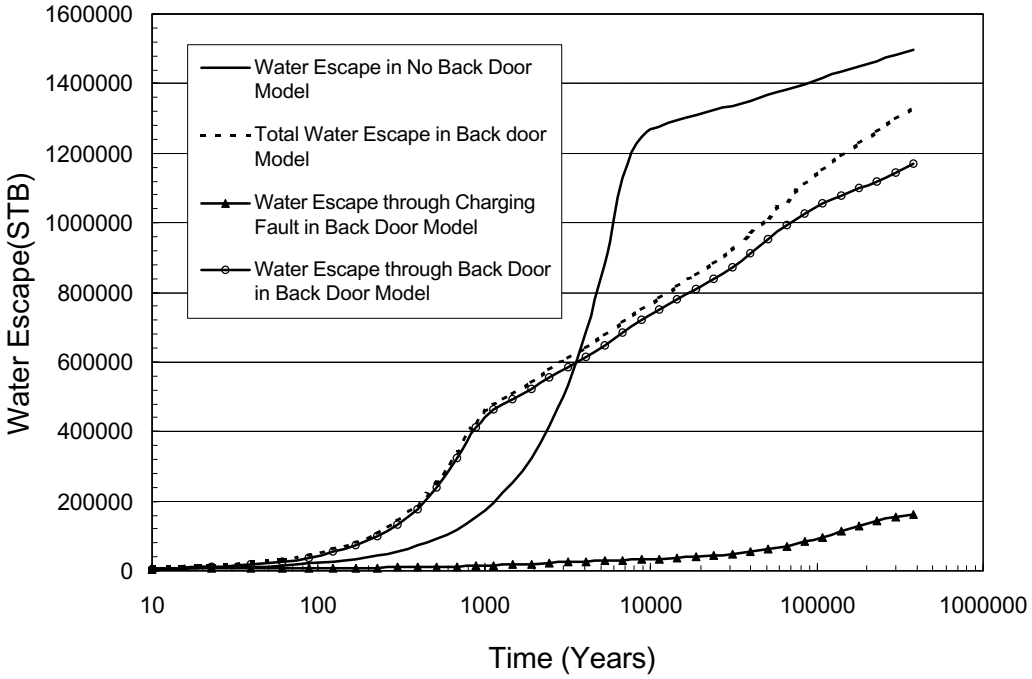

Figure 29. Water escape under hydrostatic pressure in the UDBD model both with and without an updip back door. The downdip fault is the charging fault. The permeability of the charging fault is 170 md. The permeability of the sand is constant at 100 md. If the updip back door exists, its permeability is 170 md (Data from Eclipse®).

DDBD Models: The downdip oil transportation ability of an updip fault

The downdip oil transportation ability of an updip fault is represented by a percent charge through which oil charges downdip sand. Oil charges the sand through an updip charging fault. No back door exists in this kind of models. Both oil and water are permitted to flow out of the sand only through the charging fault. The properties of the charging fault are variable. Oil saturation at 381,400 years under hydrostatic pressure is shown in Figure 30, with the updip charging fault permeabilities of 0.01 md, 1 md and 1000 md. The percent charges under hydrostatic pressure and geopressure are shown in Figures 31 and 32, respectively. All percent charges under both hydrostatic pressure and geopressure are less than 15 percent at 381,400 years, because both the buoyancy and the geopressure gradients impede the downdip oil charge.

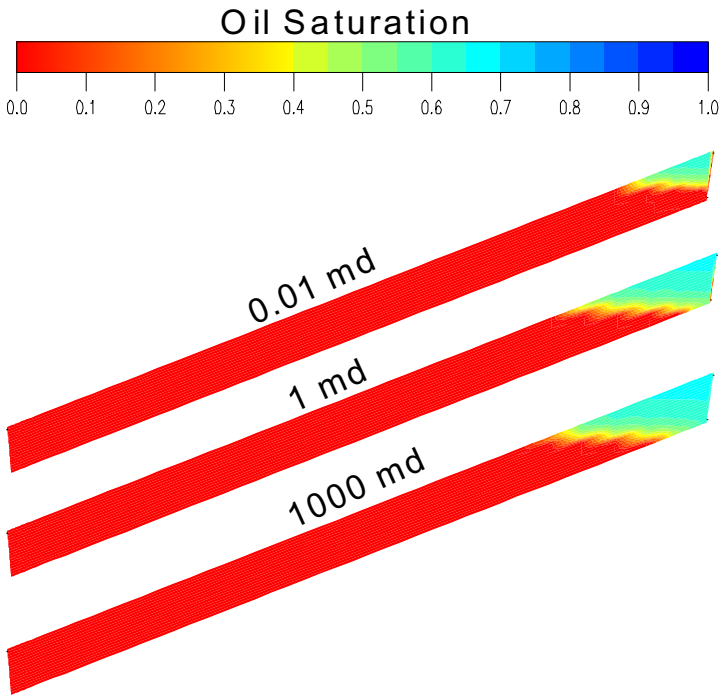

Figure 30. Oil saturation at 381,400 years under hydrostatic pressure in DDBD models without any downdip back door when the permeability of updip charging fault is 0.01 md, 1 md and 1000 md (Eclipse® figures).

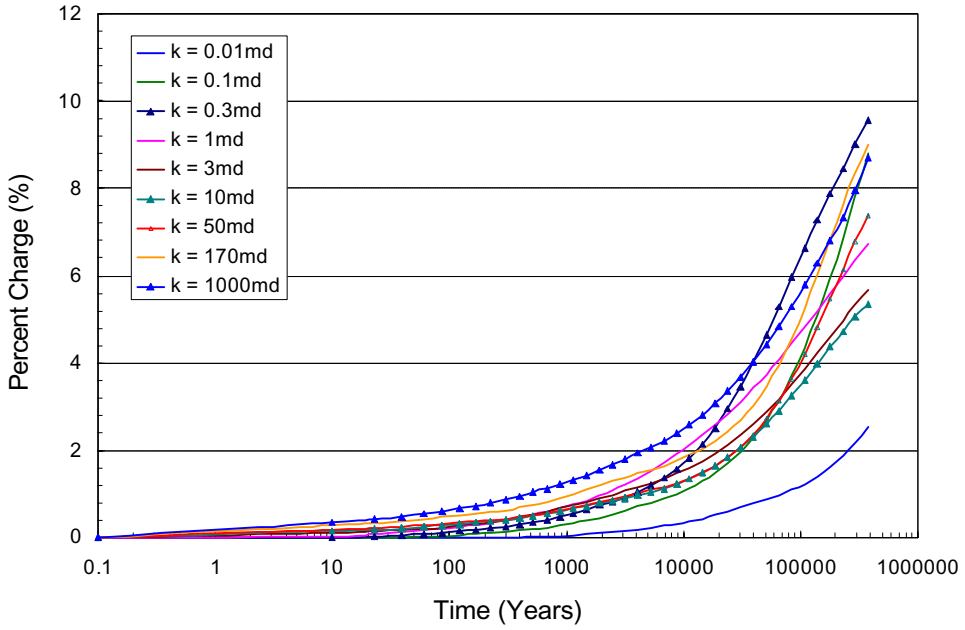

Figure 31. Percent charge under hydrostatic pressure in DDBD models without any downdip back door. Oil charges through an updip charging fault. The sand permeability is constantly 100 md. The shown permeabilities are the permeabilities of the updip charging fault (Data from Eclipse®).

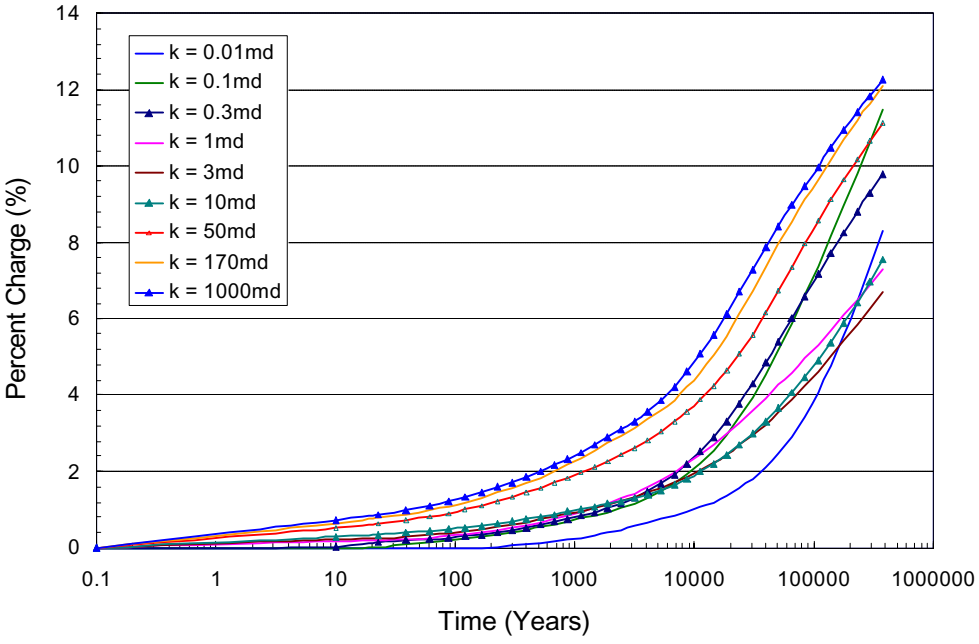

Figure 32. Percent charge under geopressure in DDBD models without any downdip back door. Oil charges through an updip charging fault. The sand permeability is constantly 100 md. The shown permeabilities are the permeabilities of the updip charging fault (Data from Eclipse®).

DDBD Models: Downdip oil charge efficiency with the aid of downdip back doors

Oil charges sand along an updip charging fault. Both oil and water are permitted to escape along a charging fault. The charging fault has constant properties, with the value of permeability being 170 md in all models. The downdip fault acts as a back door with variable properties. The percent charges under both hydrostatic pressure and geopressure are shown in Figures 33 and 34. Both the negative buoyancy gradient and the negative geopressure gradient between the updip charging fault and downdip back door impede the downdip oil charge. Therefore, the percent charges for most models under both hydrostatic pressure and geopressure are generally less than 15 percent, similar to the results obtained from the DDBD models without any downdip back door. However, the percent charge under hydrostatic pressure is over 20 percent when the permeability of the downdip back door is between 0.01 md and 0.3 md. The percent charge can be as high as 70 percent when the permeability of the downdip back door is 0.01 md. In contrast to the results obtained from the UDBD models with updip back doors, the higher the displacement pressure of the downdip back door, the higher the percent charge under hydrostatic pressure when the permeability of the downdip back door ranges from 0.01 md to 0.3 md as shown in Figure 33. Under geopressure, the same percent charge is obtained at any time for all models because geopressure and the properties of the charging fault determine the downdip oil charge behavior. The downdip back door has few effects on the downdip oil charge when under geopressure.

Communication models

So far, simulation results have shown the behavior of oil charges in very simple geological structures, and have demonstrated that updip back doors do facilitate an updip oil charge. In theory, a barrier generally impedes oil migration. For this section, communication models were constructed in order to investigate whether or not an updip back door might facilitate oil penetration of a barrier in order to charge updip sands.

This communication model has two faults: a downdip fault that is a charging fault, and an updip fault that is a back door. It also has two reservoirs separated by a central barrier. The permeability of the charging fault is considered constant at 170 md. The properties of the central barrier and the updip back door are considered to be variable.

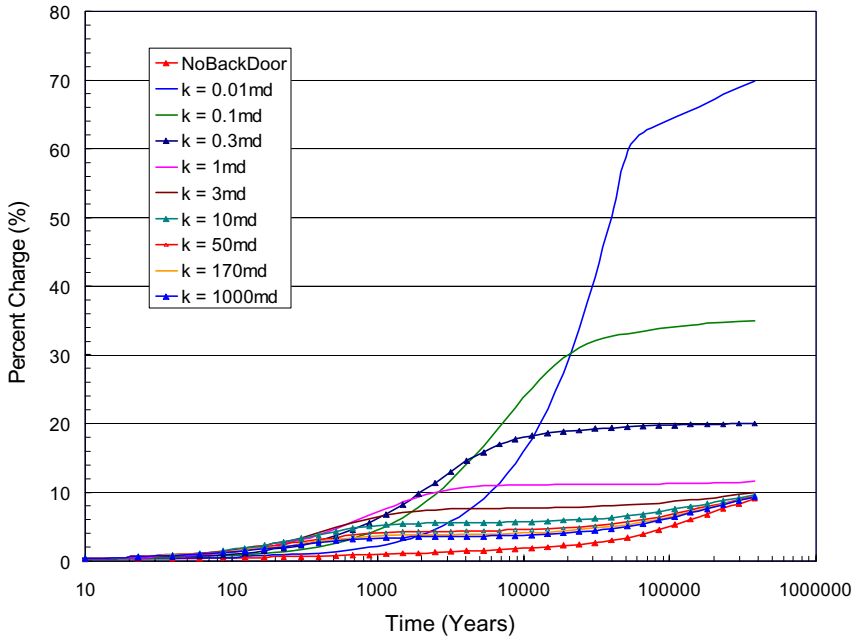

Figure 33. Percent charge under hydrostatic pressure in DDBD models with a downdip back door. Oil charges through an updip charging fault. The sand permeability is constantly 100 md. The permeability of the charging fault is constantly 170 md. The shown permeabilities are the permeability of the back door (Data from Eclipse®).

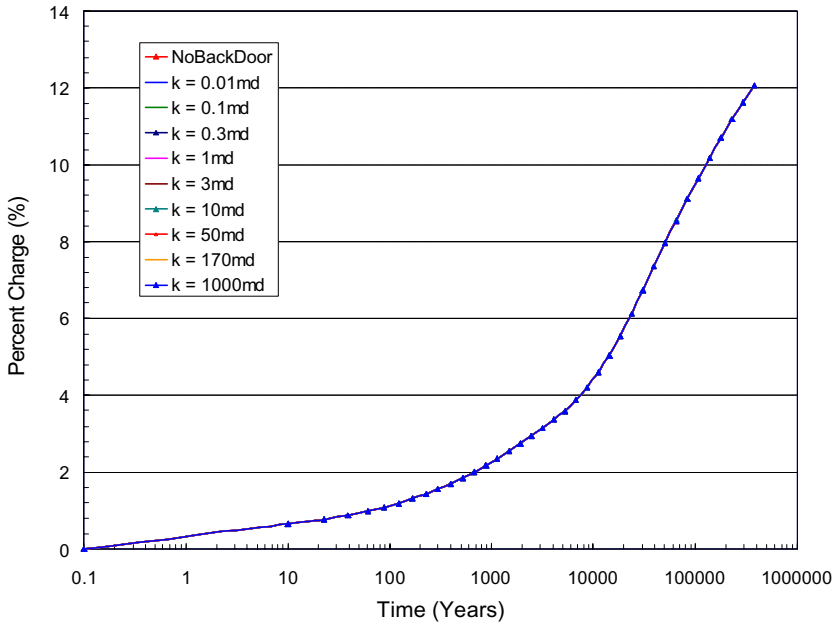

Figure 34. Percent charge under geopressure in DDBD models with a downdip back door. Oil charges through an updip charging fault. The sand permeability is constantly 100 md. The permeability of the charging fault is constantly 170 md. The shown permeabilities are the permeability of the back door (Data from Eclipse®).

The permeability of the central barrier was first set at 0.01 md, so its displacement pressure was very high, 214 psi. Oil saturation under hydrostatic pressure at 300 years, 3,200 years and 381,400 years when no updip back door exists and when the permeability of the updip back door is 0.01md and 170md is shown in Figure 35. The percent charge under hydrostatic pressure is shown in Figure 36. If there is no updip back door, no oil will charge the updip reservoir until 381,400 years. When the permeability of the barrier is 0.01 md, some oil will charge the updip reservoir after 381,400 years. Continuing to increase the permeability of the updip back door shows that when the permeability is 170 md, no oil charges the updip back door either. Obviously, oil penetrates the barrier fault under hydrostatic pressure only when the permeability of the updip back door is 0.01 md. The same properties shared by the updip back door and the central barrier could result in oil penetration. This oil penetration would result in a higher percent charge after 381,400 years if the updip back door and the central barrier have the same properties as shown in Figures 35 and 36. This, however, is a very special case.

Continuing to increase the permeability of the central barrier under hydrostatic pressure shows that when the permeability is 0.1 md, its displacement pressure is still high, 55 psi. Oil saturation at 300 years, 51,000 years, and 381,400 years when there is no updip back door and when the permeability of the updip back door is 0.1 md is shown in Figure 37. Figure 38 shows oil saturation at 381,400 years when the permeability of the updip back door is 1, 10 and 170 md. Obviously, if there is no updip back door, no oil can charge the updip reservoir. If there is an updip back door, oil will definitely charge the updip reservoir. The updip back door provides a routine for water escaping to make room for the oil charge in the updip reservoir. When the permeability of the updip back door is high, the back door also provides an easy way for oil to escape from the reservoir.

When the permeability of the updip back door is 3 md, its displacement is only 7.8 psi. Oil saturation at 381,400 years under hydrostatic pressure when there is not the updip back door and the permeability of the updip back door is 1, 10 and 170 md is shown in Figure 39. Oil can charge the updip reservoir under hydrostatic pressure even though there is no updip back door. Oil certainly charges the updip reservoir if the updip reservoir exists. Therefore, when the displacement pressure of the barrier is low, it can not act as an efficacious barrier even under hydrostatic pressure.

Geopressure facilitates an updip oil charge. The communication model simulates oil migration under geopressure. The geopressure gradient is 1.118 psi/ft within the geopressure zone where rocks cannot generate fractures because geopressure is always much less than the corresponding lithostatic pressure at the same depths within the geopressure zone. The oil saturation under geopressure at 300 years, 3,100 years and 381,400 years when the permeability of the central barrier is 0.01 md is shown in Figure 40. The percent charge when no updip backdoor exists and when the permeability of the updip back door is 0.01, 0.1, 0.3, 1, 3, 10, 50, 170 and 1000 md is shown in Figure 41. Figure 40 indicates that if an updip back door does not exist, oil cannot penetrate the barrier, but back doors mean oil penetration and a charged updip reservoir. Both Figures 40 and 41 demonstrate that the lower the displacement pressure of the updip back door, the more efficient the updip oil under geopressure. Simulation results in the communication models under both hydrostatic pressure and geopressure were nearly the same with no back door and when the permeability of the barrier was 0.01 md.

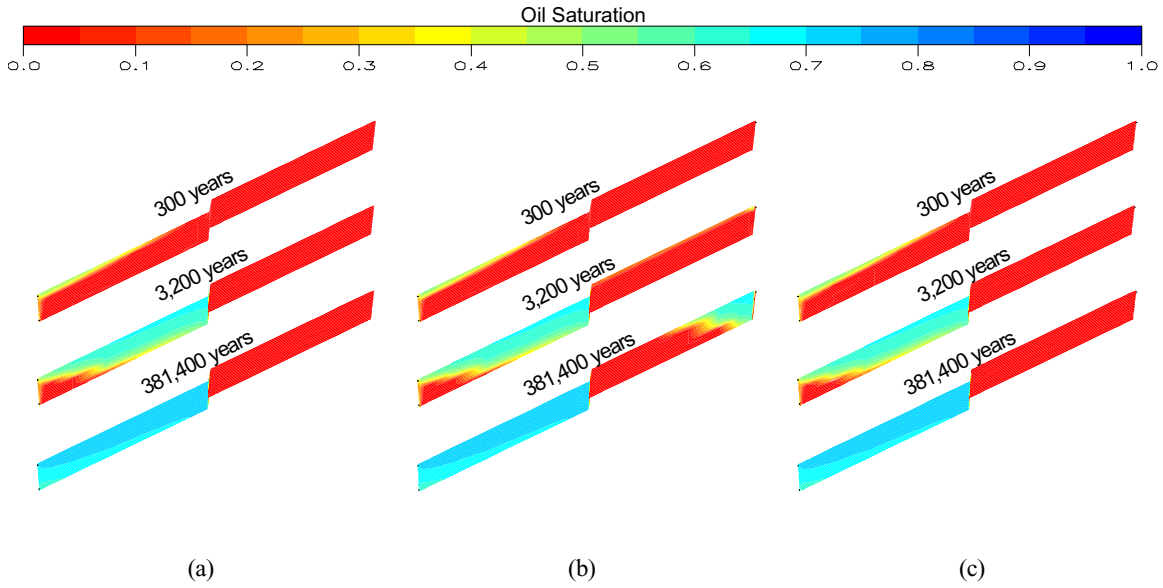

Figure 35. Oil saturation under hydrostatic pressure in communication models when (a) no updip back door exists and the permeability of the updip fault is (b) 0.01 md or (c) 170 md. The charging fault is the downdip fault. The central fault is a barrier fault. The updip fault is a back door. The permeabilities of reservoir sand, the charging fault and the barrier fault are 100 md, 170 md and 0.01 md, respectively (Eclipse® figures).

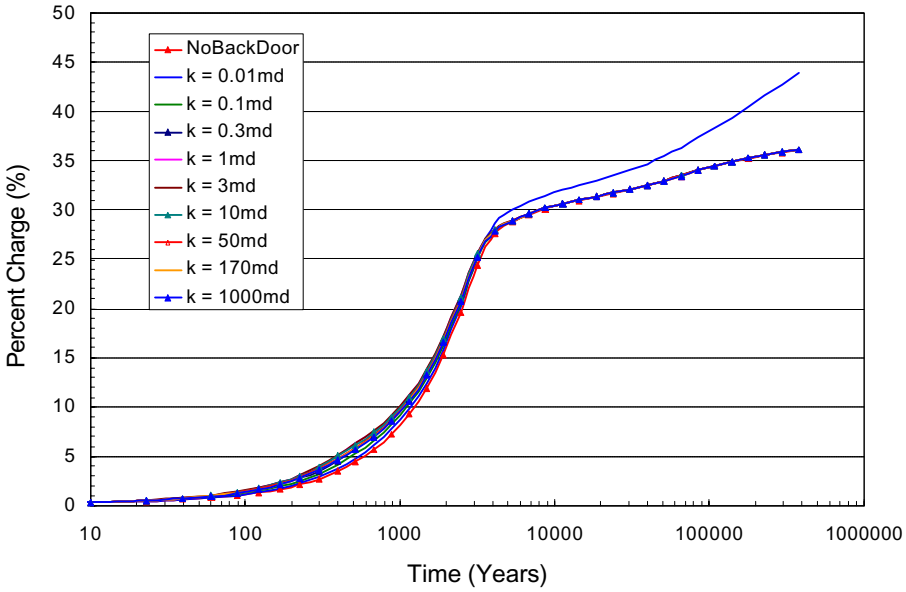

Figure 36. Percent charge under hydrostatic pressure in communication models without and with updip back doors. The charging fault is the downdip fault. The central fault is a barrier fault. The permeabilities of reservoir sand, the charging fault and the barrier fault are 100 md, 170 md and 0.01 md. The shown permeabilities are the permeabilities of the updip back door (Data from Eclipse®).

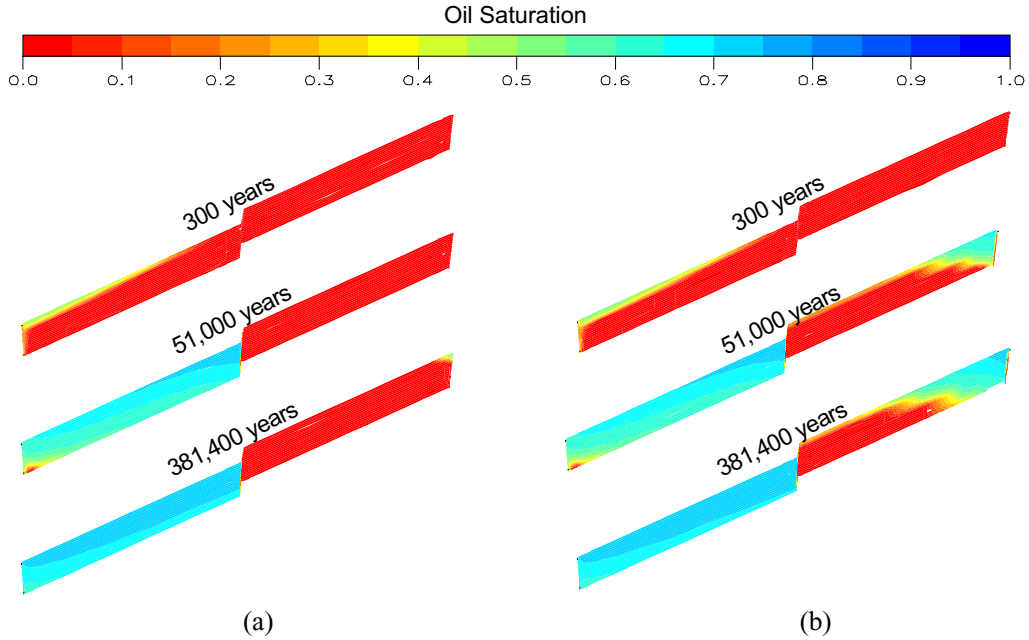

Figure 37. Oil saturation under hydrostatic pressure in communication models when (a) no updip back door exists and (b) the permeability of the updip fault is 0.1 md. The permeabilities of reservoir sand, charging fault and central barrier are 100 md, 170 md and 0.1 md, respectively (Eclipse® figures).

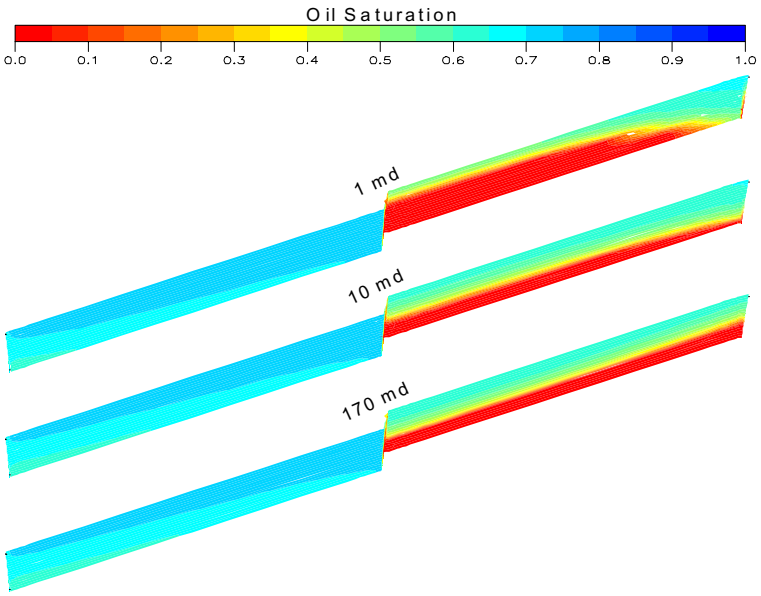

Figure 38. Oil saturation under hydrostatic pressure in communication models when the permeability of the updip fault is 1 md, 10 md and 170 md. The permeabilities of reservoir sand, charging fault and central barrier are 100 md, 170 md and 0.1 md, respectively (Eclipse® figures).

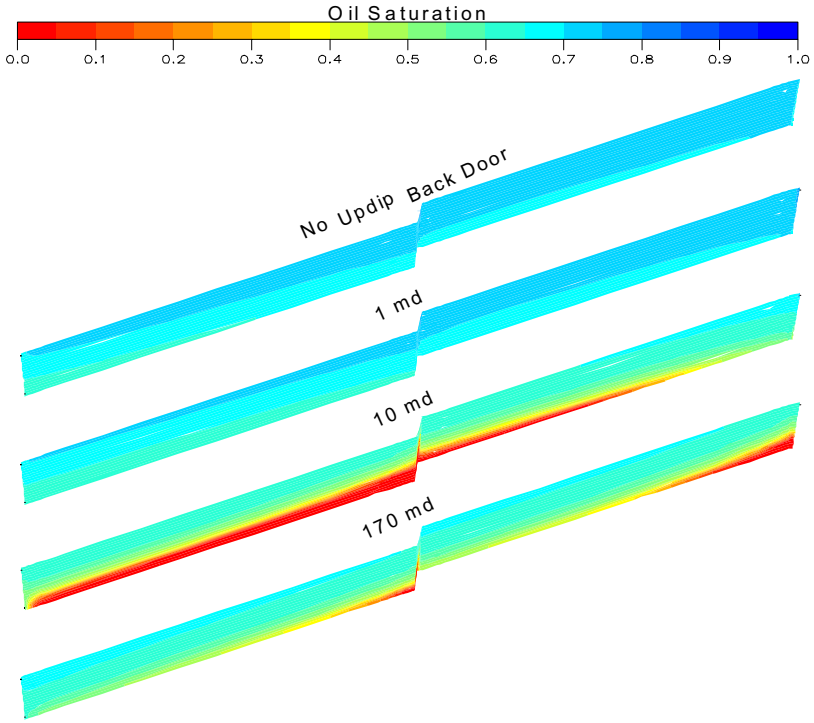

Figure 39. Oil saturation under hydrostatic pressure in communication models when there is not the updip back door and the permeability of the updip fault is 1 md, 10 md and 170 md. The permeabilities of reservoir sand, charging fault and central barrier are 100 md, 170 md and 3 md, respectively (Eclipse® figures).

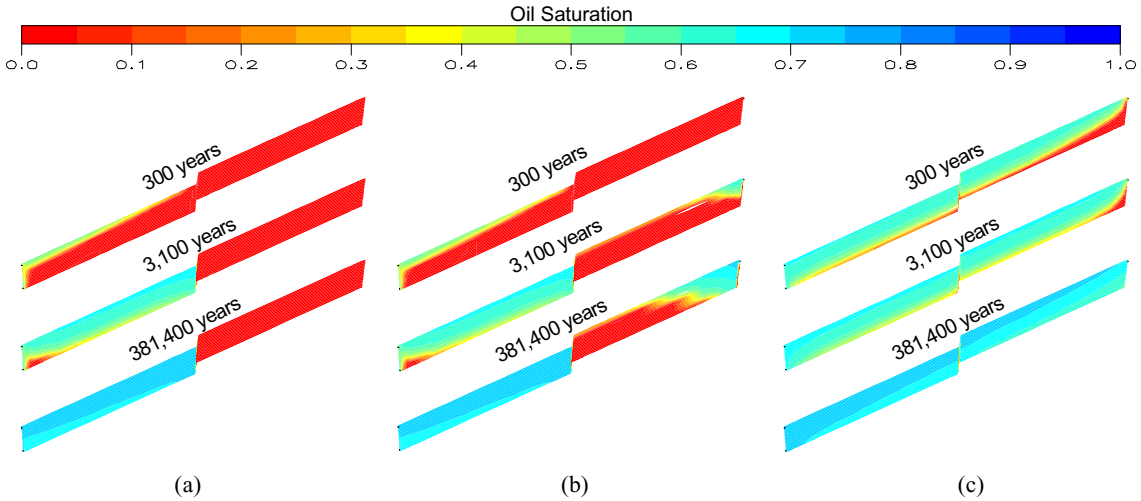

Figure 40. Oil saturation under geopressure in communication models when (a) no back door updip exists and the permeability of the updip back door is (b) 0.01 md or (c) 10 md. The permeabilities of reservoir sand, the charging fault and the central barrier are 100 md, 170 md and 0.01 md, respectively (Eclipse® figures).

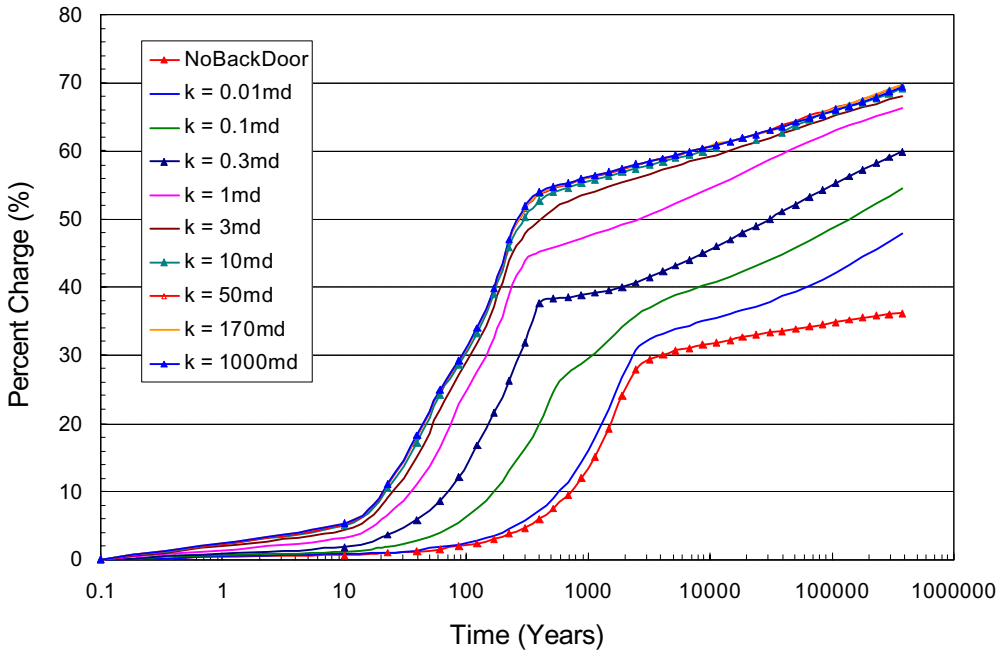

Figure 41. Percent charge under geopressure in communication models without and with the updip back doors. The permeabilities of reservoir sand, the charging fault and the central barrier are 100 md, 170 md and 0.01 md, respectively. The shown permeabilities are the permeabilities of the updip back door (Data from Eclipse®).

DISCUSSION

Simulation results indicate that charge time is a critical factor affecting the percent charge. In this study, continuous oil charging was assumed to last 381,400 years. Although the oil charge might not be continuous, total charge time can practically be assumed to last to up to hundred thousand years. For example, hydrocarbon charges lasted 250,000 years in the Ship Shoal 274/293 field. Simulations have shown that within 1,000 years, those UDBD models with an updip back door under hydrostatic pressure, UDBD models without a back door, and almost all DDBD models had less than a 20 percent charge, except those UDBD models with updip back doors under geopressure. A commercial oil accumulation has a percent charge of at least 20 percent. Therefore, if total charge time is too short, commercial oil accumulation should not be expected. Simulations indicate that the total charge time should be at least 10,000 years for commercial oil accumulation under hydrostatic pressure.

Under hydrostatic pressure, the updip oil transportation ability of a charging fault through which oil can charge an updip sand is determined by the properties of the charging fault. The lower the displacement pressure of the downdip charging fault, the higher its updip oil transportation ability. In contrast, the properties of a charging fault have minimal effects on its downdip oil transportation because both the negative buoyancy gradient and the negative geopressure gradient impede any downdip oil charge.

An updip back door generally improves updip oil charge efficiency. The lower the displacement pressure of an updip back door, the more efficient its updip oil charge. However, the lower the displacement pressure of an updip back door, the easier it is for oil to escape, thus causing a lower percent charge than that resulting in models where the displacement pressure of the back door is made higher, if the charging time is long enough. A downdip back door has a limited effect on its downdip oil charge because the negative buoyancy gradient between the downdip back door and an updip charging fault always impedes the downdip oil charge. However, simulations indicate that a downdip backdoor might have a “charging window” under hydrostatic pressure. Only when the properties of the downdip back door lie within the range of this charging window can the downdip back door improve a downdip oil charge. Within this charge window, the higher the displacement pressure of the downdip fault, the more efficient the downdip oil charge. In this charging window the permeability of the downdip back door will be between 0.01 md

and 0.3 md and the corresponding displacement pressure of the downdip back door will range from 28 psi to 214 psi when the permeability of the updip charging fault is 170 md.

Geopressure exists. Evidence which includes temperature, pressure, salinity anomalies, mud volcanoes, biotic communities and active venting sites all supports the theory that the expulsion of hydrocarbons from source rocks within some geopressured zones is mainly focused along faults in the northern Gulf of Mexico (Nunn, 1996; Roberts and Nunn, 1996; Kim, 1998; and Kulander, 1998). Geopressure generally enhances an updip oil transportation ability of a fault and updip oil charge because geopressure acts with the buoyancy. On the other hand, because the geopressure gradient between a downdip back door and an updip charging fault must be negative, geopressure will impede the downdip oil transportation ability of a fault and downdip oil charge even though a downdip back door charging window exists under hydrostatic pressure.

Reservoir sands are often separated by barriers. Simulations in the communication models show that if the displacement pressure of a barrier is less than or equal to 7.8 psi, oil can penetrate the barrier to charge the updip sand under hydrostatic pressure, both with or without an updip back door. If the displacement of the barrier is 55 psi, oil can charge the updip reservoir under hydrostatic pressure only when an updip back door exists. Only when the displacement pressure of a barrier is high enough, for example 214 psi, can the barrier act as a true prohibitor of oil migration under hydrostatic pressure. In this case, an updip back door cannot help oil penetrate a barrier under hydrostatic pressure, except when a central barrier and an updip back door have the same properties. In that case, however, the improvement of an oil percent charge is very limited as shown in Figure 36. On the contrary, an updip back door facilitates oil penetration of a central barrier under geopressure, and hence greatly improves an oil charge. Meanwhile, similar to the results of the updip back door obtained from the UDBD models, the lower the displacement pressure of an updip back door, the more efficient an oil charge. Oil penetration in communication models under geopressure results from two reasons. Geopressure facilitates oil penetration and an updip back door provides a routine for water escape, thus causing a reduced differential of capillary pressures between juxtaposed sands or fault-zone materials to initial the oil penetration.

Therefore, in a two-phase (oil and water) system, patterns of oil charge can be affected by four factors: charge time, the oil transportation ability of charging faults, back doors, and geopressure. The charge time

must be long enough and the updip oil transportation ability of a charging fault must be large enough. In addition, both updip back doors and geopressure enhance an updip oil charge.

SUMMARY

Oil charge of fault-compartmentalized sand intervals simultaneously separated by impermeable shale is affected by four factors: charge time, the oil transportation ability of charging faults, back doors and geopressure. The charging time must be long enough to result in commercial oil accumulations in oil-water systems under hydrostatic pressure, according to my data, at least 10,000 years.

The updip oil transportation ability of a fault is determined by the properties of that fault. The lower the displacement pressure of the fault, the higher its updip oil transportation ability is. On the contrary, the downdip oil transportation ability of a fault is generally lower and does not result in commercial downdip oil accumulations.

Updip back doors generally improve an updip oil charge. Moreover, the lower the displacement pressure of an updip back door, the more efficient the updip oil charge. In contrast to the common role of an updip back door during an updip oil charge, downdip back doors generally have few effects on a downdip oil charge.

Geopressure enhances the updip oil transportation of a fault, and improves the positive effects of updip back doors on updip oil charges. Geopressure and updip back doors usually result in a more efficient updip oil charge. A physical barrier may not be a barrier to oil migration with the aid of geopressure and updip back doors.

CHAPTER V

MIGRATION PATHWAYS IN OIL-WATER SYSTEMS

This chapter is mainly concerned with how faults control oil migration in oil-water systems when oil actively charges in stacked fault-compartmentalized reservoirs. More complex numerical models are constructed here than those models in chapter III. First examined was how faults affect oil migration pathways in geological structures when two fault-bounded reservoirs are separated by impermeable shale. Second, oil charges in stacked fault-bounded reservoirs through growth faults were investigated under both hydrostatic pressure and geopressure. Finally, interreservoir migration, an important mechanism for oil accumulation and trap identification, is simulated in these geological structures.

INTRODUCTION

In chapter III, how charging faults, back door faults and pressure distribution affect oil migration and entrapment in faulted structures was investigated. Besides these factors, geological structures can also have great influences on oil migration and remigration since geological structures are usually complex. For example, hydrocarbon migration and remigration in the Ship Shoal 274/293 and the South Eugene Island 330 fields (Nunn, 1996; and Roberts and Nunn, 1996) were mainly prompted by growth faults. Crude oil found in individual sand intervals, driven from a single source system within geopressure zones, resulted from multiple phases of hydrocarbon migration and remigration in the Ship Shoal 274/293 field. Observations from the Ship Shoal 274/293 field suggested that the presentation of antithetic faults insure hydrocarbon charge, probably because migration and remigration along these faults were more likely to result in hydrocarbon migration due to geometric relationship between faults and reservoirs. Therefore, how geological structures affect hydrocarbon migration and remigration should be further studied, based on the results of investigation conducted for Chapter III. This chapter mainly deals with two specific goals:

The first goal is to understand how geological structures affect oil migration pathways during an active oil charge. More complex numerical models with at least stacked fault-bounded reservoirs were built to accomplish the goal. The most complex numerical models were ones with growth faults. By changing the

properties of bounding faults, fluid flow in these models indicated how faults affect hydrocarbon migration pathways in faulted structures.

The second goal concerns interreservoir migration when an oil source dries up. Interreservoir migration, one kind of hydrocarbon remigration, is hydrocarbon migration from lower reservoirs to upper reservoirs through bounding faults in stacked fault-compartmentalized reservoirs without oil supply. Interreservoir migration is an important mechanism for oil accumulation and trap identification. Numerical simulations demonstrate that anomalously high oil column heights are generally maintained in stacked fault-compartmentalized reservoirs during an active oil charge. The anomalously high oil column heights could cause interreservoir migration after an oil supply stops. Therefore, it is necessary to investigate interreservoir migration without oil supply.

SIMULATION MODELS

As in the previous chapter, the permeability of reservoirs is considered constant at 100 md, and faults at 0.3 ft wide. The permeabilities of the charging faults in this study could be 0.1 md, 10 md, or 170 md, and the permeabilities of the backdoor faults could be 1 md, 10 md, 50 md or 1000 md.

Model 1

This kind of model consists of a porous and permeable dipping reservoir above a impermeable dipping shale, both above a second porous and permeable dipping reservoir bounded by faults at either end as shown in Figure 42. The left-end fault is antithetic to the dipping sands, while the right-end fault is synthetic to the dipping sands. Black oil is allowed to charge the sands through the left-end fault. The right-end fault acts as an updip back door. Permeable sands juxtaposed against impermeable shale are simulated in this kind of models. The dip angles of the two sands and the shale in this numerical model are all 5° as shown in Figure 42. The dip angle of the left-end fault is 70°, antithetic to the sands. The dip angle of the right-end fault is 60°, synthetic to the sands. The thickness of the two sands is 70 ft. The thickness of the shale is only 10 ft. An injection well and two production wells are both introduced into this numerical model. Black oil is allowed to enter into the reservoir through the injection well, and in this numerical model any fluid can flow out of the reservoir through the production well. $P_{injector}$ is the bottom hole pressure of the injection well in this numerical model. P_d and P_u are the bottom hole pressures of the

production wells located in the charging fault and back door, respectively. Constant well bottom hole pressures, $P_{injector}$, P_d and P_u, are maintained as boundary conditions in the numerical models. In order to guarantee that oil injected from the charging fault and the fluids (both water and oil) escape from the charging fault and the back door, $P_{injector}$ is kept 5 psi higher than the initial pressure of the cell where the injection well is connected. At the same time, P_d and P_u are kept 10 psi lower than the initial pressures of cells where they are connected.

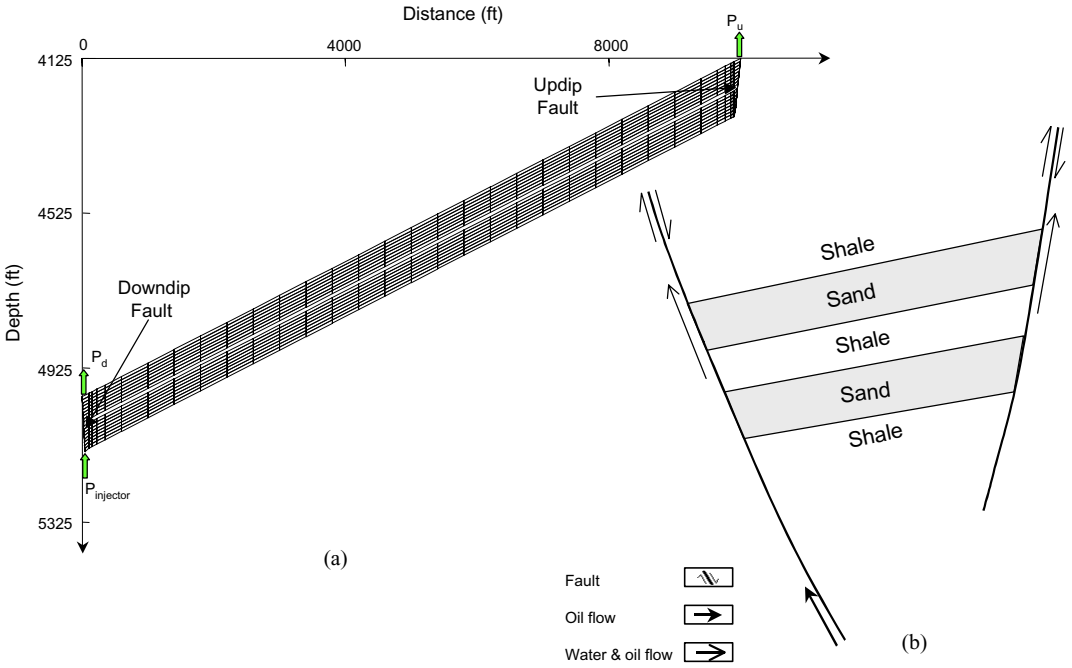

Figure 42. Model 1: (a) numerical model and (b) conceptual model. Two sands separated by impermeable shale are bounded by two faults. The left-end fault is a charging fault. The right-end fault is a back door. The dip angles of the sands are 5°. The charging fault dips 70°, antithetic to the sands. The back door dips 60°, synthetic to the sands.

Model 2

The conceptual and numerical models correspond to the kind of the models shown in Figure 43. The geological structure of these kinds of models is the same as the structure of Model 1, except that the right-

end fault is the charging fault and the left-end fault is a back door. Constant well bottom hole pressures, $P_{injector}$, P_d and P_u, are also maintained as boundary conditions in this numerical model, as in Model 1. Permeable sands juxtaposed against impermeable shale are continuously simulated in both of these kinds of models.

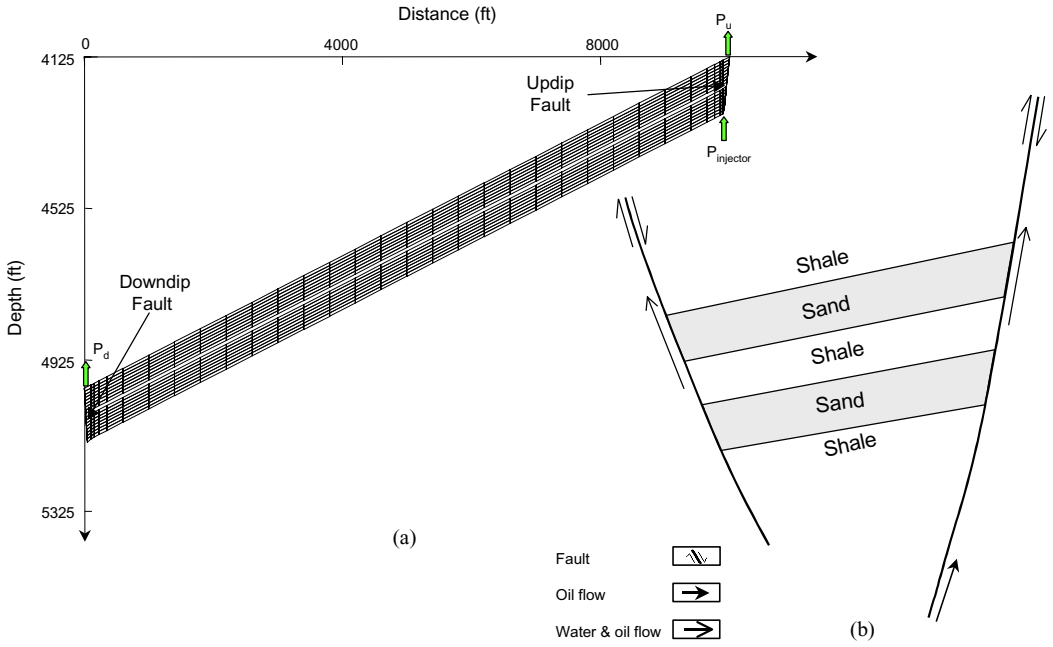

Figure 43. Model 2: (a) numerical model and (b) conceptual model. Two sands separated by impermeable shale are bounded by two faults. The left-end fault is a back door. The right-end fault is a charging fault. The dip angles of the sands are 5°. The charging fault dips 60°, antithetic to the sands. The back door dips 70°, synthetic to the sands.

Model 3

Here, an impermeable dipping shale lies between two porous and permeable dipping reservoirs, bounded by faults at either end as shown in Figure 44. They are offset by a central fault. The throw along this central fault is 30 ft. and this central fault is a charging fault. The left-end fault is a downdip back door, and the right-end fault acts as an updip back door. Black oil is allowed to enter into the reservoir through the charging fault. Fluid can flow out of the sand through the charging fault and through both back doors. The dip angles of the two sands and the shale in this numerical model are all 5° as shown in Figure 44. The dip angle of the charging fault is 68°, synthetic to the dipping sands. The dip angle of the downdip back door is

70°, antithetic to the sands. The dip angle of the updip back door is 60°, synthetic to the sands. An additional production well connected to the charging fault is added to allow fluids to flow out of the sands. P_c is the bottom hole pressure of the production well located in the charging fault. $P_{injector}$, P_c, P_d and P_u are maintained as constant pressures in this numerical model. $P_{injector}$ is kept 5 psi higher than the initial pressure of the cell where the injection well is connected, while P_c, P_d and P_u are kept 10 psi lower than the initial pressures of cells where they are connected, respectively.

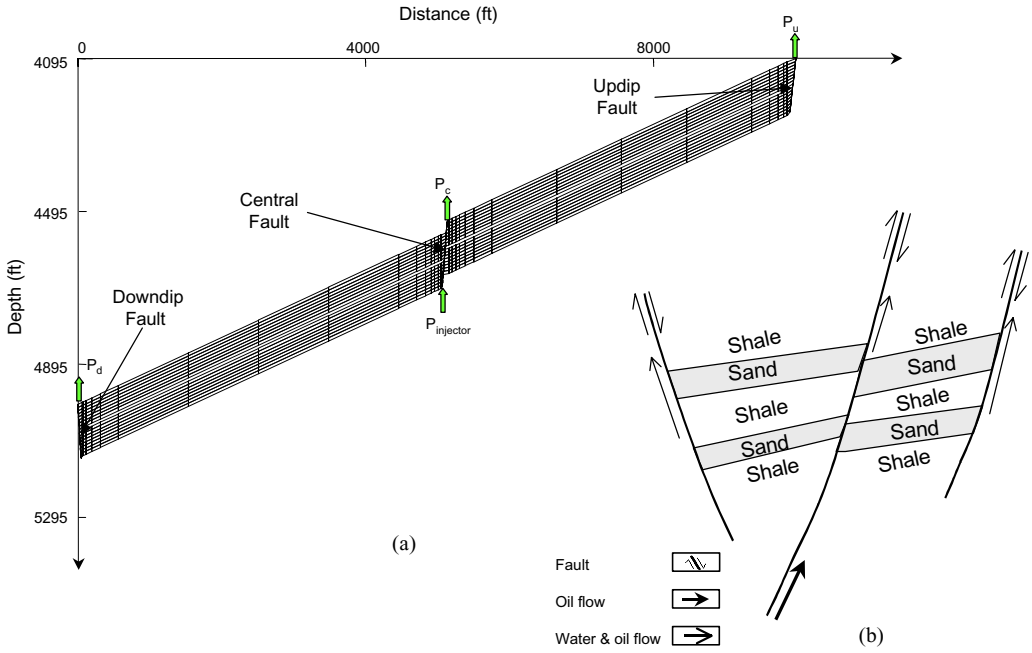

Figure 44. Model 3: (a) numerical model and (b) conceptual model. Two sands separated by impermeable shale are bounded by faults. The left-end fault is a downdip back door. The right-end fault is an updip back door. The central fault is a charging fault. The dip angles of the sands are 5°. The downdip back door dips 60°, antithetic to the sands. The charging fault dips 68°, synthetic to the sands. The updip back door dips 70°, synthetic to the sands. The thrown along the central fault in the numerical model is 30 ft.

Growth fault model

The numerical growth fault model where sands are separated by shale is shown in Figure 45. Both sand A and sand X are bounded by a downdip fault and an antithetic fault. Sand B, sand Y and sand V are

bounded by an antithetic fault and a synthetic fault. A synthetic fault and an updip fault are bounding sands C and Z. Both sand U and sand W are bounded by only one fault, the former bounded by an antithetic fault and the later by a synthetic fault. Oil charges reservoirs through the growth fault and any fluid (either water or oil) can flow out of the reservoir through that same growth fault shown in Figure 45. No fluids can flow out of the reservoirs either through the downdip or updip faults.

As a sequence, oil can charge both sand U and sand W, and fluids can flow out of them only through the antithetic or synthetic fault, respectively. Oil can charge sands B, Y and V, and any fluid can flow out of them through the synthetic fault and the antithetic fault. Sand X and sand Z can be charged by oil only through the antithetic fault and the synthetic fault, respectively. However, any fluid can flow out of sand X and sand Z through these two faults. Oil can charge sand A and sand C through the two faults, but any fluid can flow out of them only through a fault.

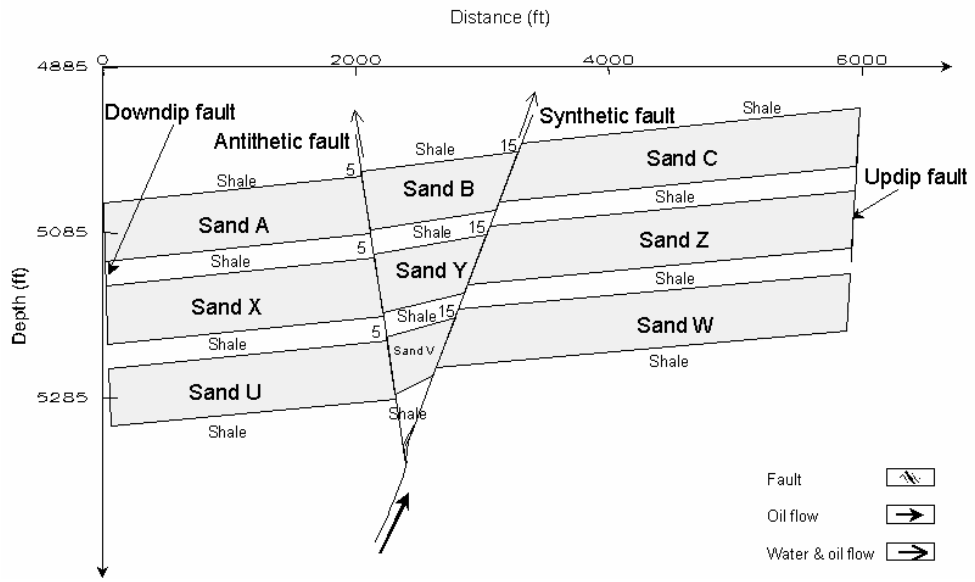

Figure 45. Growth fault model. Reservoir sands are 70 ft thick and shale is 30 ft thick. The reservoir sands and shale are 1° dipping. The downdip fault is 78° dipping, antithetic to the sands. The antithetic fault is dipping 45°, antithetic to sands. The synthetic fault and the updip fault are synthetic to sands, dipping 21° and 69°, respectively. Selected throw shown in feet.

For simplicity and the purpose of describing the effects of growth faults on oil migration, the properties of the downdip and updip faults are the same. Their permeabilities are considered to be constant at 10 md

in all growth fault models. $P_{injector}$, P_d and P_u are maintained at constant pressures in this numerical model, as before.

SIMULATION RESULTS

Migration

Black oil was allowed to continuously enter into reservoirs through the charging fault. The oil transportation ability of the charging fault was determined by its properties. The higher the displacement pressure of the charging fault, the lower its oil transportation ability. Updip back doors facilitated water escape from the sands in order to make room for an oil charge. How the back doors affect hydrocarbon migration depends upon their properties. On the one hand, the lower the displacement of a back door, the easier it is for water to escape from a reservoir through that back door. On the other hand, the lower the displacement of a back door, the easier it is for oil to flow out of a reservoir through an updip back door.

Migration: Model 1

The permeability of the charging fault was first considered to be 170 md. The permeability of the updip back door is kept variable. The time-dependent oil saturation under hydrostatic pressure is shown in Figure 46. Since the oil transportation ability of the charging fault is high and its displacement pressure is lower than the displacement pressure of the reservoir, oil flows along the charging fault and charges both reservoirs. When the permeability of the updip back door is 1 md, the back door actually acts as a barrier to oil migration. Water cannot easily escape from these reservoirs to make room for an oil charge, thus causing a slow oil charge within 5,000 years as shown in Figure 47. After 5,000 years, oil accumulates in the upper part of the two sands, causing a higher oil charge percent shown in Figures 46 and 47. When the permeability of the back door is 50 md or 1000 md, the back door provides a routine for water escape, thus resulting in a faster oil charge. However, since the back door has nearly no seal capacity to retain oil, oil also flows out of the sands through the back door, thus causing a low percent charge after 5,000 years, as compared to the percent charge when the permeability of the back door is 1 md.

When the permeability of the charging fault is 10 md, the oil transportation ability of the charging fault is lower and its displacement pressure higher, as compared to a charging fault whose permeability is 170 md. The charging fault generally causes a lower percent charge under hydrostatic pressure as shown in Figure

47. When the permeability of an updip back door is 1 md and the back door has a high displacement pressure, oil first charges and accumulates in the lower sand, and then charges the upper sand since water cannot easily escape from the back door shown in Figure 48. When the permeability of a back door is 50 md or 1000 md, the upper sand is bypassed by the oil shown in Figure 48. The charging fault, the lower reservoir and the updip back door comprise a routine for oil migration. Because the displacement pressure is low when the permeability of a back door is 50 md or 1000 md, only a little oil can be retained in these reservoirs shown in Figure 48.

Geopressure may exist. Simulation results show that geopressure has the following effects on oil migration. First, geopressure results in a faster oil charge and higher percent charge shown in Figures 49 and 50. Second, oil always migrates into both the upper and lower reservoirs if the charge time is long enough. Finally, when the permeability of an updip back door is 1 md and hence has a high displacement pressure, the upper reservoir is favored by the oil, in contrast to the results obtained under hydrostatic pressure. A charging fault with high oil transportation ability can cause lower sands to be bypassed by oil.

Migration: Model 2

Oil saturation at 400 years, 39,700 years and 381,400 years under hydrostatic pressure when the permeability of the updip charging fault is 170 md and the permeability of the downdip back door is 50 md is shown in Figure 51. The oil saturation of different models at 381,400 years is shown in Figure 52. Because the negative buoyancy gradient between an updip charging fault and a downdip back door prevents oil from entering into both reservoirs, a very limited amount of oil migrates into them shown in Figures 51, 52 and 53. Simulation results show that a downdip back door has a little effect on oil migration under hydrostatic pressure.

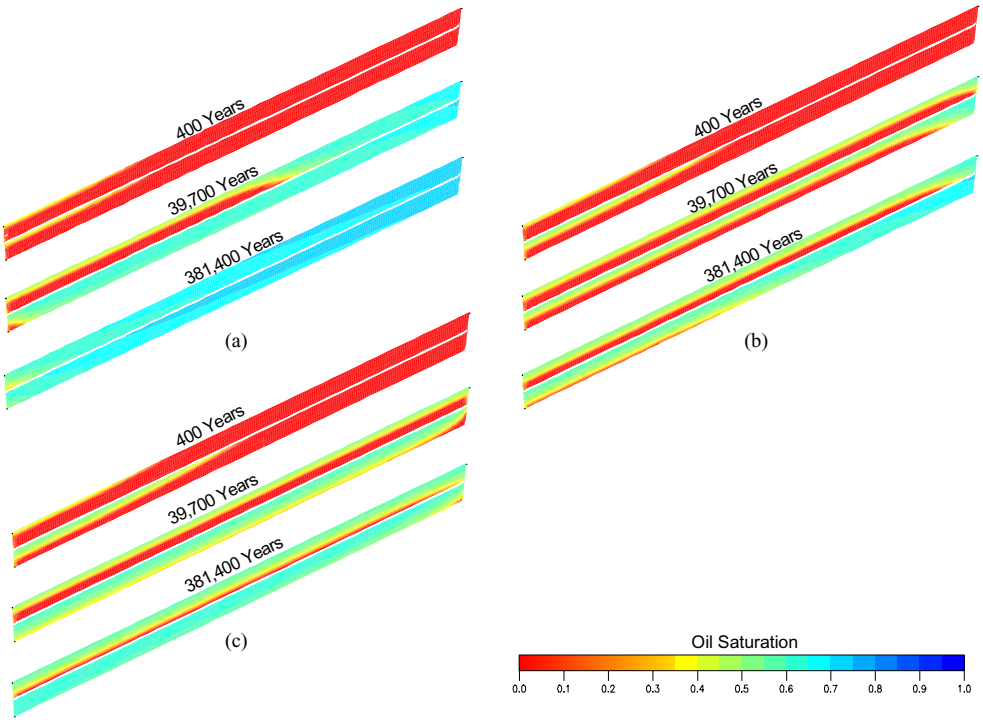

Figure 46. Oil saturation under hydrostatic pressure in model 1 when the permeability of updip back door is (a) 1 md, (b) 50 md, or (c) 1000 md. The permeability of downdip charging fault is 170 md (Eclipse® figures).

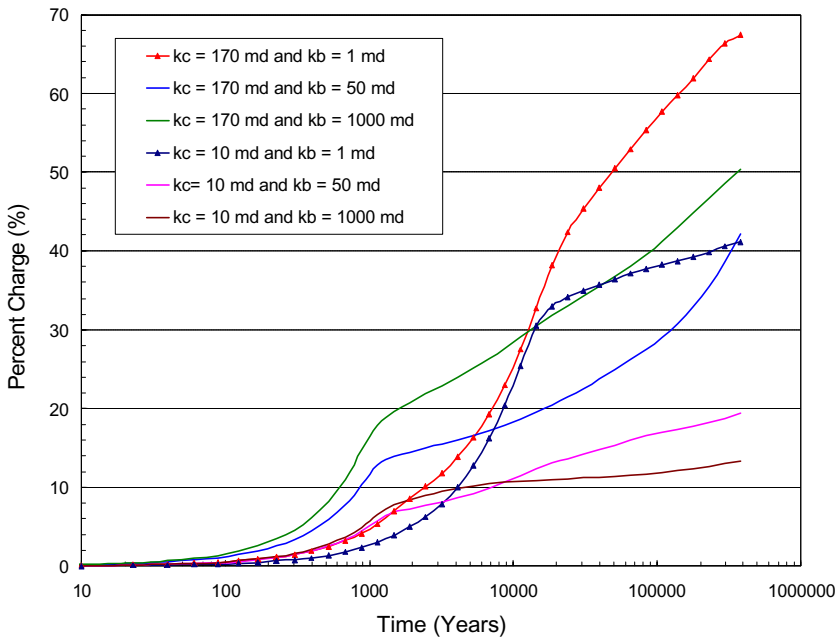

Figure 47. Percent charge under hydrostatic pressure in model 1 when oil charges through a downdip fault. The updip fault is a back door. kc is the permeability of the charging fault and kb is the permeability of the updip back door (Data from Eclipse®).

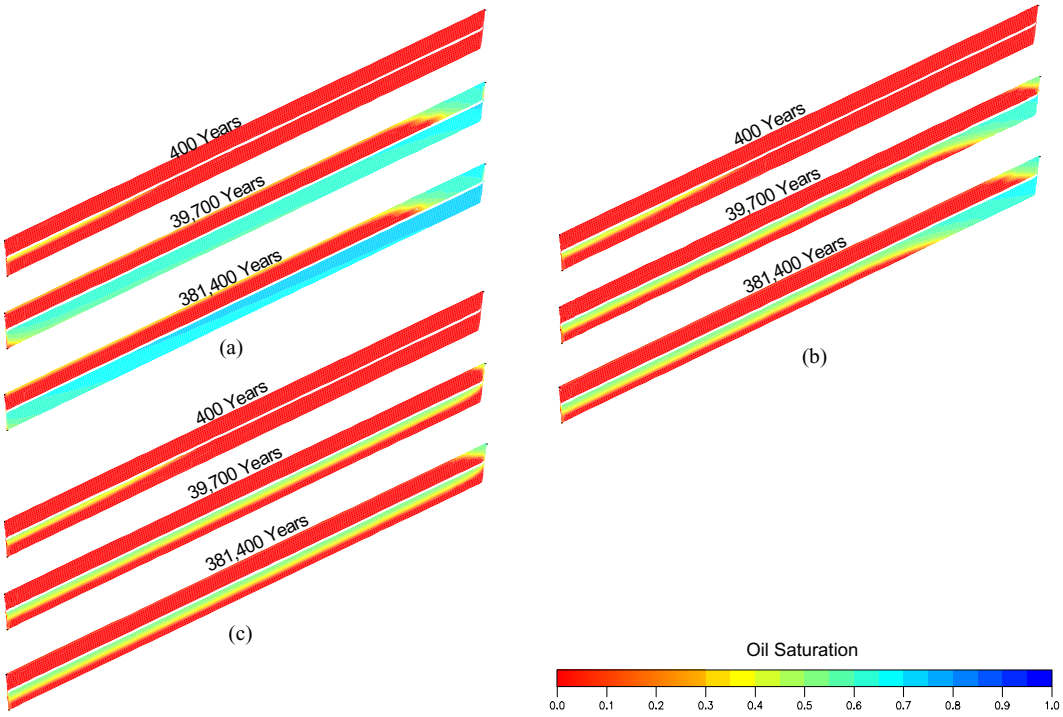

Figure 48. Oil saturation under hydrostatic pressure when the permeability of updip back door is (a) 1 md, (b) 50 md, and (c) 1000 md in model 1. The permeability of downdip charging fault is 10 md (Eclipse® figures).

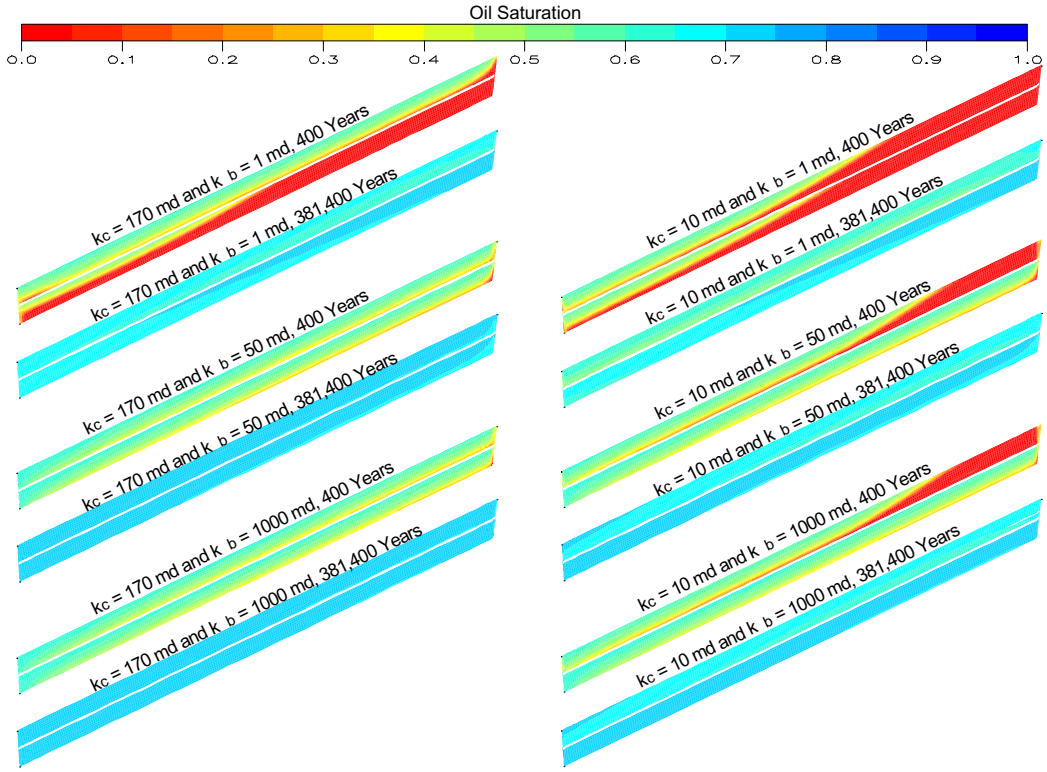

Figure 49. Oil saturation under geopressure when oil charges through a downdip charging fault and the permeability of updip back door is variable in model 1. kc is the permeability of the charging fault and kb is the permeability of the updip back door (Eclipse® figures).

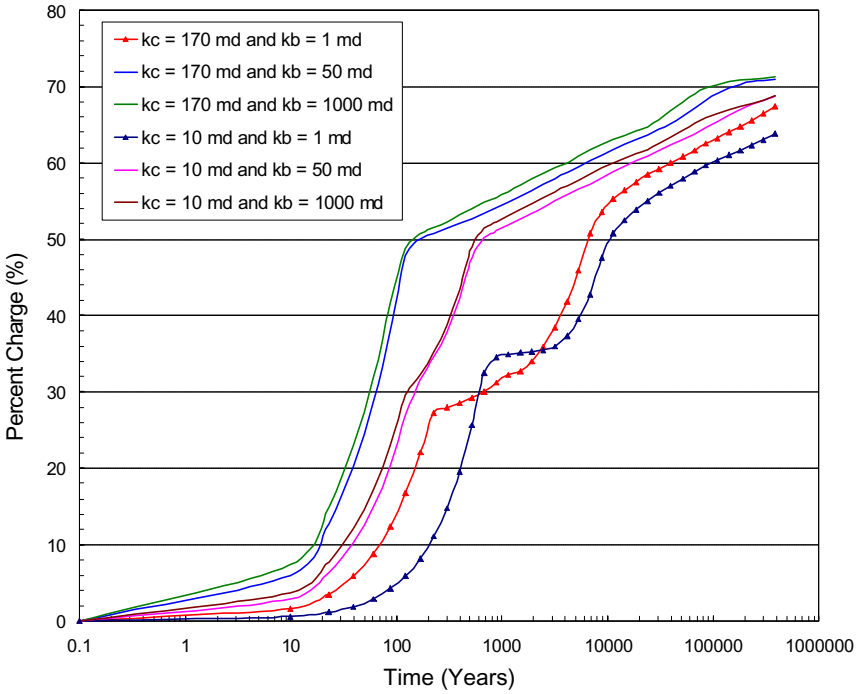

Figure 50. Percent charge under geopressure when oil charges through a downdip fault in model 1. The property of updip back door is variable. kc is the permeability of the charging fault and kb is the permeability of the updip back door (Data from Eclipse®).

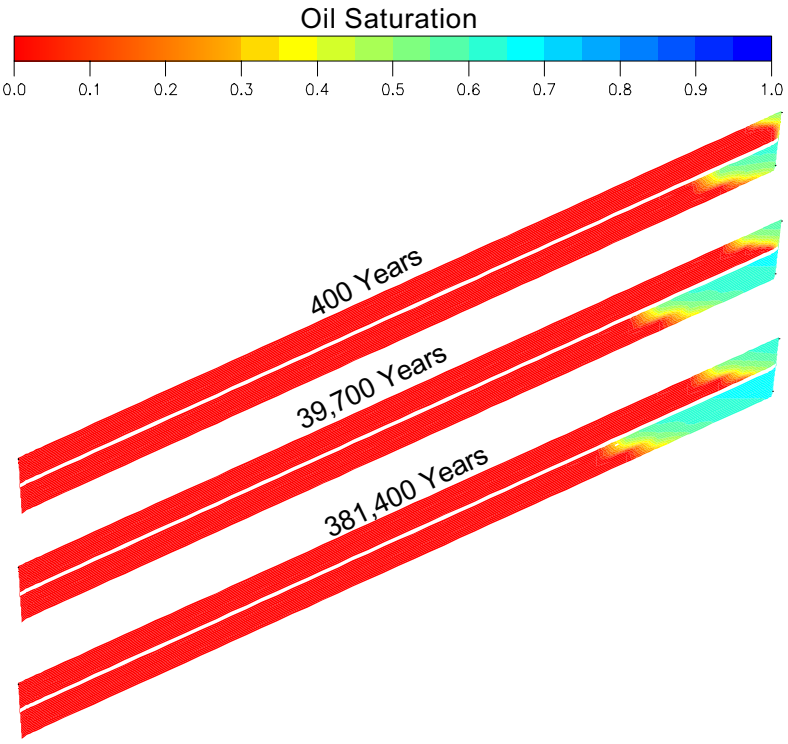

Figure 51. Oil saturation under hydrostatic pressure in model 2 when the permeability of updip charging fault is 170 md and the permeability of the downdip back door is 50 md (Eclipse® figures).

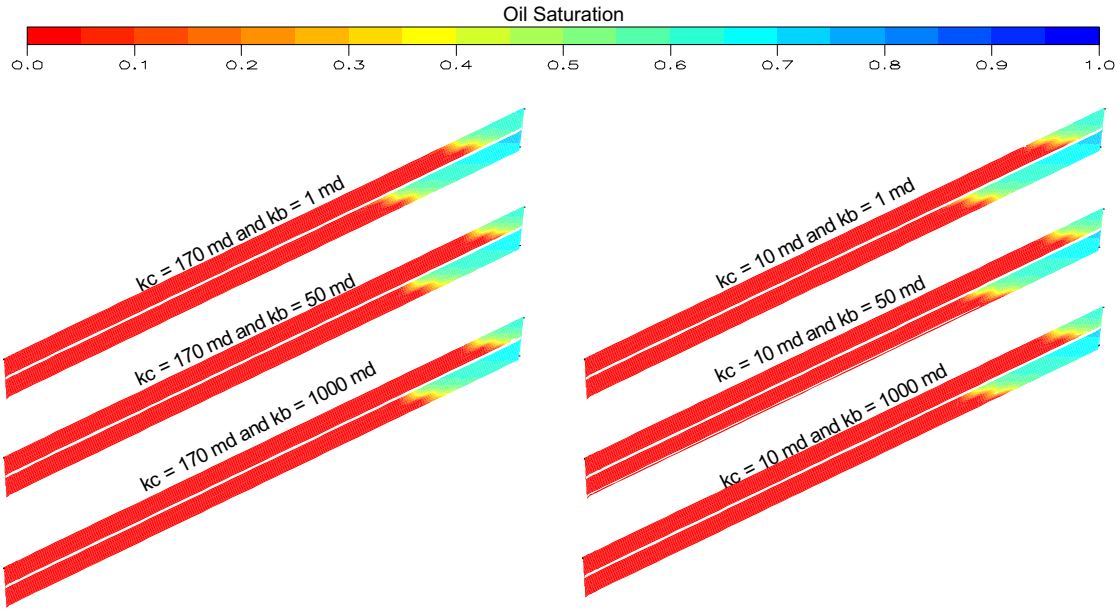

Figure 52. Oil saturation at 381,400 years under hydrostatic pressure when oil charges through an updip fault in model 2. kc is the permeability of the charging fault and kb is the permeability of downdip back door (Eclipse® figures).

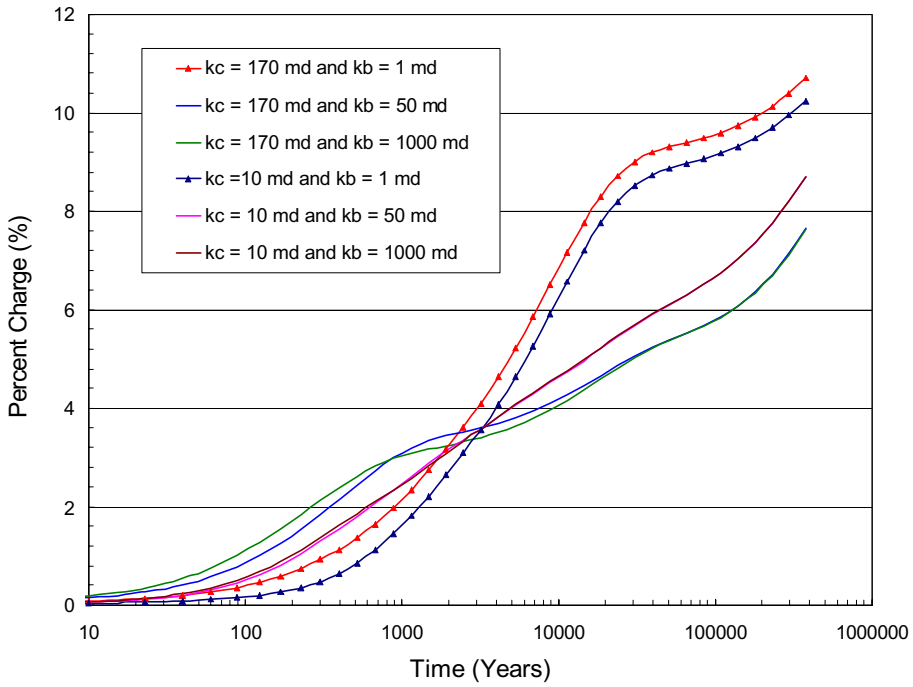

Figure 53. Percent charge under hydrostatic pressure when oil charges reservoir sands through the updip fault in model 2. kc is the permeability of the charging fault and kb is the permeability of the updip back door (Data from Eclipse®).

Charge patterns obtained from numerical simulations under geopressure are very different from those under hydrostatic pressure shown in Figures 54 and 55. Oil always charges and favors lower sands under geopressure. This is in contrast to the simulation results obtained under hydrostatic pressure. The reason why lower sands are filled is that geopressure facilitates water escape from the sand, thus making room for an oil charge. Water escapes from the lower sand so that oil can charge the lower sand first. While water escapes and oil charges, the gradient of geopressure reduces shown in Figure 56, thus causing the geopressure zone to gradually transfer to a normal hydrostatic pressure zone. This is the reason why interreservoir migration must be investigated under hydrostatic pressure alone. Hydrostatic pressure usually prevents a downdip oil charge. This can explain why lower sands are more frequently filled, because a significant amount of oil charges the lower sands and a higher percent charge is obtained as compared to the charge percent obtained under hydrostatic pressure (see Figures 53 and 57). Figure 53 shows that a downdip back door whose permeability is 1 md can cause a slow oil charge.

Migration: Model 3

Figure 58 shows the oil saturation of different models at 381,400 years under hydrostatic pressure. As is shown, both updip reservoirs are charged by oil under hydrostatic pressure, but a very limited amount of oil charges the downdip reservoirs even though the permeability of the downdip back door is very high. Buoyancy and an updip back door cause the oil to charge both updip reservoirs. Under geopressure, the lower downdip reservoir and both updip reservoirs are charged by oil shown in Figure 59. The oil charging the lower downdip sand under geopressure is consistent with simulation results obtained from Model 2.

Growth fault model

Under hydrostatic pressure, the properties of antithetic fault and synthetic faults are the same first with their permeabilities at 170 md, thus causing the lower sands to fill first, and only later allowing the upper sands to fill as shown in Figure 60. Because of geological structures, sands A, X and U are not favored by oil charges. The patterns of oil show that charges in sands B, C and Y are complex. Oil charges sands B and Y partly through the synthetic fault and partly through the antithetic fault shown in Figure 61. Oil charges into sand C partly through the synthetic fault and partly through the updip fault shown in Figure 61. The fact that oil first charges sands B and Y through the synthetic fault implies that oil is more likely to

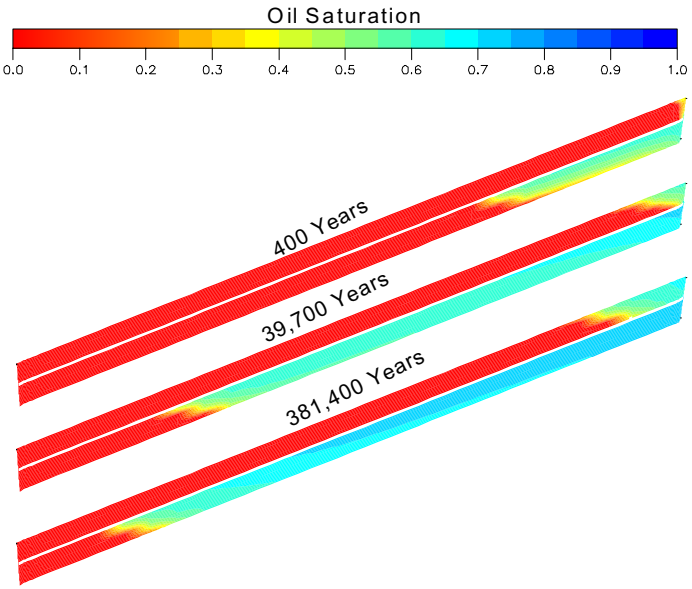

Figure 54. Oil saturation under geopressure when the permeability of updip charging fault is 170 md and the permeability of downdip back door is 50 md in model 2 (Eclipse® figures).

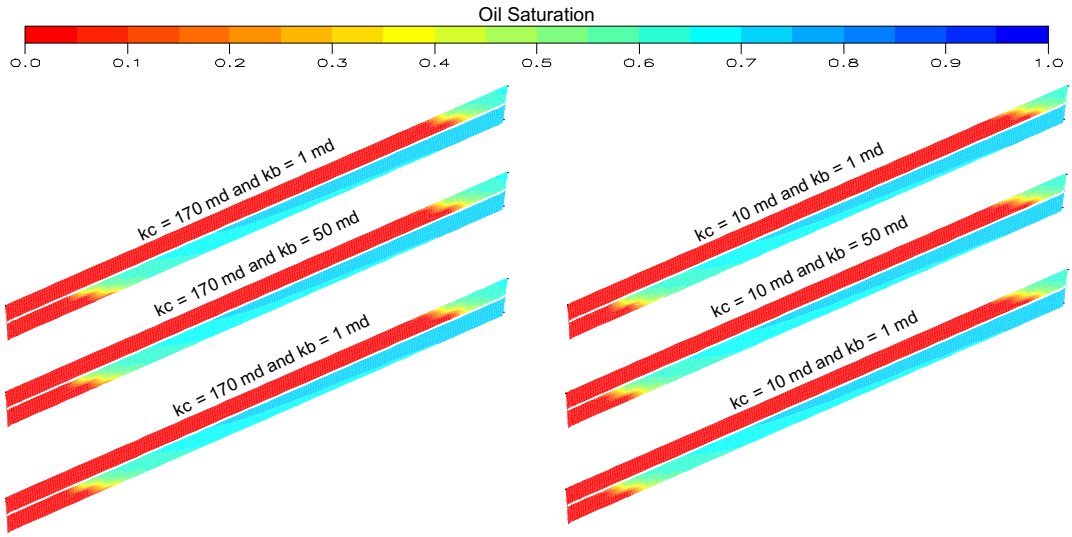

Figure 55. Oil saturation at 381,400 years under geopressure in model 2. kc is the permeability of the charging fault and kb is the permeability of the updip back door (Eclipse® figures).

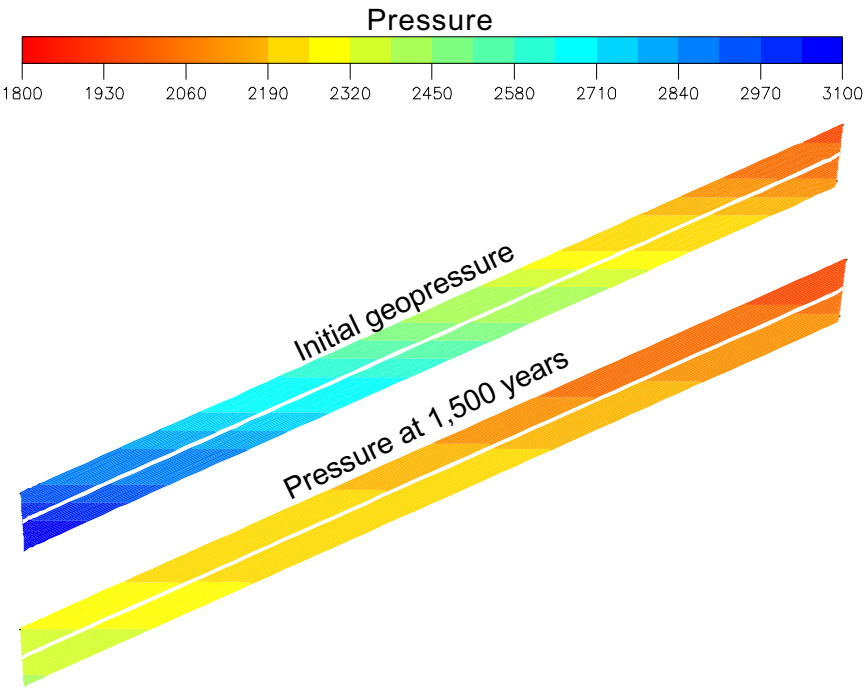

Figure 56. Pressure at 1500 years under initial geopressure when the permeability of updip charging fault is 170 md and the permeability of downdip back door is 50 md in model 2 (Eclipse® figures).

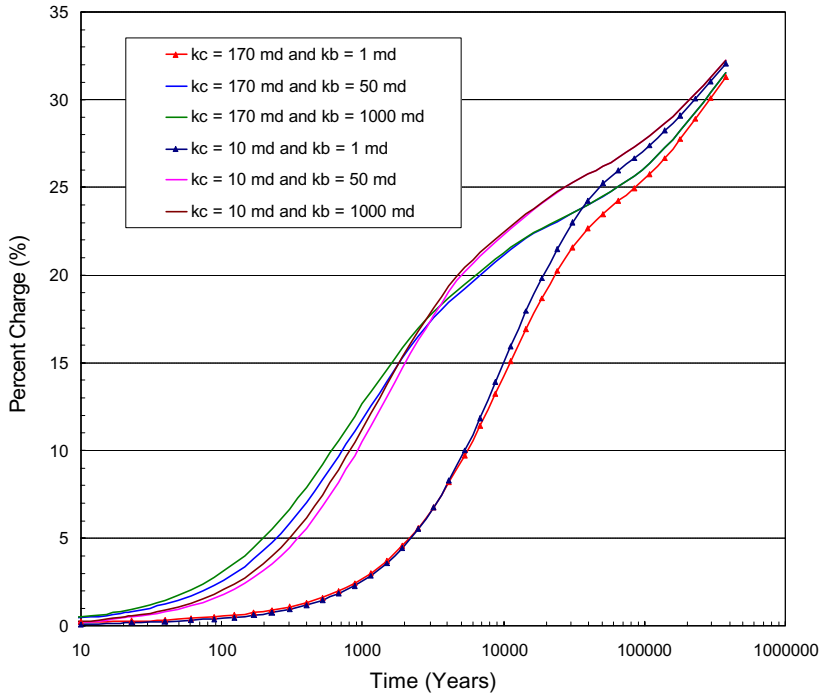

Figure 57. Percent charge under geopressure when oil charges through the updip fault and the downdip fault acts as a back door in model 2. kc is the permeability of the charging fault and kb is the permeability of the updip back door (Data from Eclipse®).

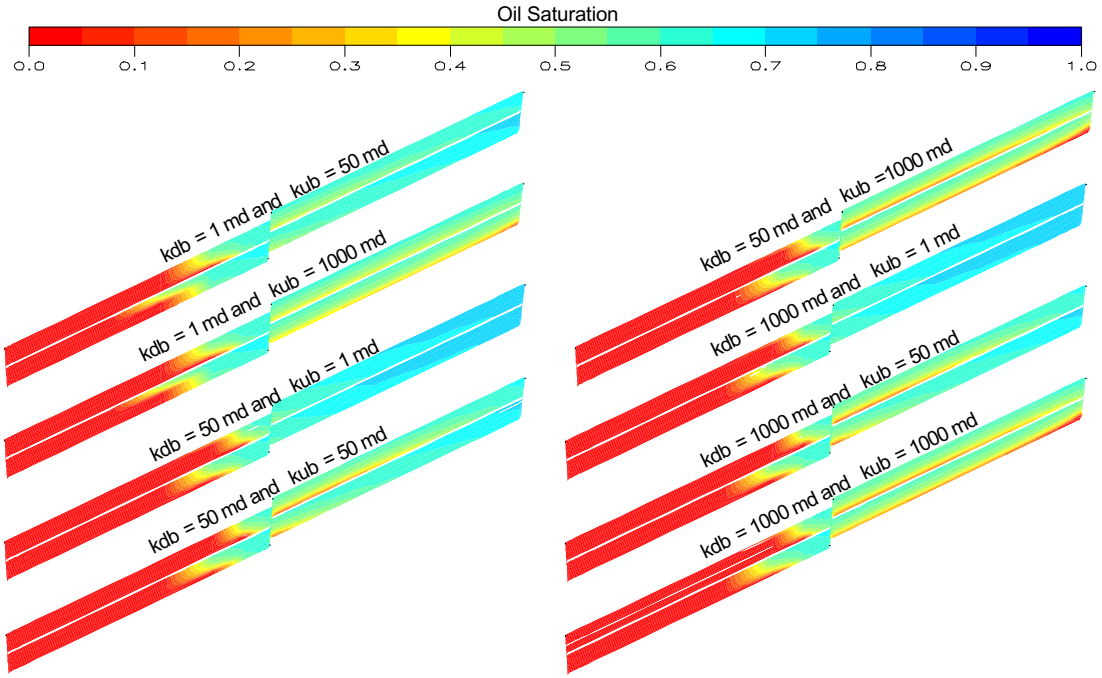

Figure 58. Oil saturation at 381,400 years under hydrostatic pressure when the permeability of the central fault is 170 md in mode 3. kdb is the permeability of downdip back door and kub is the permeability of updip back door (Eclipse® figures).

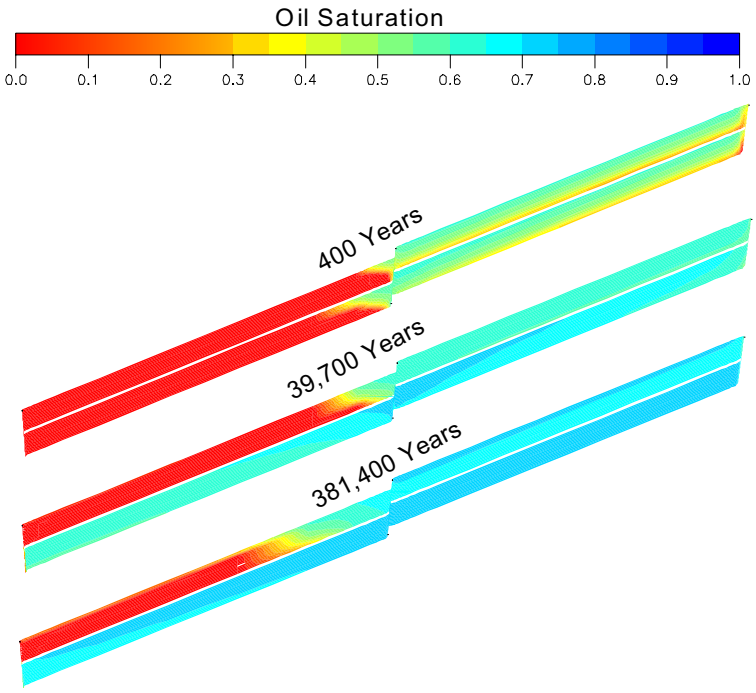

Figure 59. Oil saturation under geopressure when the permeability of the central charging fault, the downdip back door and the updip back door are 170 md, 1 md and 1000 md, respectively, in mode 3 (Eclipse® figures).

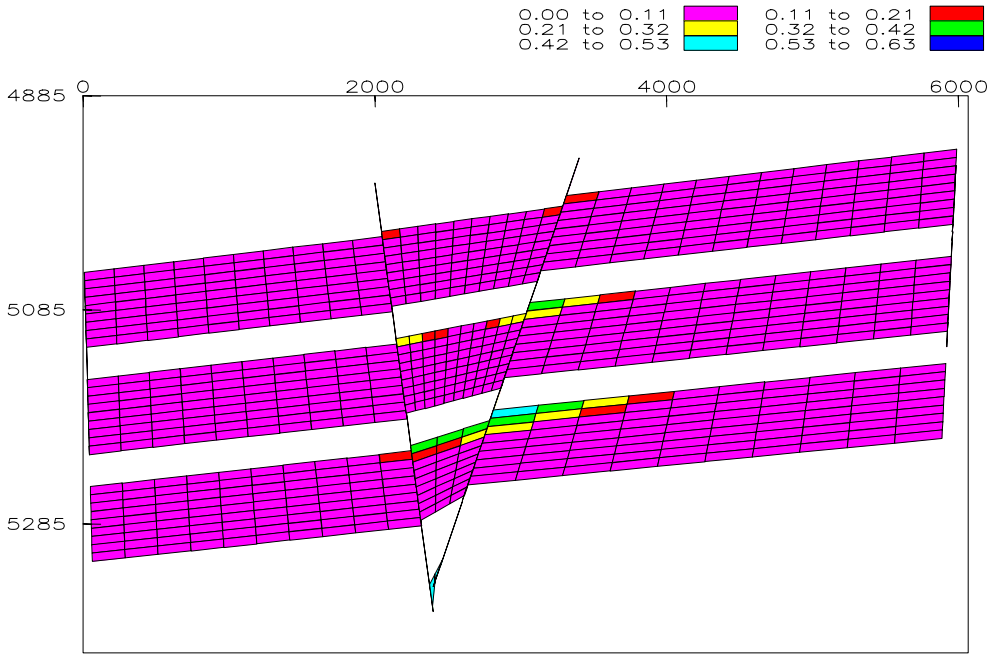

Figure 60a. Oil saturation at 200 years under hydrostatic pressure when the permeabilities of antithetic fault and synthetic fault are 170 md (Eclipse® figures).

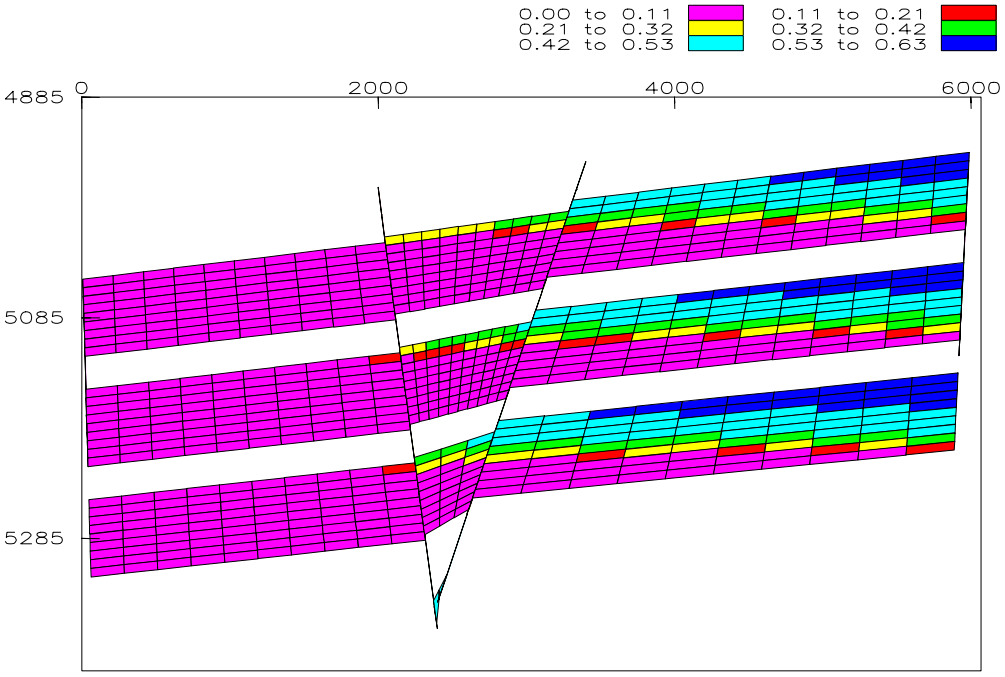

Figure 60b. Oil saturation at 5,300 years under hydrostatic pressure when the permeabilities of antithetic fault and synthetic fault are 170 md (Eclipse® figures).

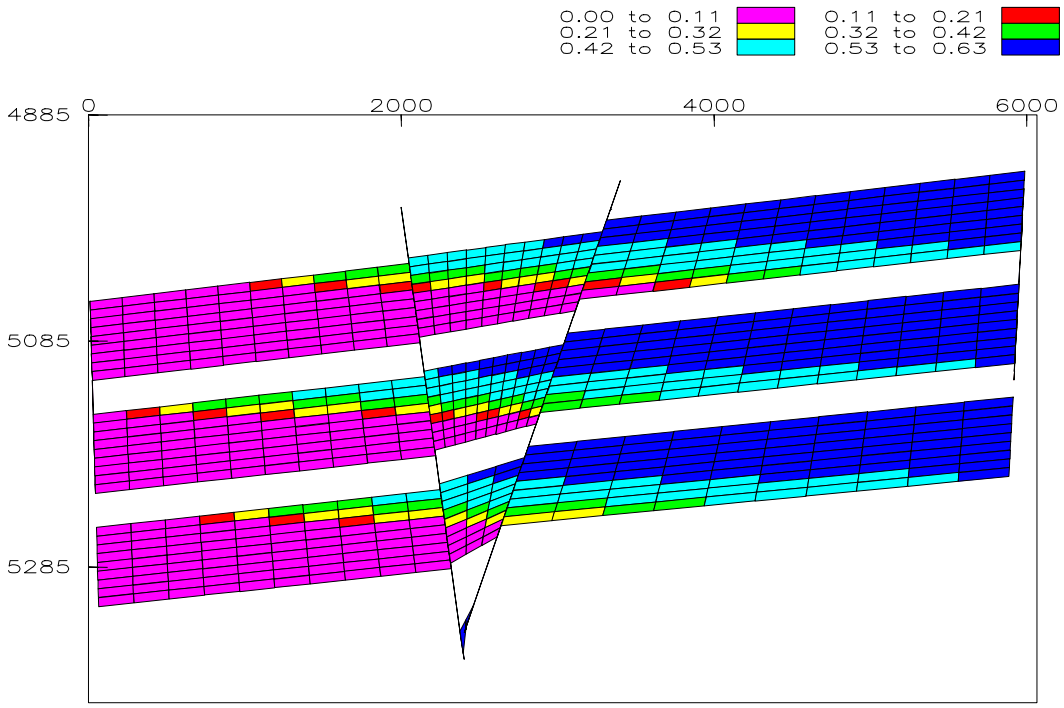

Figure 60c. Oil saturation at 65,700 years under hydrostatic pressure when the permeabilities of antithetic fault and synthetic fault are 170 md (Eclipse® figures).

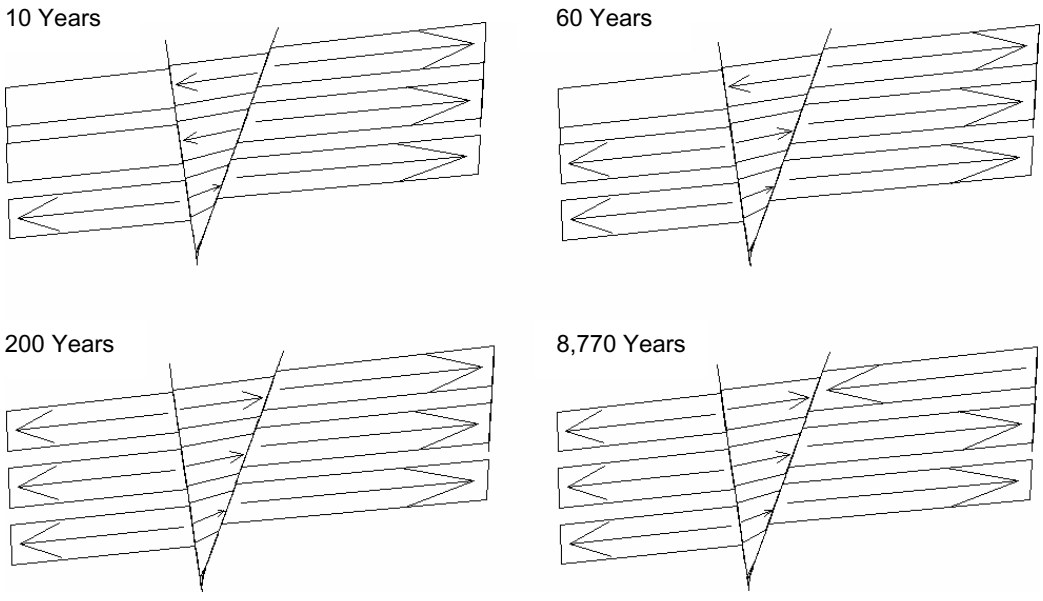

Figure 61. Oil flow under hydrostatic pressure when the permeabilities of antithetic fault and synthetic fault are 170 md, respectively (Eclipse® figures).

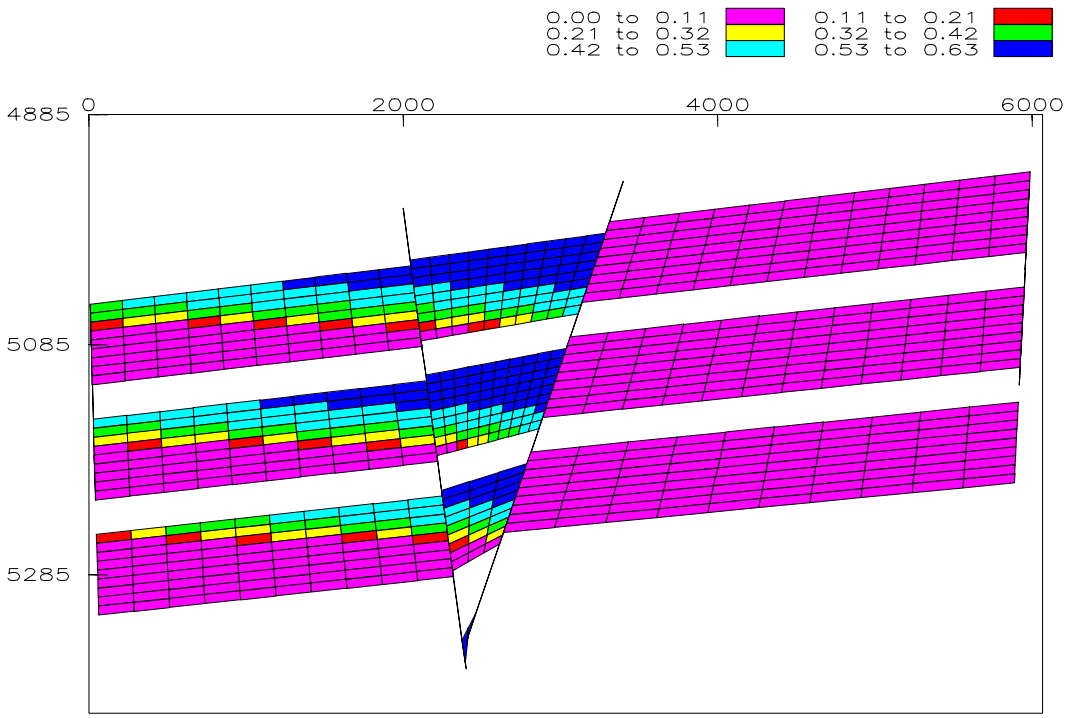

Figure 62. Oil saturation at 65,700 years under hydrostatic pressure when the permeability of antithetic fault is 170 md and the permeability of synthetic fault is 0.1 md (Eclipse® figures).

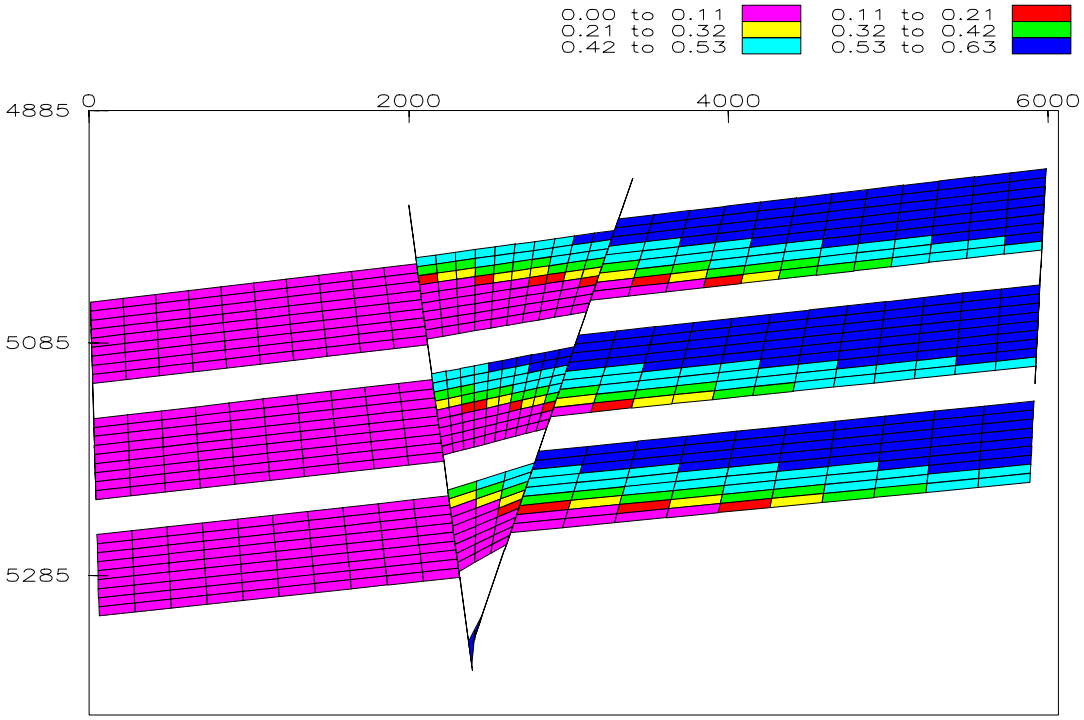

Figure 63. Oil saturation at 65,700 years under hydrostatic pressure when the permeability of antithetic fault is 0.1 md and the permeability of synthetic fault is 170 md (Eclipse® figures).

migrate along a synthetic fault than along an antithetic fault. If the permeability of a synthetic fault is 0.1 md and the permeability of an antithetic fault is 170 md, sands C, Z and W will be bypassed (see Figure 62), even though these sands are favored because of geological structures (see Figure 60). In contrast to these conclusions, if the permeability of a synthetic fault is 170 md and the permeability of an antithetic fault is 0.1 md, sands A, X and U will be bypassed (see Figure 63).

Under geopressure, sands A, X and U are not favored either (Figure 64) as they aren't under hydrostatic pressure when the properties of the synthetic fault and the antithetic fault were the same. However, more oil charges these three sands under geopressure than under hydrostatic pressure. Meanwhile, since sand X has a downdip back door, a significant amount more of oil charges sand X than sand U. If the permeability of the antithetic fault is 170 md and the permeability of the synthetic fault is 0.1 md, sands C, Z and W will be bypassed early on (Figure 65(a)), as they were under hydrostatic pressure. However, both sands Z and C are charged if the charging time is long enough as shown in Figures 65(b) and 65(c). An updip back door in

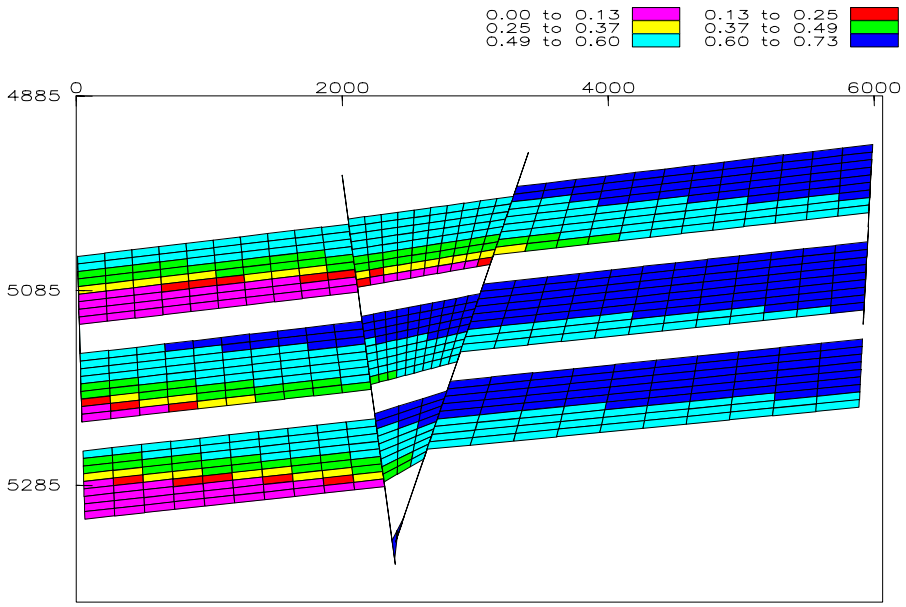

Figure 64. Oil saturation at 65,700 years under geopressure when the permeabilities of the antithetic fault and synthetic fault are 170 md (Eclipse® figures).

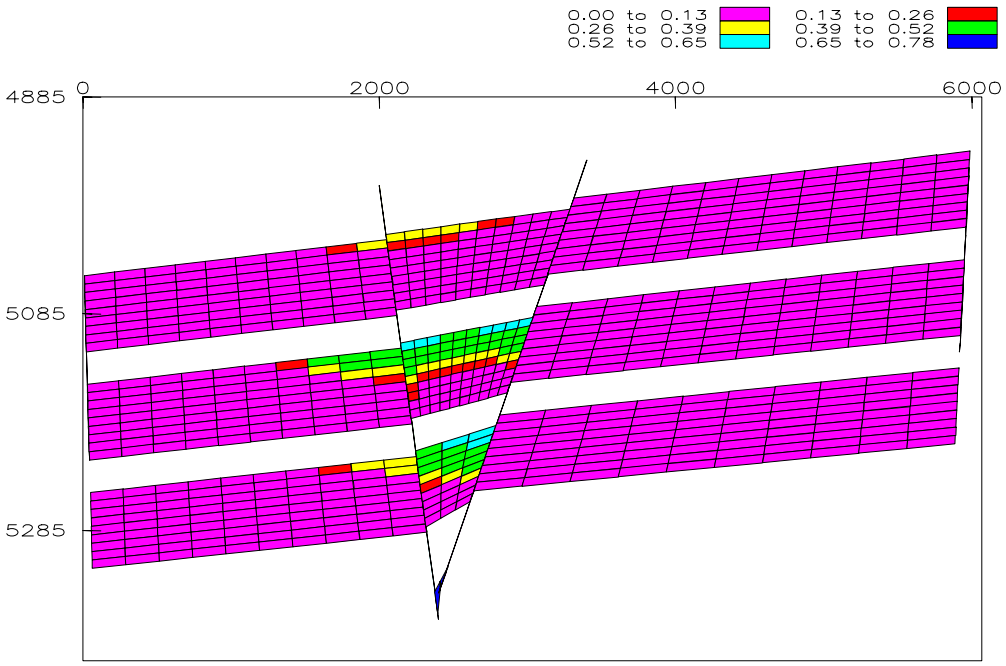

Figure 65a. Oil saturation at 200 years under geopressure when the permeability of antithetic fault is 170 md and the permeability of synthetic fault is 0.1 md (Eclipse® figures).

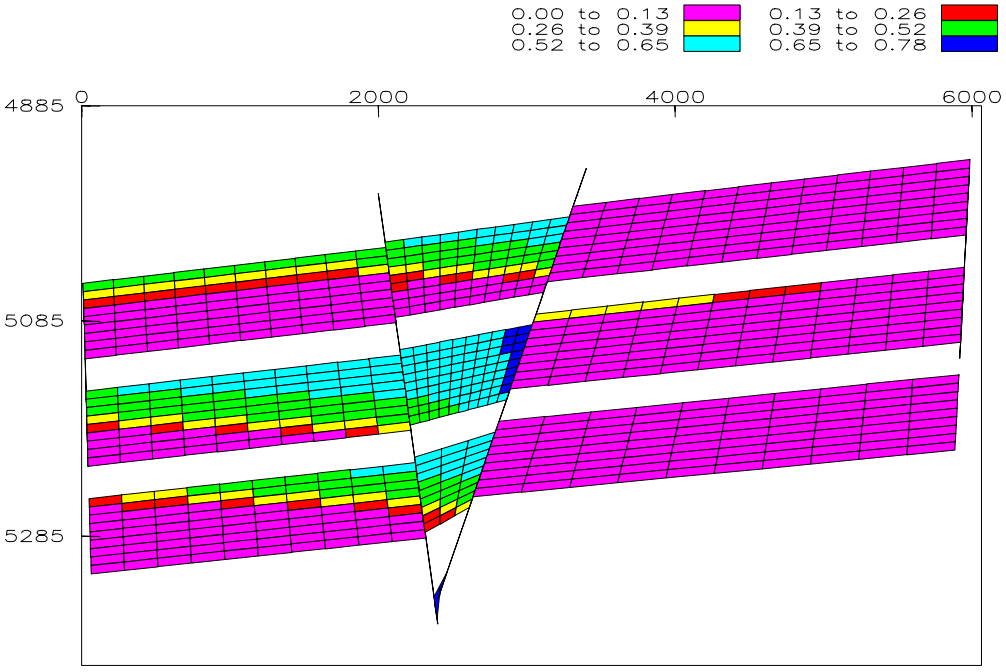

Figure 65b. Oil saturation at 5,300 years under geopressure when the permeability of antithetic fault is 170 md and the permeability of synthetic fault is 0.1 md (Eclipse® figures).

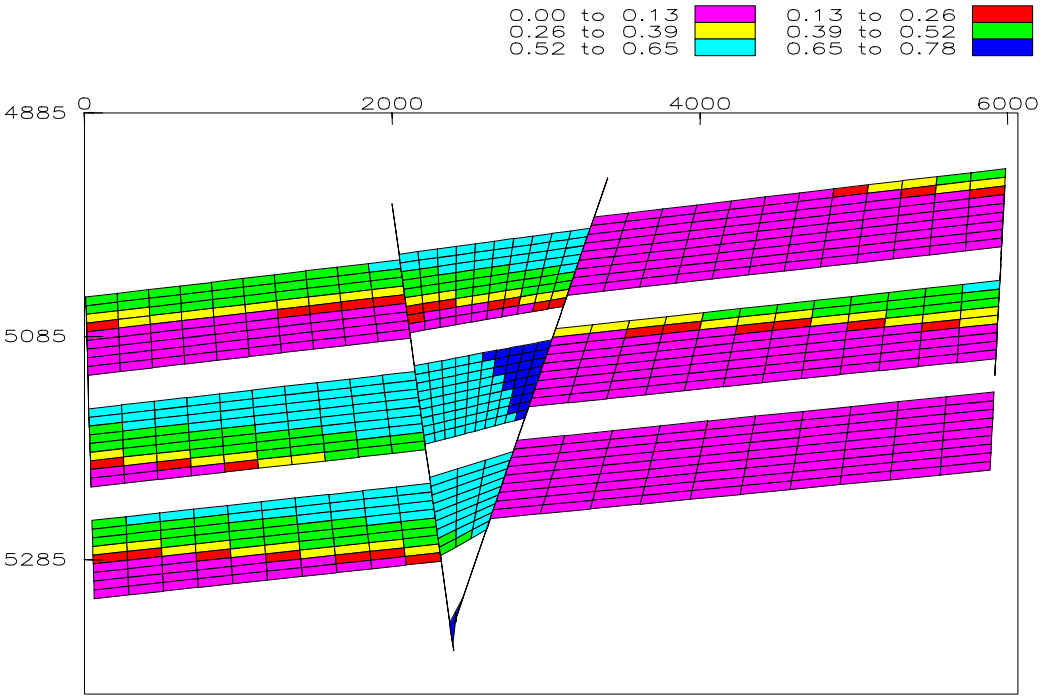

Figure 65c. Oil saturation at 18,700 years under geopressure when the permeability of antithetic fault is 170 md and the permeability of synthetic fault is 0.1 md (Eclipse® figures).

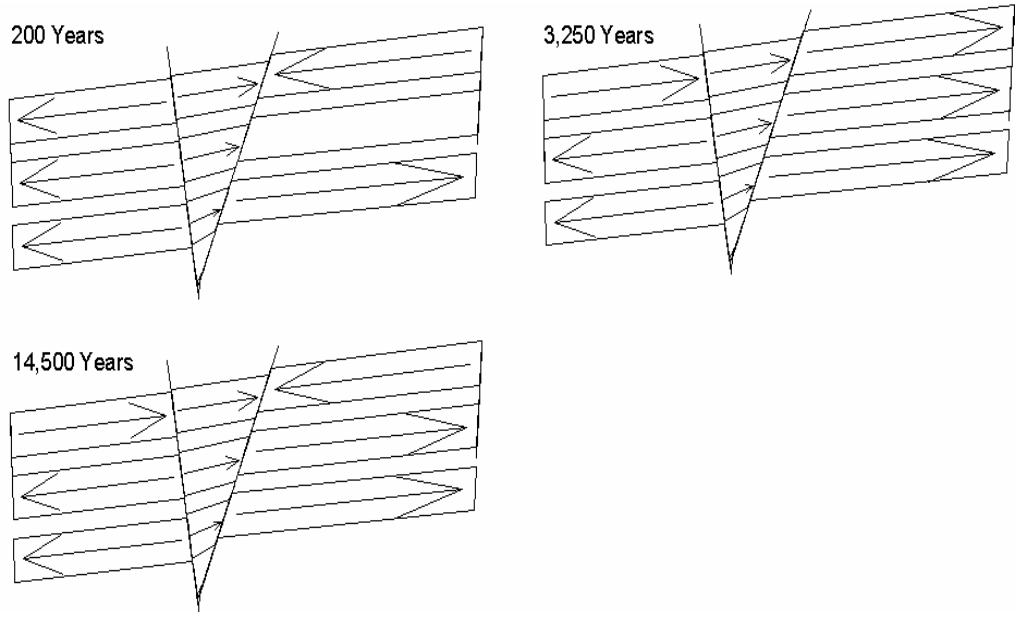

Figure 66. Oil flow under geopressure when the permeability of antithetic fault is 170 md and the permeability of synthetic fault is 0.1 md (Eclipse® figures).

sand Z causes more oil to charge sand Y than sands B and V, and consequently some oil in sand Y charges sand Z. Oil charges sand C partly through an updip fault and partly through a synthetic fault (Figure 66). Sand W is bypassed because it doesn't have an updip back door. If the permeability of an antithetic fault is 0.1 md and the permeability of a synthetic fault is 170 md, sands A, X and U will still be bypassed until 2,500 years have passed. At the same time, more oil will charge sands Y and Z because of back doors (Figure 67).

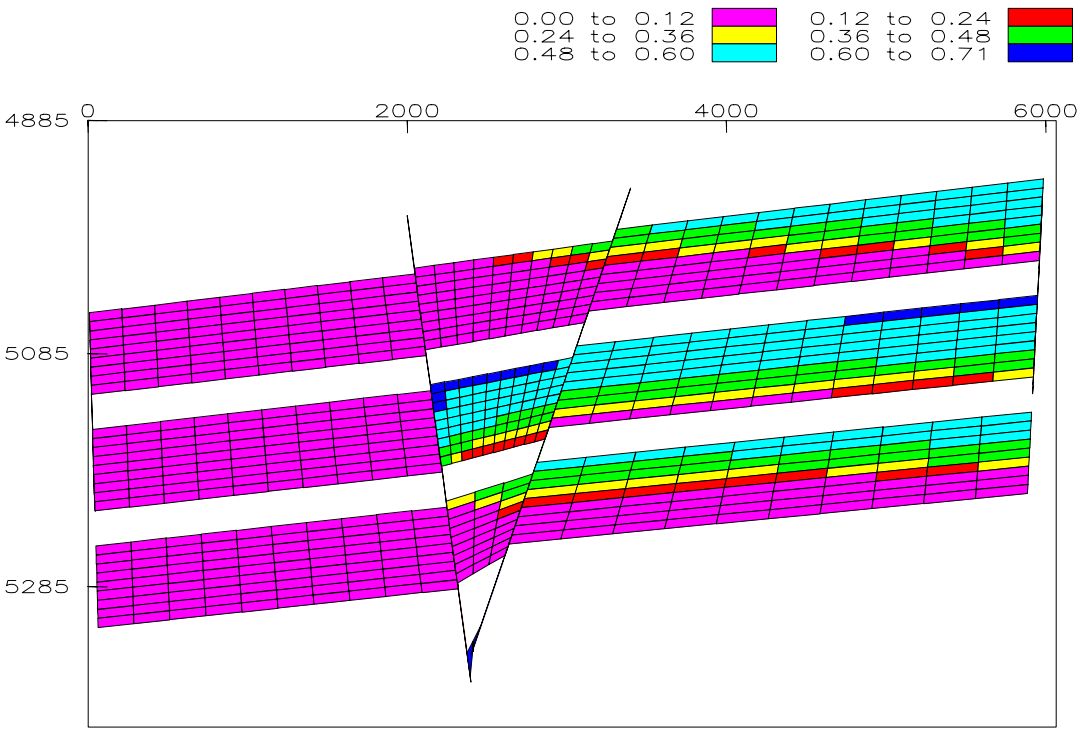

Figure 67. Oil saturation at 2,500 years under geopressure when the permeability of the antithetic fault is 0.1 md and the permeability of the synthetic fault is 170 md (Eclipse® figures).

Interreservoir migration

So far, continuous oil charging has been assumed to last several hundred thousands years. It has been found that anomalously high hydrocarbon column heights can be maintained in stacked fault-bounded reservoirs during active charges. Once the reservoirs are isolated from the source, the difference between the displacement pressures of the bounding fault and the adjacent reservoir sand must limit the oil column

height. Interreservoir migration between stacked fault-bounded reservoirs under hydrostatic pressure will occur only when the oil supply dries up.

The same numerical models shown in Figures 42 and 43 are used here to study interreservoir migration. Faults act as routines for this interreservoir migration. However, no oil is allowed to enter reservoirs through bounding faults. Since no oil enters into the model system, no fluid can flow out through either fault because of the material balance in these numerical simulations. The model system itself consists of a closed system. The initial oil saturation in all models is shown in Figure 68.

If a downdip fault exists but there is no updip fault to act as a routine for interreservoir migration, oil independently moves updip in both reservoirs at the same time that oil migrates from the lower reservoir into the upper reservoir through the downdip fault (Figure 69). The first oil movement continues until buoyancy can no long move oil updip in both reservoirs. Oil will then accumulate in the upper parts of the two sands. The second oil movement from the lower sand to the upper will continue until one of two conditions is met. The first condition is that any oil-water contact in the lower sand reaches the section of the downdip fault and the top of the lower sand. The second condition is that the oil column height reaches a height that the downdip fault can retain because of its displacement pressure. Meanwhile, the lower the displacement pressure of the downdip fault, the faster and larger the second oil movement from the lower sand to the upper (Figure 69).

If there is an updip fault for interreservoir oil migration between the two reservoir sands but there is no downdip fault, oil will independently move updip in the two sands (Figure 70). At the same time, oil will migrate from the lower sand to the upper through the updip fault. The lower the displacement pressure of the downdip fault, the faster the oil will move through the fault and the greater the amount of oil that will migrate into the upper sand.

If both an updip and a downdip faults exist to act as routines for interreservoir migration, oil can migrate from the lower sand to the upper at the same time that water flows from the upper sand to the lower sand through the two faults (Figure 71). Interreservoir migration is very fast and oil-water contacts in both sands should reach the same level. Oil will continuously and independently move updip in both sands at the same time that same oil-water contacts in the two sands are maintained.

DISCUSSION

Migration

Simulation results show that which sand between the two in Model 1 is favored under hydrostatic pressure is mainly determined by the oil transportation ability of the charging fault and the properties of the updip back door. If the charging time is long enough, the lower the displacement pressure of the charging fault, the more favored the upper sand. Oil could bypass the lower sand completely. The higher the displacement pressure of the charging fault, the more favored the lower sand is. Meanwhile, it is required that the displacement pressure of the updip back door be low enough so that the downdip charging fault, one of the two reservoirs and the updip backdoor fault consist of an oil migration pathway. Otherwise, oil migration could be prevented by the back door so that oil only very slowly charges both reservoirs. Generally, the lower reservoir sands are favored under hydrostatic pressure. This is in contrast to the results that show that the upper reservoir is generally favored under geopressure. The reason why the upper reservoir is favored is that a significant amount of oil enters though the charging fault under geopressure, but water cannot escape from both reservoirs to make room for oil charges through the charging fault or the updip back door. Oil migrates along the charging fault, but only some of the entered oil escapes through the same charging fault because both oil and water are trying to escape through it at an early charge time. Therefore, the `upper sand is favored under geopressure. Moreover, the lower the displacement pressure of the charging fault, the more favored the upper reservoir will be.

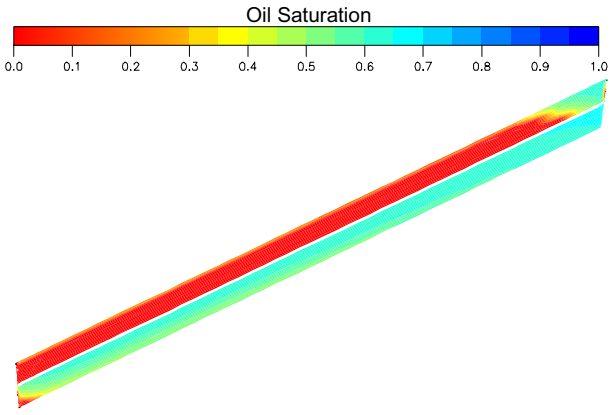

Figure 68. Initial oil saturation in all numerical models used to study interreservoir oil migration (Eclipse® figures).

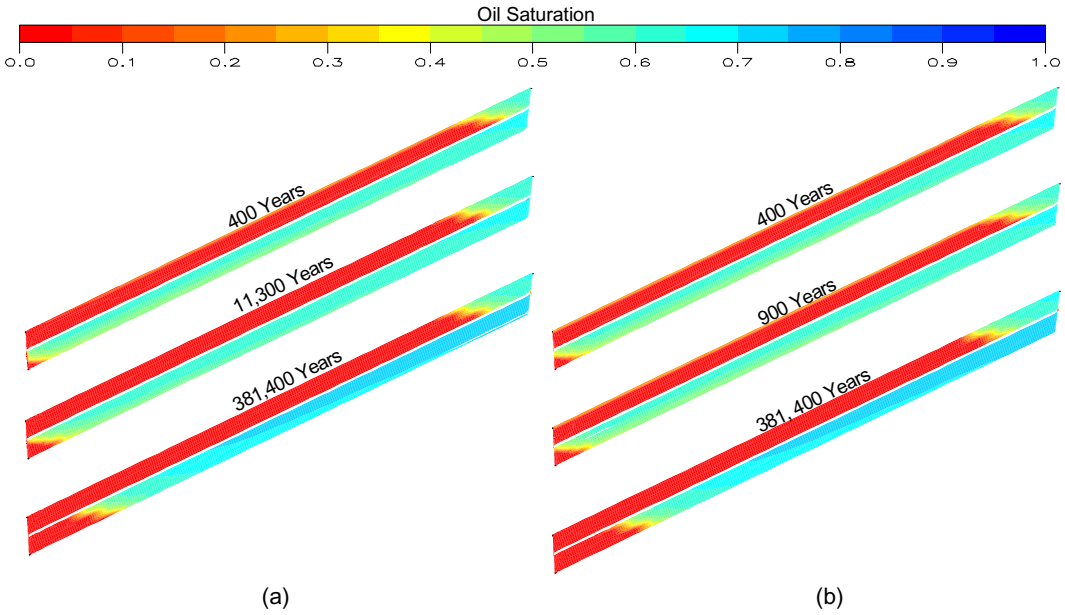

Figure 69. Oil saturation during the interreservoir migration when no updip fault exists and the permeability of downdip fault is (a) 1 md or (b) 170 md (Eclipse® figures).

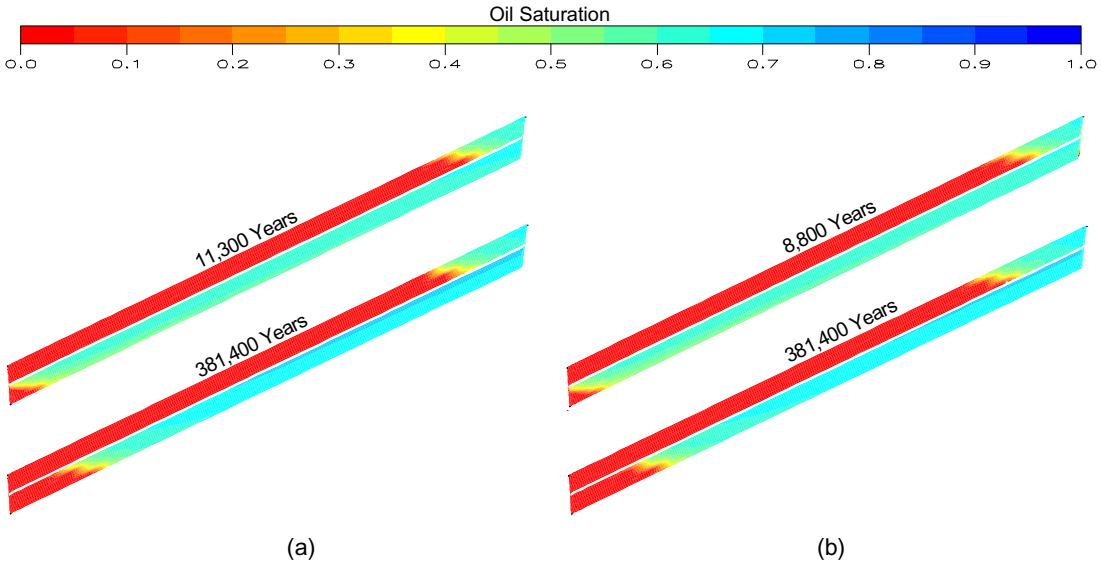

Figure 70. Oil saturation during the interreservoir migration when no downdip fault exists and the permeability of updip fault is (a) 1 md or (b) 170 md (Eclipse® figures).

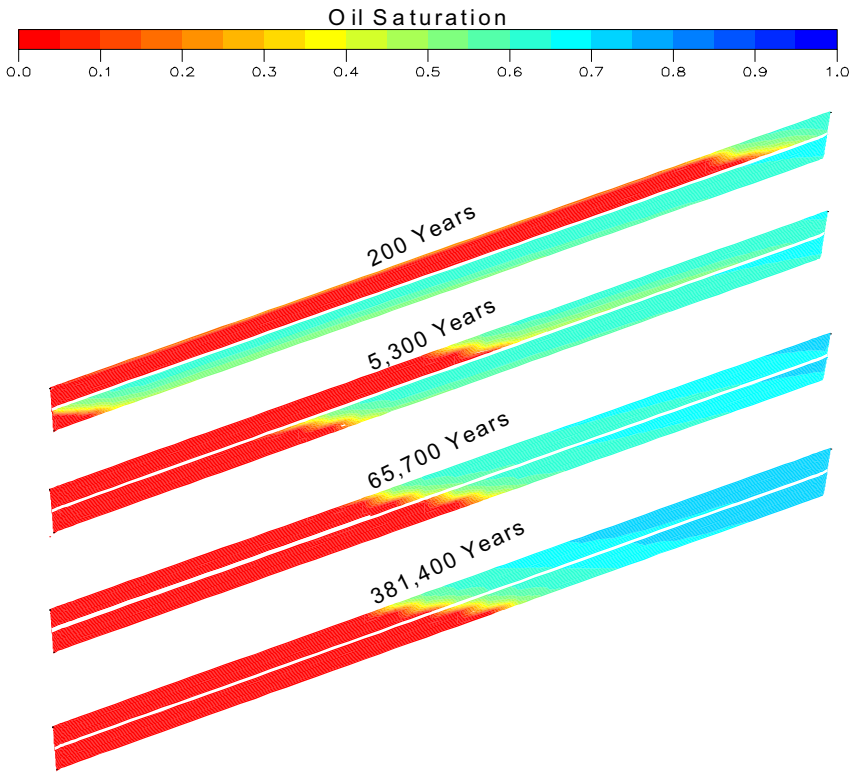

Figure 71. Oil saturation during interreservoir migration when the permeabilities of downdip fault and updip fault are 1 md and 170 md, respectively (Eclipse® figures).

The negative buoyancy gradient between the updip charging fault and the downdip back door impedes oil migration into both downdip reservoirs under hydrostatic pressure, as shown in Model 2. However, because pressure changes during simulation, oil can significantly charge the lower reservoir under geopressure. The results that the zone under geopressure gradually transfers to the zone under hydrostatic pressure because of oil migration are consistent with the results obtained in the northern Gulf of Mexico (Nunn, 1996). The results that oil charges the lower downdip reservoir under geopressure are in contrast to the results regarding the effects of back doors on oil percent charges which state that only a very limited amount of oil charges a downdip sand under both hydrostatic pressure and geopressure. Obviously, geological structures can greatly change oil charging patterns under geopressure.

The above discussions regard geological structures where sands juxtapose against shale. When oil charges through a charging fault along which sands juxtapose against sands, the results obtained in Models 1 and 2 are applicable. The downdip lower reservoir also fills under geopressure.

When oil migrates along growth faults, lower and updip sands are favored under hydrostatic pressure when the properties of the antithetic and synthetic faults are the same (Figure 61). However, when one of the two faults has a higher displacement pressure than the other, either the synthetic or antithetic fault will impede oil migration along itself as shown in Figures 62 and 63. Under geopressure, lower and updip sands are still favored, but more oil charges the downdip sands than under hydrostatic pressure (sands A, X and U in Figure 64). The role of the downdip back door and the results obtained under geopressure in Model 2 explains the reason why more oil charges downdip sands than upper ones. When the synthetic fault has a high displacement pressure, geopressure and an updip back door can facilitate oil migration along the synthetic fault and penetrate it to charge the updip sands (sands C and Z in Figure 65). However, it is difficult for oil to migrate along an antithetic fault or to penetrate it when it has a high displacement pressure, even if a downdip back door exists under geopressure. This causes the downdip sands to usually be dry as shown in Figure 67.

Interreservoir migration

Interreservoir migration through faults along which sands juxtapose against shale has been simulated for this study. Once a fault exists, interreservoir migration does not stop until the trapped oil column height reaches the height the fault can retain because of its displacement pressure. Even though a fault might be a downdip fault and its permeability very small, buoyancy force should definitely motivate interreservoir migration to begin and continue. Interreservoir migration is a very long process when under hydrostatic pressure. The models for studying interreservoir migration consist of closed systems in this study. If more series of sand and shale lie over the sand-shale-sand structure along both bounding faults, oil will continuously migrate from lower sands to upper sands while water could flow from the upper sands to the lower through the bounding faults.

SUMMARY

Both oil migration during active charges and the interreservoir migration without oil supplies are affected by the following factors: charge time for active charges or migration time without an oil supply, pressure, the oil transportation ability of the charging faults, the properties of back doors, and the geological

structure. Reservoirs may not fill because of the fact that either the charge time or the migration was not enough.

The combination of charging faults, reservoirs, back doors, their relationships and the pressure all determine oil migration pathways. Any one of these factors can change migration pathways. Generally, lower reservoirs and updip sands are favored and oil migration into downdip reservoirs should not be expected. Geopressure and updip back doors facilitate oil charges in updip reservoirs.

Interreservoir migration among stacked fault-bounded reservoirs is an important mechanism for oil accumulation and trap identification. Once stacked fault-bounded reservoirs are commercially charged, interreservoir migration driven only by the buoyancy force is a very slow process even when the displacement pressure of the bounding faults is very low. Therefore, commercial oil accumulation could be found in these stacked fault-bounded reservoirs.

CHAPTER VI

THE ROLE OF BACK DOORS IN OIL-GAS-WATER SYSTEMS

This chapter focuses on the role of back doors on hydrocarbon migration and entrapment in oil-gas-water systems. The role of a back door on gas migration and entrapment is especially emphasized. First, simulations were conducted on a single fault-bounded reservoir in order to describe the role of back doors on hydrocarbon migration and entrapment in such simple geological structures. This is key to understanding the patterns of hydrocarbon migration and entrapment in complex geological structures related to faults. Second, hydrocarbon migration along growth faults was simulated in order to investigate how hydrocarbons charge stacked reservoirs through these growth faults.

INTRODUCTION

In the northern Gulf of Mexico, hydrocarbons commonly charge into stacked fault-compartmentalized reservoirs along faults and were retained in appropriate traps. The diverse distribution of oil and gas in the Ship Shoal 274/293 field implied that an early stage of oil and gas charges were followed and disturbed by a late stage of gas migration along growth faults. Gas can be found updip or downdip from oil in the field.

Therefore, a further understanding of the role of back doors on hydrocarbon migration and entrapment in three-phase systems is the final goal of this study. The roles of downdip and updip back doors in the simplest models, where a single reservoir is bounded by faults, were the first to be individually investigated. With the fundamentals obtained from all previous work, an attempt to better understand the effects of back doors in growth fault models in three-phase systems was then made.

NUMERICAL MODELS

To allow oil and gas to enter stacked fault-bounded reservoirs through a charging fault, two injection wells were connected to the charging fault. Oil was allowed to enter numerical models through one injection well and gas was allowed to enter through the other. A constant oil flow rate and a constant gas flow rate related to the two injection wells were specified as boundary conditions. The oil injection rate was kept constant at 10 STB/day, and the gas injection rate was constant at 30 mcf/day. Therefore, the GOR

was 3,000 for all models. Such high flow rates could increase reservoir pressure, but the maximum pressure that was allowed in these numerical models was set so that it was always less than the lithostatic pressure at the corresponding depths, thus preventing rocks from fracturing. Water saturation was initially 100%.

UDBD model

The same conceptual and numerical models shown in Figure 18 were applied here. Constant well bottom hole pressures, P_d and P_u were specified as a part of the boundary conditions in these numerical models. P_d and P_u were 10 psi lower than the corresponding pressures of the cells where they were respectively connected.

DDBD model

The conceptual model and corresponding numerical model are shown in Figure 19. Constant P_d and P_u were specified as a part of the boundary conditions in the numerical model, as in the above UDBD model.

Three-fault model

The corresponding conceptual model was shown in Figure 20 but the central fault here is a charging fault. Numerical grids are shown in Figure 72 without any throw along the central fault. Fluids can flow out of the system through the downdip fault, the central fault and the updip fault, as shown in Figure 72. Constant pressures P_d, P_c and P_u were assigned to be 10 psi less than the corresponding cell pressures as a part of the boundary conditions.

Growth model

The kind of model used was shown in Figure 45. Constant P_d (the bottom hole pressure of a production well connected to an antithetic fault) and P_u (the bottom hole pressure of a production well connected to a synthetic fault) were assigned as a part of the boundary conditions in the numerical model, as in the above UDBD model.

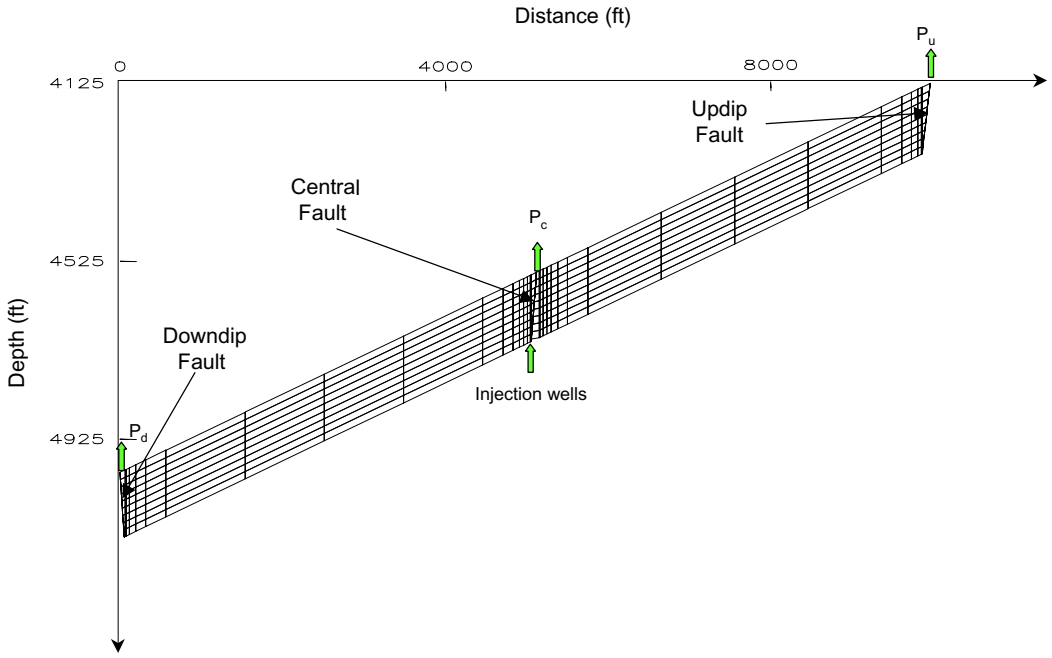

Figure 72. Three-fault model. The central fault is a charging fault. The updip and downdip faults are both back doors. Oil and gas charge through the charging fault. Oil, gas and water can escape from both the charging fault and the back doors. Constant pressures P_d, P_c and P_u are specified as a part of the boundary conditions.

SIMULATION RESULTS

UDBD model

Both oil and gas saturation under hydrostatic pressure when the permeability of the downdip charging fault is 50 md and there is no updip back door is shown in Figure 73. When comparing oil saturation to gas saturation at 400 years, gas obviously charges faster than oil. No updip back door to allow for fluid escape causes both oil and gas to accumulate in the reservoir, but gas is updip from oil in the reservoir since gas weighs less than oil. The oil and gas saturation at 1,500 years and 5,300 years demonstrate that gas accumulation in the upper dip part of the sand forces oil to move down. If the charge time is long enough, some oil will finally escape from the reservoir through the charging fault. At 5,300 years, gas dominates the reservoir and only a little oil remains. If the charging time is longer than 5,300 years and gas continues to be in supply, very little oil will be retained in the reservoir.

If the permeability of the downdip charging fault is 50 md and the permeability of the updip back door is 170 md, oil, gas and water can all escape through the charging fault and the updip back door. However, the updip back door will have different effects on all of them. Gas escapes more easily than water, but water more easily than oil. Therefore, gas occupies a thin upper layer of the reservoir as shown in Figure 74. Some gas escapes from the reservoir through the downdip charging fault, at the same time that other gas escapes through the updip back door. Oil charges the updip sand because the updip back door acts as a routine for water to escape from the reservoir (Figure 74).

Simulations show that an updip back door is necessary for oil to charge sand from the downdip charging fault under both hydrostatic pressure and geopressure (Figures 73, 74, 75, and 76). The oil percent charges under hydrostatic pressure and under geopressure listed in Figures 75 and 76 show that some oil already charging the updip reservoir escapes from it through the downdip charging fault due to gas accumulation in its upper part, but only if there is no updip back door. Updip back doors do not affect gas accumulation in updip sands, even though the permeability of the back door might be very low, for example, only 0.1 md (Figures 75 and 76).

DDBD model

Oil and gas saturation under hydrostatic pressure is shown in Figure 77 when the permeabilities of the downdip and updip back doors are 170 md and 50 md, respectively, with simultaneous oil and gas charges in the downdip reservoir through the updip charging fault. Since gas is less dense and viscous than oil, gas can easily escape from the model system through the charging fault, leaving the reservoir uncharged by gas. Gas percent charges shown in Figures 78 and 79 in the reservoir are always less than 0.5 percent within 5,300 years under hydrostatic pressure and geopressure.

In contrast, a very limited amount of oil charges the downdip reservoir (Figures 77, 78 and 79). Oil percent charges under hydrostatic pressure in (Figure 78) show that oil charging the downdip reservoir is related to the downdip back door, which obviously acts as a routine for water escape in order to make room for the oil charge. The lower the displacement pressure of the downdip back door, the more efficient the downdip oil charge under hydrostatic pressure. This is in contrast to the results obtained in investigations of oil-water systems. However, the oil percent charge under geopressure is determined by the geopressure

gradient and the properties of the updip charging fault (Figure 79). This is consistent with the results obtained from oil-water systems.

Three-fault model

Hydrocarbon charging of fault-bounded reservoirs through fault along which sands juxtapose against shale was investigated here. The three-fault models were designed to investigate this type of situation. If the permeability of the charging fault is 50 md and the permeabilities of the back doors are possibly 0.1 md and 170 md, oil and gas saturation at 5,300 years in the 4 possible models under hydrostatic pressure is shown in Figure 80. Oil and gas percent charges under hydrostatic pressure are shown in Figures 81. The corresponding saturation and percent charges under geopressure are shown in Figure 82 and 83, respectively.

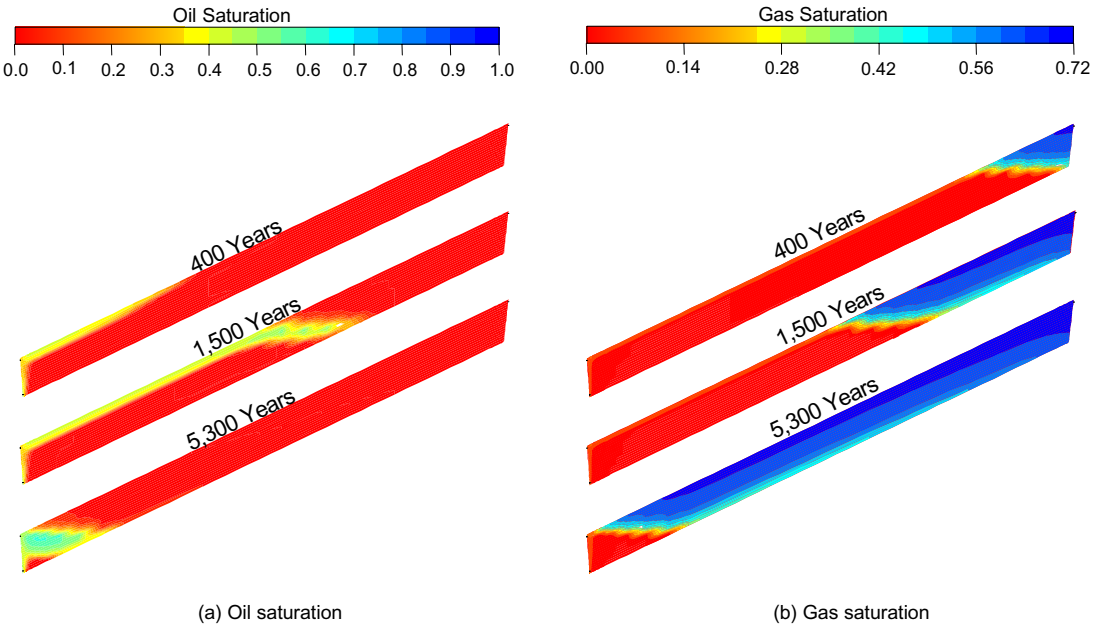

Figure 73. Oil and gas saturation under hydrostatic pressure when the permeability of the downdip charging fault is 50 md and no updip back door exists in the UDBD model (Eclipse® figures).

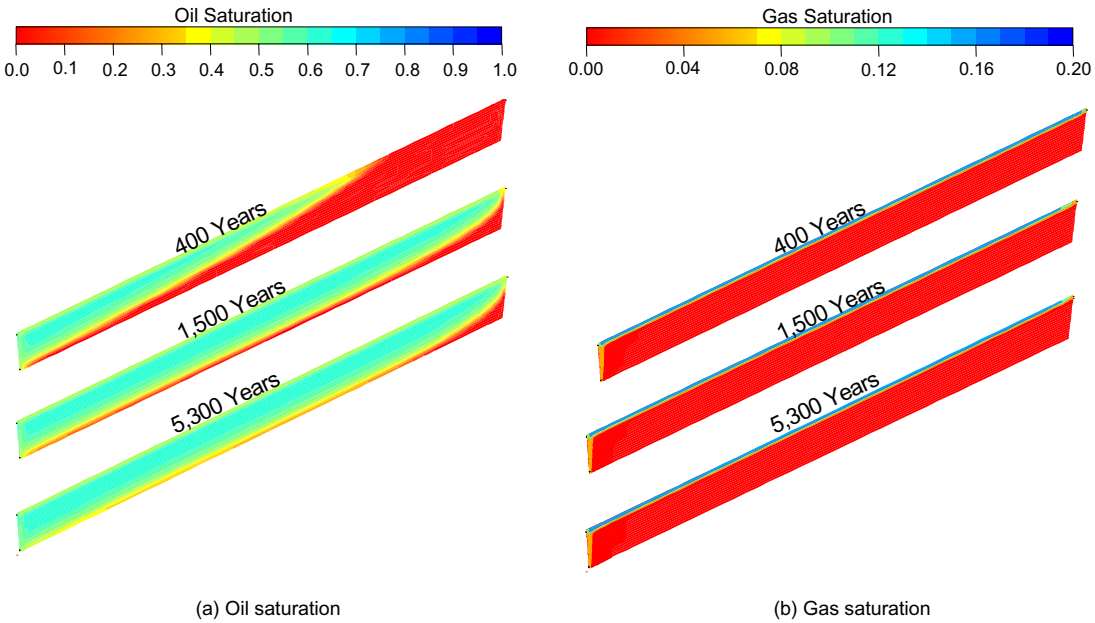

(a) Oil saturation (b) Gas saturation

Figure 74. Oil and gas saturation under hydrostatic pressure when the permeability of the downdip charging fault is 50 md and the permeability of updip back door is 170 md in the UDBD model (Eclipse® figures).

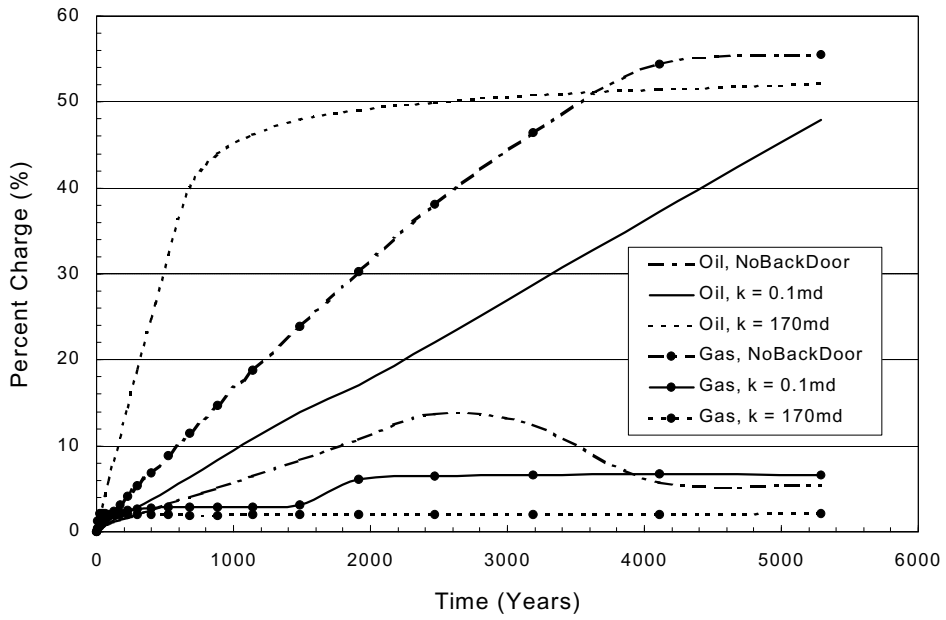

Figure 75. Oil and gas percent charges under hydrostatic pressure when the permeability of the downdip charging fault is 50 md and the permeability of updip back door is 0 md (no back door), 0.1 md and 170 md in the UDBD model (Data from Eclipse®).

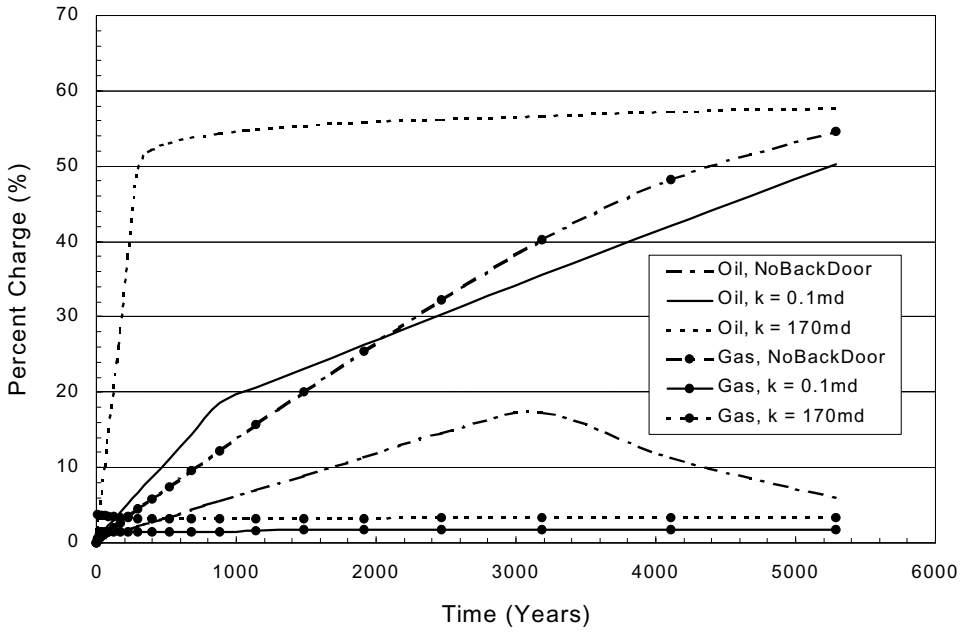

Figure 76. Oil and gas percent charges under geopressure when the permeability of the downdip charging fault is 50 md and the permeability of the updip back door is 0 md (no back door), 0.1 md and 170 md in the UDBD model (Data from Eclipse®).

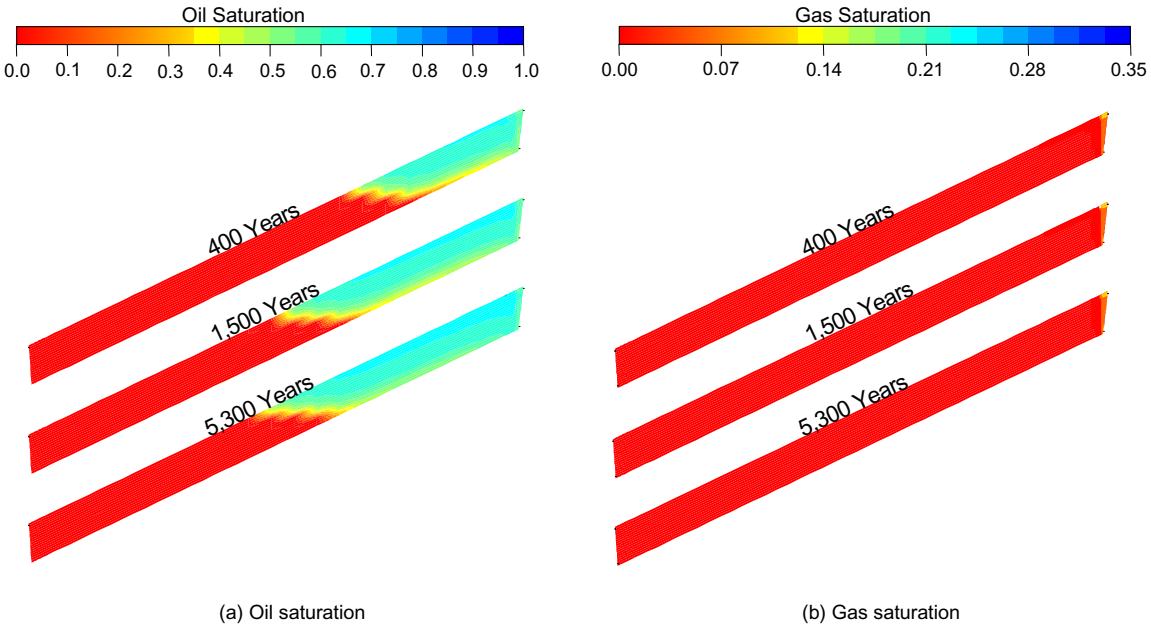

Figure 77. Oil and gas saturation under hydrostatic pressure when the permeability of the updip charging fault is 50 md and the permeability of the downdip back door is 170 md in the UDBD model (Eclipse® figures).

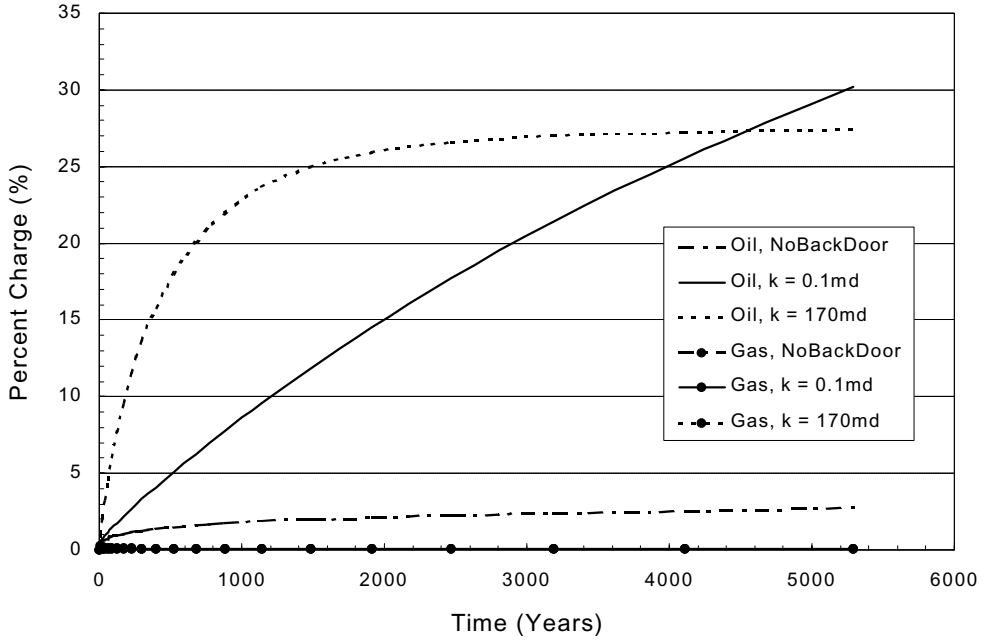

Figure 78. Oil and gas percent charges under hydrostatic pressure when the permeability of the updip charging fault is 50 md and the permeability of the downdip back door is 0 md (no back door), 0.1 md and 170 md in the DDBD model (Data from Eclipse®).

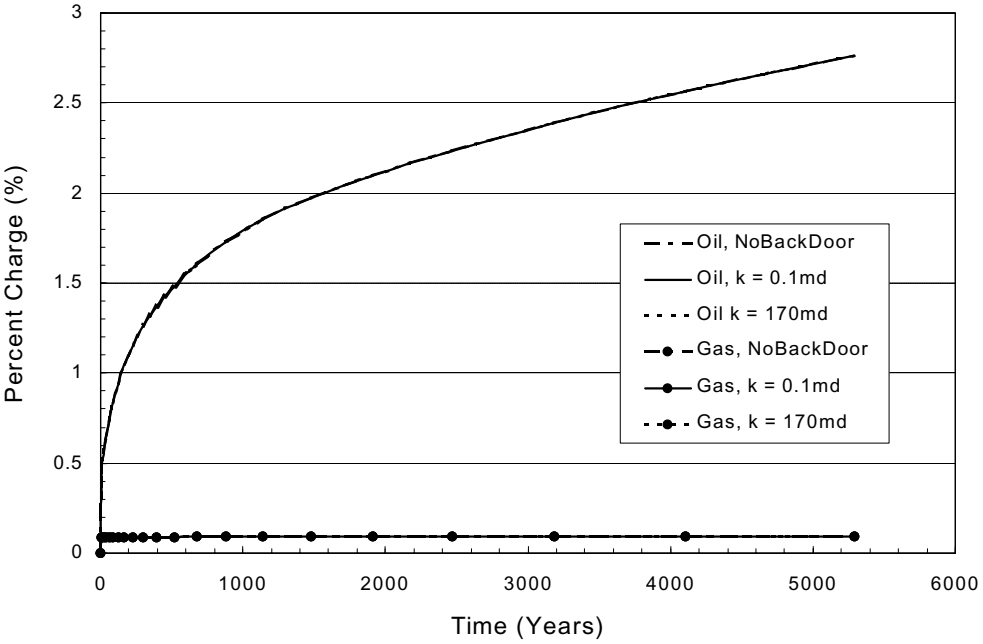

Figure 79. Oil and gas percent charges under geopressure when the permeability of the updip charging fault is 50 md and the permeability of the downdip back door is 0 md (no back door), 0.1 md and 170 md in the DDBD model (Data from Eclipse®).

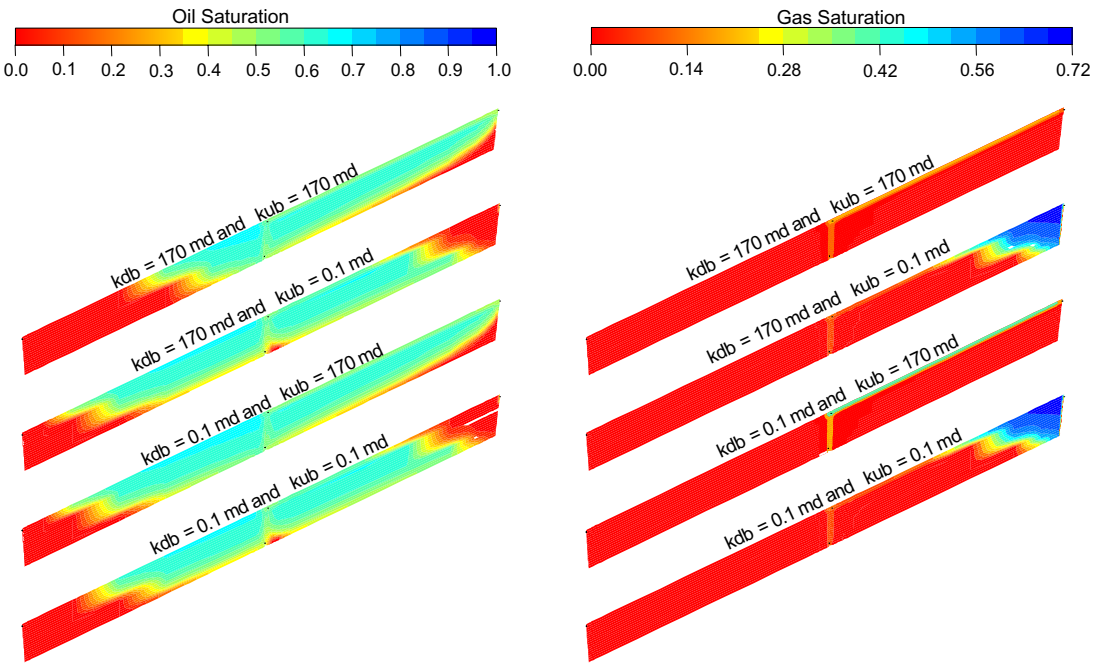

Figure 80. Oil and gas saturations at 5,300 years under hydrostatic pressure when the permeability of central charging fault is 50 md and the permeabilities of back doors are variable in the three-fault model. kdb and kub are the permeabilities of the downdip back door and the updip back door, respectively (Eclipse® figures).

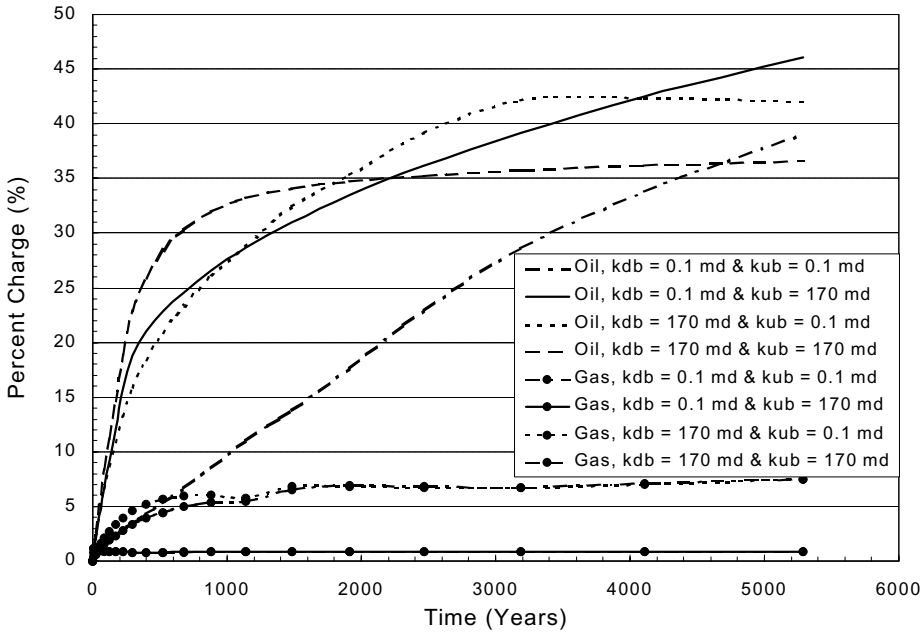

Figure 81. Oil and gas percent charges under hydrostatic pressure when the permeability of central charging fault is 50 md and the permeabilities of back doors are variable in the three-fault model. kdb and kub are the permeabilities of the downdip back door and the updip back door, respectively (Data from Eclipse®).

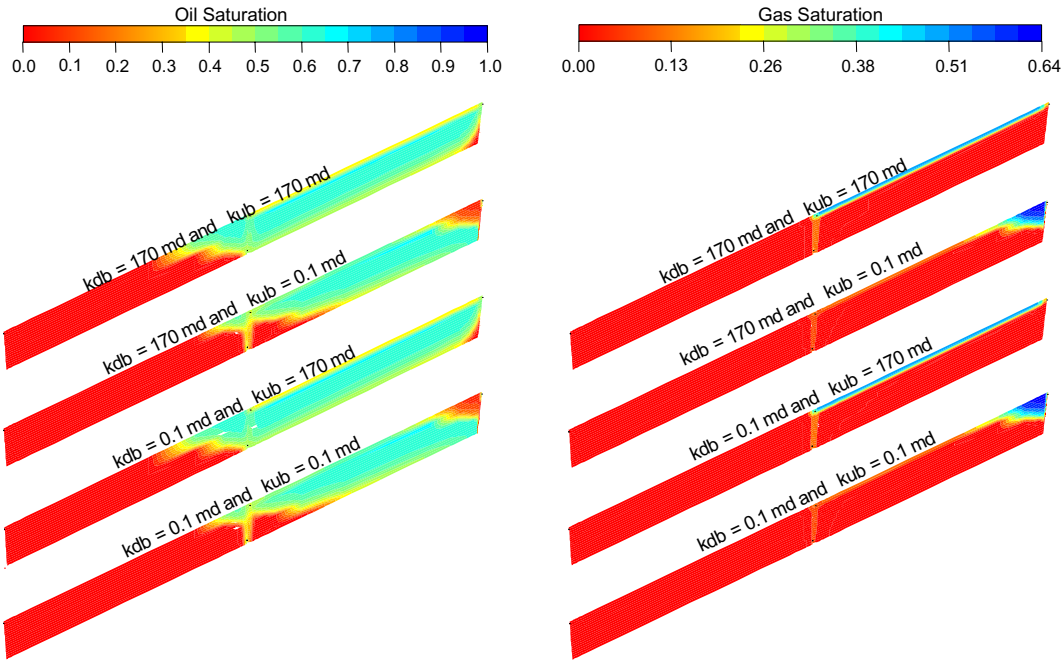

Figure 82. Oil and gas saturations at 5,300 years under geopressure when the permeability of central charging fault is 50 md and the permeabilities of back doors are variable. kdb and kub are the permeabilities of the downdip back door and the updip back door, respectively (Eclipse® figures).

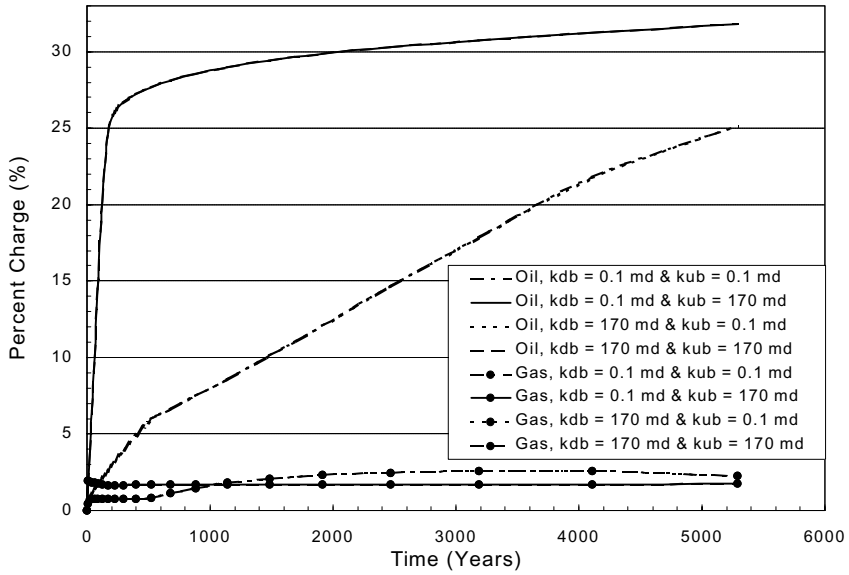

Figure 83. Oil and gas percent charges under geopressure when the permeability of central charging fault is 50 md and the permeabilities of back doors are variable. kdb and kub are the permeabilities of the downdip back door and the updip back door, respectively, in the three-fault model (Data from Eclipse®).

Under hydrostatic pressure, simulations show that an updip reservoir is favored by gas, and an updip back door with a high displacement pressure is necessary to retain gas in the reservoir. No gas will charge the downdip reservoir (Figures 80 and 81). Different from gas charging patterns under hydrostatic pressure, oil charges both the updip reservoir and the downdip reservoir, depending on the properties of the charging fault, the downdip back door and the updip back door (Figures 80 and 81). Gas affects oil charging an updip reservoir. More gas accumulation causes less oil to charge the updip reservoir. However, gas has little effect on a downdip oil charge. Very little gas charges the downdip reservoir, and a very limited amount of oil can charge downdip sands, since the negative buoyancy gradient impedes the downdip oil charge and water cannot easily escape from the downdip reservoir through the downdip back door.

Under geopressure, the same results are obtained as under hydrostatic pressure (Figures 82 and 83). Less oil can charge into the downdip sand because of the geopressure gradient. The properties of the central charging fault and the updip back door determine any oil charge patterns.

Growth fault model

Because a gas charge is usually fast and the results obtained in previous work can be applied to this growth fault model, simulation time was kept to only 170 years. When the permeability of the antithetic and the synthetic faults are both 50 md , the resulting oil saturation under hydrostatic pressure is as shown in Figure 84, and the gas saturation is as shown in Figure 85. Both the downdip and the updip back doors facilitate oil charges in the middle-layer reservoirs (sands X, Y and Z). Oil simultaneously charges the middle sands (sands B, Y and V) through the antithetic and the synthetic faults. Gas easily escapes from reservoirs since gas is less dense and viscous than oil in sands C and W with an updip back door. More gas accumulates in sand C than in sand W because gas simultaneously charges the sand through the synthetic and the updip faults, and gas cannot escape from the sand through the updip back door. The updip sands (C, Z and W) are favored rather than the downdip sands (A, X and U) by both oil and gas. The same results are obtained under geopressure (Figures 86 and 87).

If the antithetic fault has a high displacement pressure but the synthetic fault has a low displacement pressure, oil charges into the middle sands, Y and U, because of the geological structures as shown in Figure 88. In theory, oil should charge sand B, but since the charge is not long enough, only a very small amount of oil charges the sand. Since the throw along the antithetic fault is small, as is the dip angle of the

reservoirs, oil can charge sands A, X and U. The downdip back door results in more oil charging sand X than sand U. A short charge time causes very little oil to charge sand A. Sand W is bypassed by the oil entirely because that sand doesn't have an updip back door and the oil transportation ability of the synthetic fault is very low. The updip back door connected to sand Z results in more gas charging sand Y than sand V (Figure 89). Gas accumulates in sand Y because the synthetic fault has a high displacement pressure. No gas charges sand W. By comparing the gas saturation in updip sands C, Z and W (Figure 89), several gas migration pathways can simultaneously exist: first, the synthetic fault could be a migration pathway alone; second, the synthetic fault, sand Z and the updip fault could comprise a migration pathway; third, the antithetic fault, sand Y and the synthetic fault might combine to be a gas migration pathway; and a final possible gas migration pathway could include the antithetical fault, sand Y, the synthetic and the updip faults. The same results as those from hydrocarbon migration and entrapment can be obtained under geopressure (Figures 90 and 91).

Finally, if the antithetic fault has a low displacement pressure, but the synthetic fault has a high displacement pressure, in theory the updip sands C, Z and W must be favored and hydrocarbons could charge the middle sands because of geological structures. This was demonstrated by simulations, even though the degree of favor was very different among these sands because of the properties of both the charging faults and the back doors (Figures 92, 93, 94 and 95). Sand X cannot be charged by oil in a two-system system under both hydrostatic pressure and geopressure (Figures 63 and 67), but oil can charge the sand under both hydrostatic pressure and geopressure in three-phase systems. As comparing to oil saturation in sands X and U (Figures 92 and 94), a downdip back door results in an oil charge in sand X. Very little oil can charge sand X through an antithetic fault. Most oil originally comes from sand Y across the antithetic fault. Meanwhile, gas can occupy the lower top part of sand Y during an active charge under hydrostatic pressure and geopressure. The reason why gas can occupy the lower top part of sand Y is that oil charging into the sand through the synthetic fault drives gas downdip along the top of the sand.

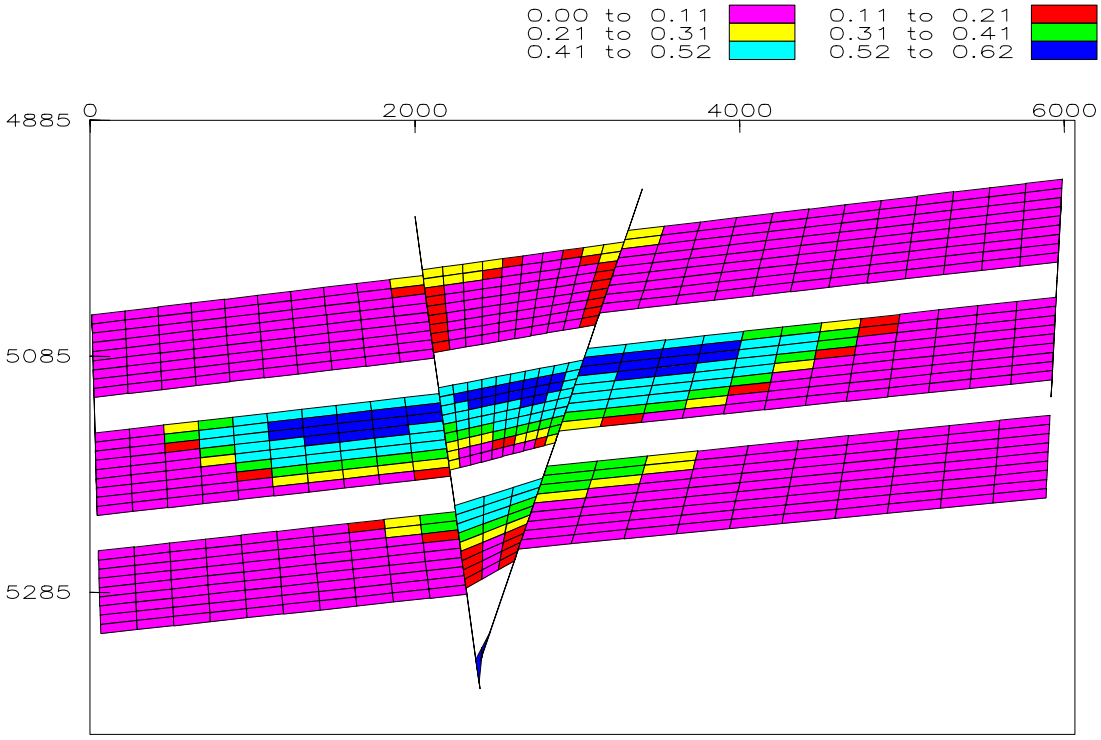

Figure 84. Oil saturation at 170 years under hydrostatic pressure in oil-gas-water systems when the permeabilities of the antithetical and synthetic faults are 50 md each (Eclipse® figures).

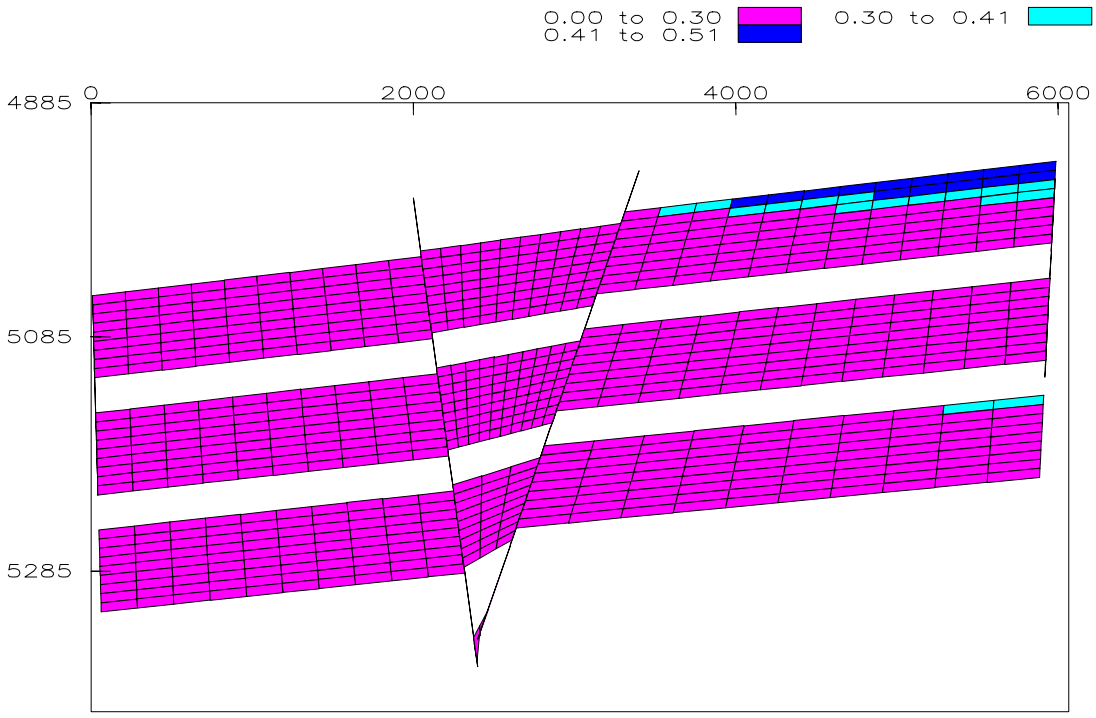

Figure 85. Gas saturation at 170 years under hydrostatic pressure in oil-gas-water systems when the permeabilities of the antithetical and the synthetic faults are 50 md each (Eclipse® figures).

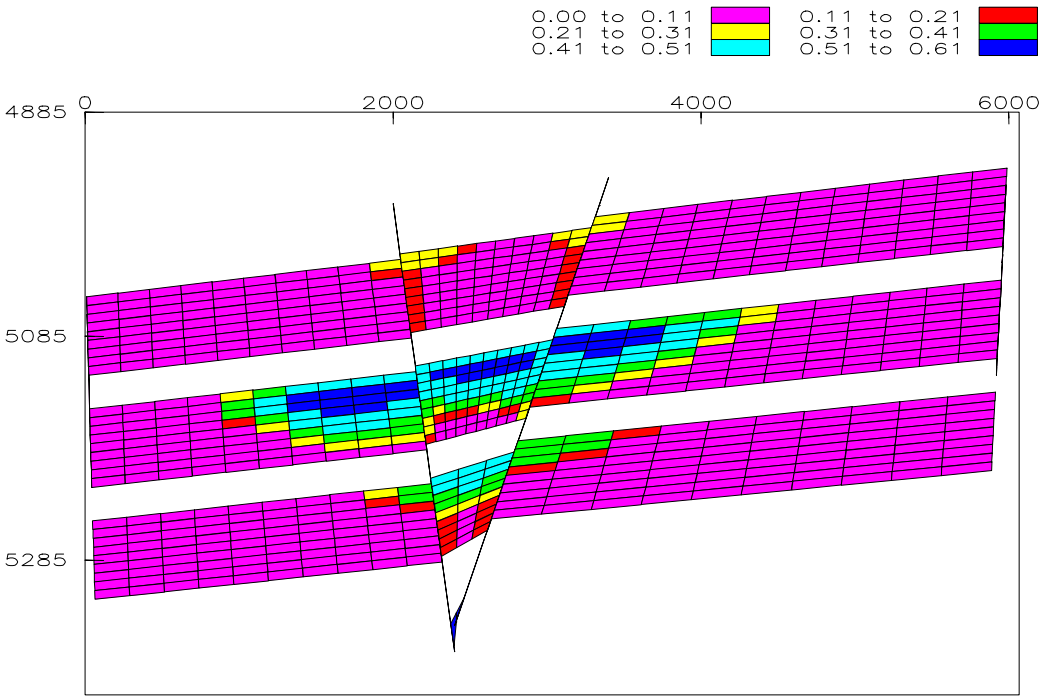

Figure 86. Oil saturation at 120 years under geopressure in oil-gas-water systems when the permeabilities of the antithetical and the synthetic faults are 50 md each (Eclipse® figures).

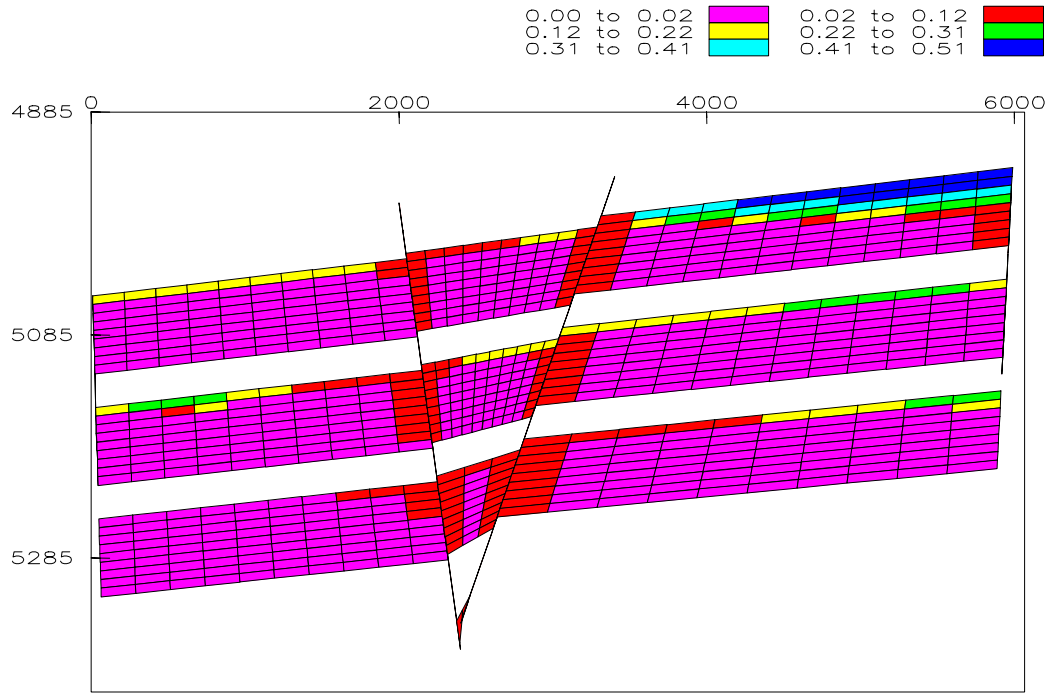

Figure 87. Gas saturation at 120 years under geopressure in oil-gas-water systems when the permeabilities of antithetical and the synthetic faults are 50 md each (Eclipse® figures).

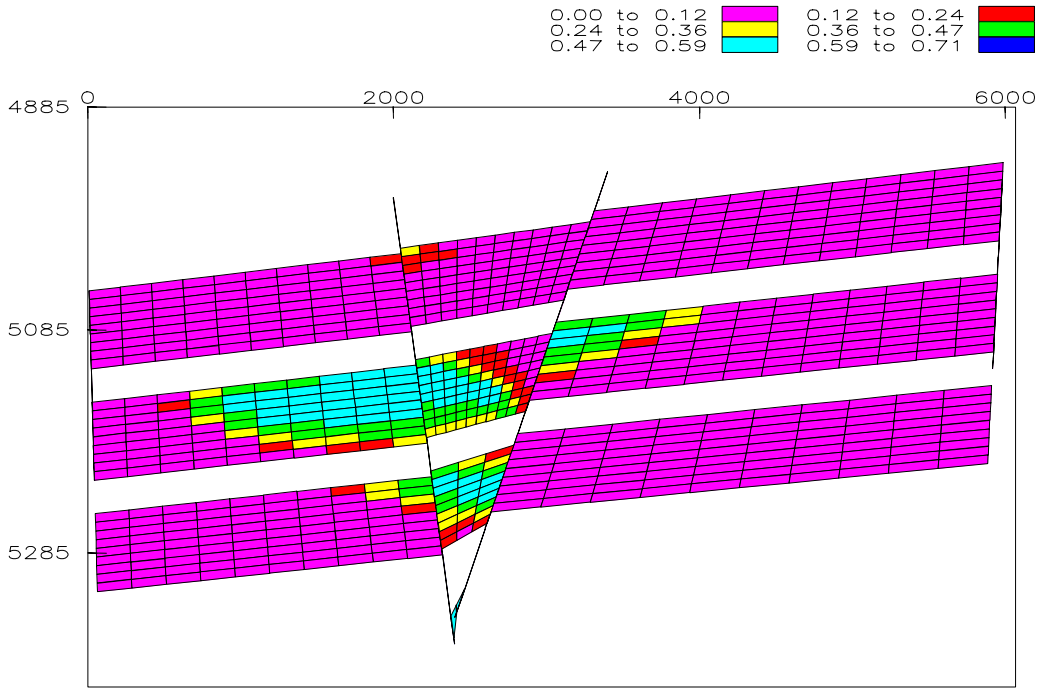

Figure 88. Oil saturation at 170 years under hydrostatic pressure in oil-gas-water systems when the permeability of antithetical is 50 md and the permeability of the synthetic fault is 0.1 md (Eclipse® figures).

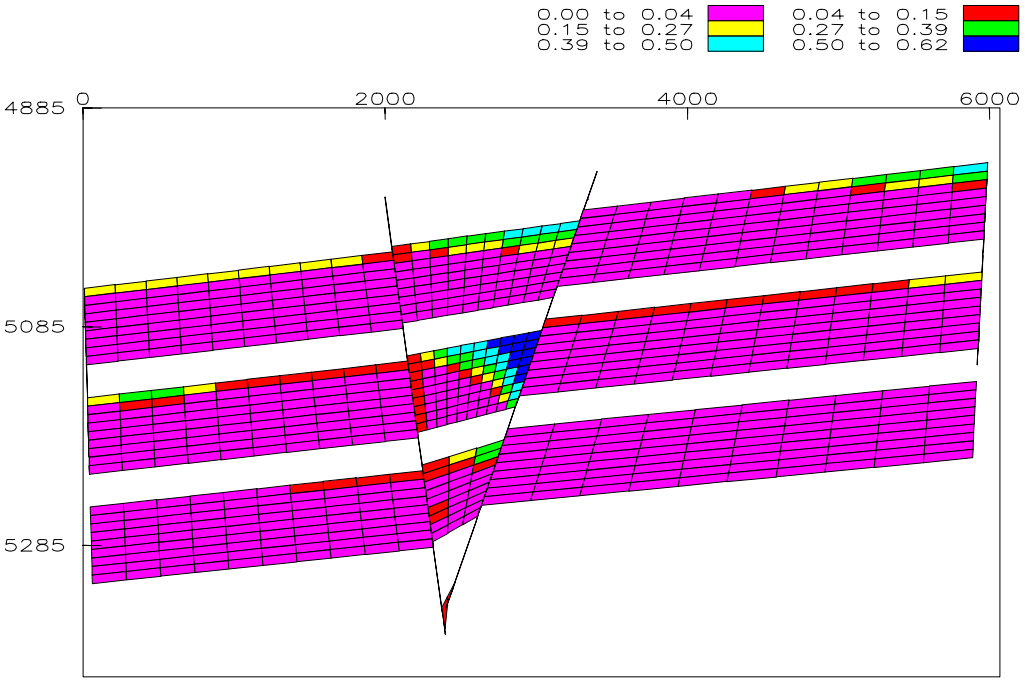

Figure 89. Gas saturation at 170 years under hydrostatic pressure in oil-gas-water systems when the permeability of antithetical fault is 50 md and the permeability of the synthetic fault is 0.1 md (Eclipse® figures).

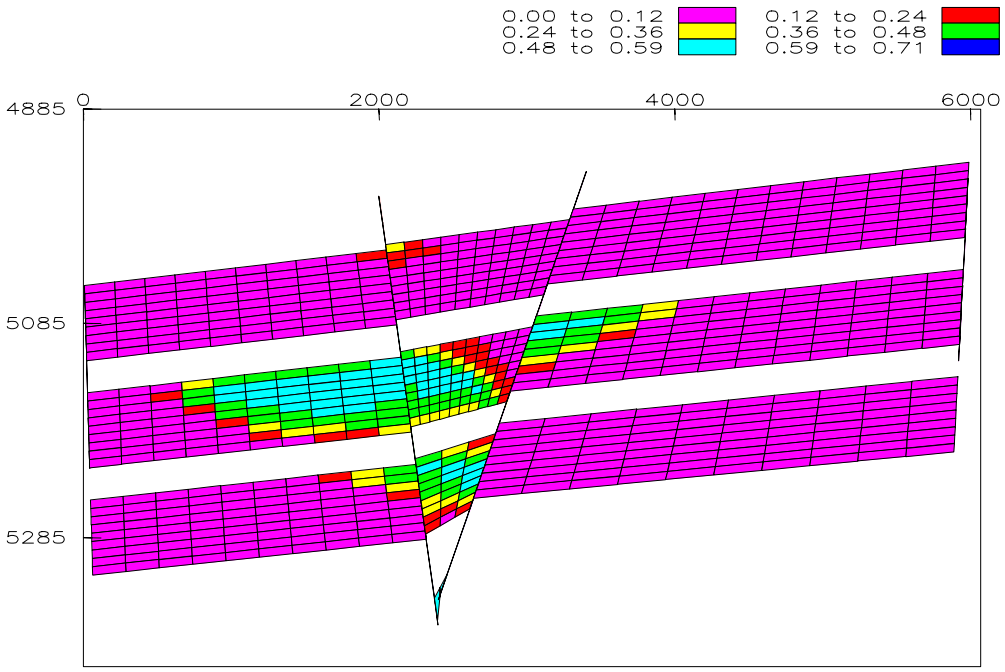

Figure 90. Oil saturation at 170 years under geopressure in oil-gas-water systems when the permeability of antithetical fault is 50 md and the permeability of the synthetic fault is 0.1 md (Eclipse® figures).

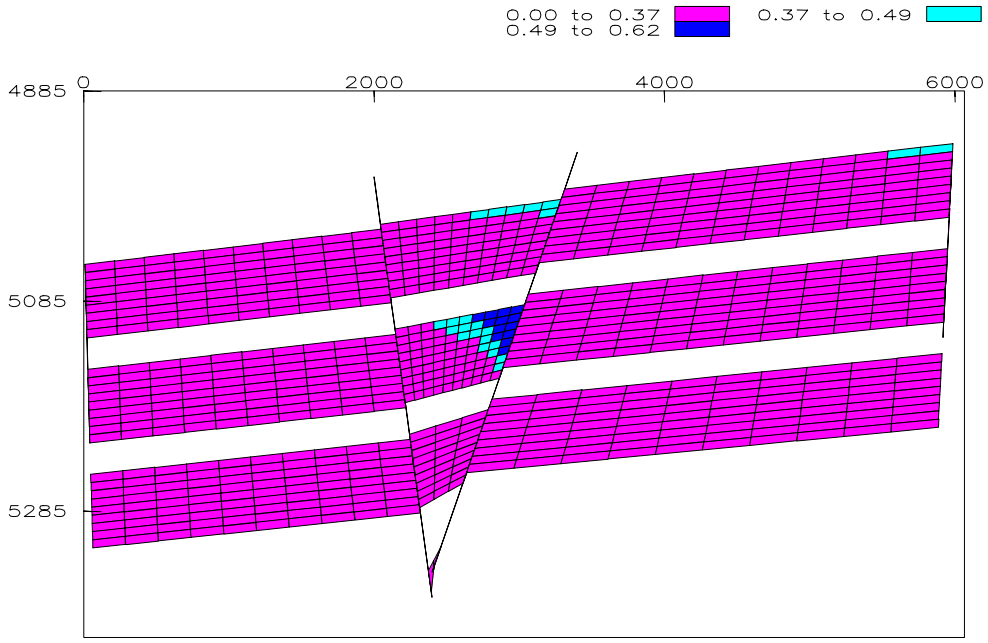

Figure 91. Gas saturation at 170 years under geopressure in oil-gas-water systems when the permeability of antithetical fault is 50 md and the permeability of the synthetic fault is 0.1 md (Eclipse® figures).

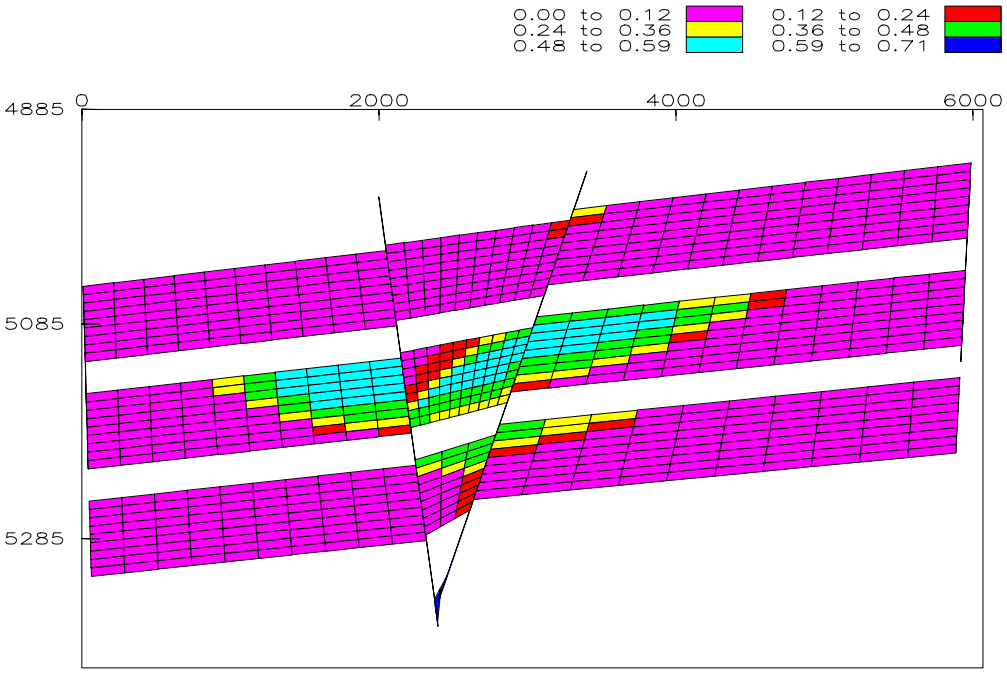

Figure 92. Oil saturation at 170 years under hydrostatic pressure in oil-gas-water systems when the permeability of antithetical fault is 0.1 md and the permeability of the synthetic fault is 50 md (Eclipse® figures).

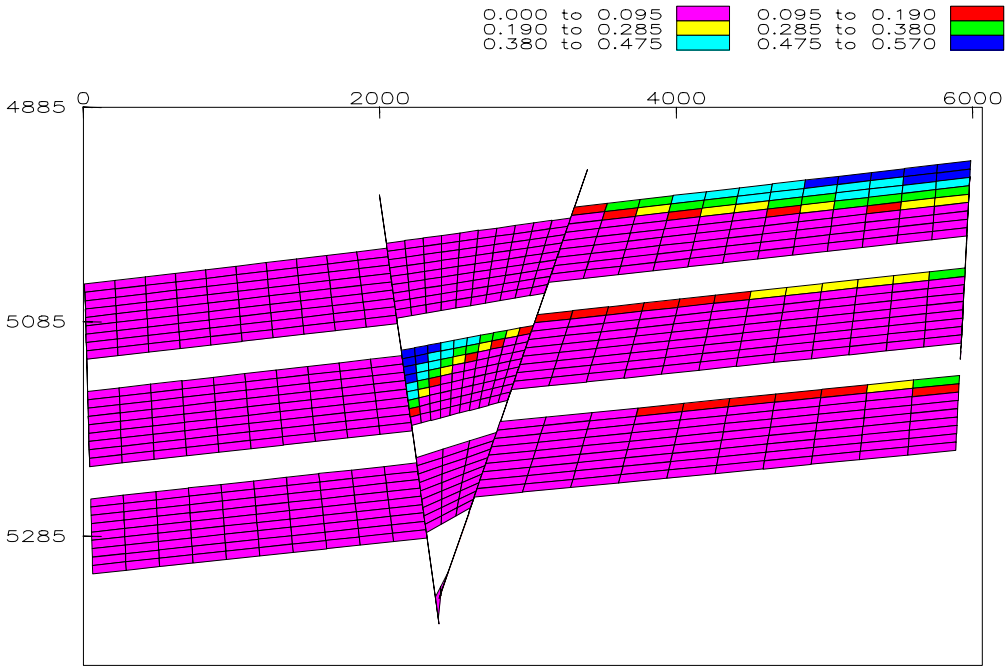

Figure 93. Gas saturation at 170 years under hydrostatic pressure in oil-gas-water systems when the permeability of antithetical fault is 0.1 md and the permeability of the synthetic fault is 50 md (Eclipse® figures).

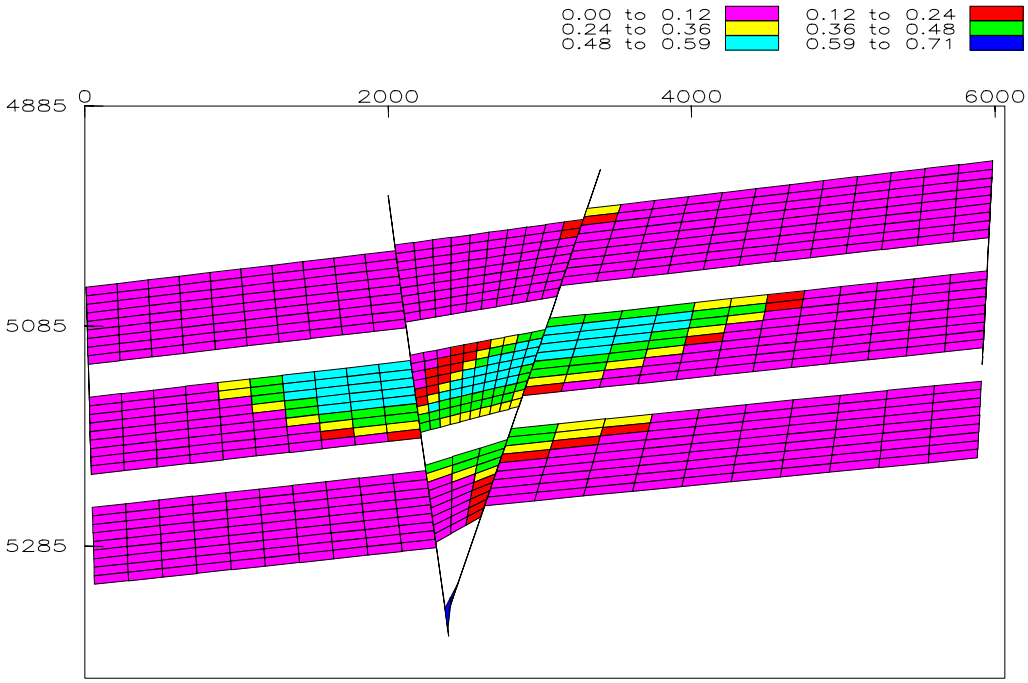

Figure 94. Oil saturation at 170 years under geopressure in oil-gas-water systems when the permeability of antithetical fault is 0.1 md and the permeability of the synthetic fault is 50 md (Eclipse® figures).

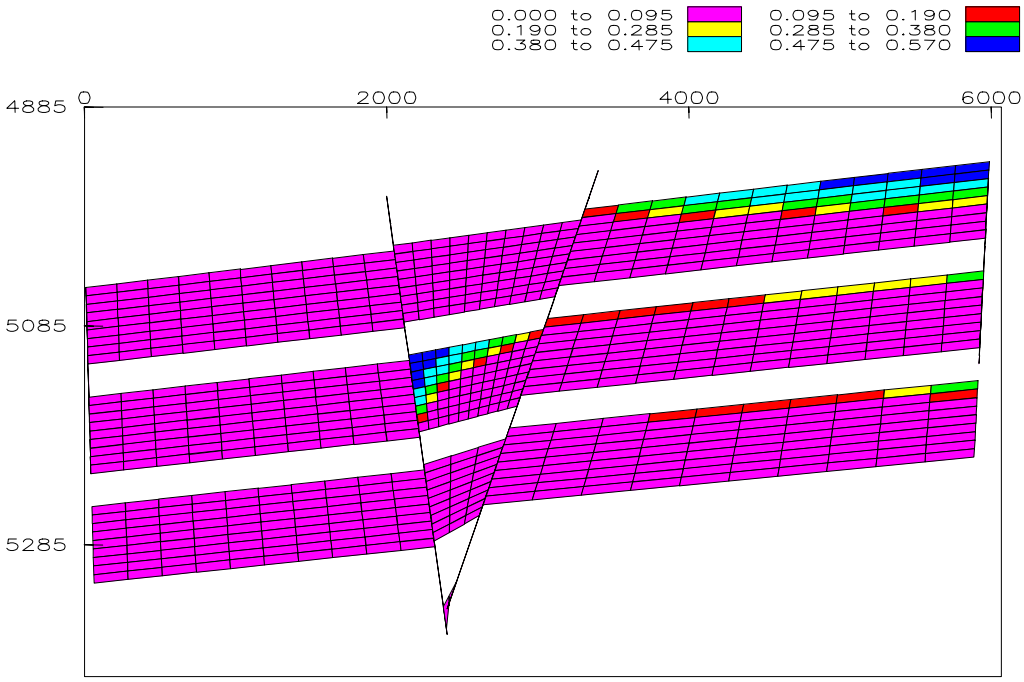

Figure 95. Gas saturation at 170 years under geopressure in oil-gas-water systems when the permeability of antithetical fault is 0.1 md and the permeability of the synthetic fault is 50 md (Eclipse® figures).

DISCUSSION

The oil and gas saturation shown in Figure 73 implies that only gas can be found in lower stacked fault-bounded reservoirs if the sands can trap gas (as in the UDBD models) without any updip back door, or the displacement pressure of the updip back door is very high, assumed the separation of oil and gas. This is consistent with the structural differential entrapment model (Gussow, 1954). However, hydrocarbon migration and entrapment are generally complex in stacked fault-bounded reservoirs, even though this study has ignored phase behavior among any two phases in the three-phase systems. The hydrocarbon charge patterns described in the structural differential entrapment model (Gussow, 1954) and the stratigraphic differential entrapment model (Petroleum Research Inc., 1960) are not sufficient to predict and describe hydrocarbon migration and entrapment.

The oil saturation shown in Figures 75 and 76 indicates that the time required for a commercial updip oil charge is greatly reduced in the three-phase systems because of the existence of gas, which greatly reduces the viscosity of the fluid. If oil can charge an updip reservoir, oil percent charges of 20 percent can be reached within several thousand years. Gas percent charges of 20 percent can charge can be reached within several thousand years in a closed updip sand, even under hydrostatic pressure (Figures 75 and 76).

Dipmeter data from the Ship Shoal 274/293 field has indicated that normal faults commonly have a shear zone at their base which acts as a seal. An attempt to simulate hydrocarbon migration along such a fault is made by using the UDBD models, the DDBD models and the three-fault model. This type of simulation is fundamental to understanding hydrocarbon migration along growth faults. The properties of the growth faults and the back doors determine the patterns of hydrocarbon migration and entrapment. One high permeability fault between two growth faults, plus updip reservoirs, resulted in the patterns of hydrocarbon distribution similar to those observed in the Ship Shoal 274/293 field.

Simulations indicate that oil can be found updip from gas during active charges. Oil might also further drive gas into downdip reservoirs. Since it is a dynamic process, it has not been observed in fields.

SUMMARY

As compared to the charge time necessary for oil to charge into reservoirs in two-phase systems, the charge time required for hydrocarbon charges in reservoirs is greatly reduced in the three-phase systems because of the presence of gas.

Simulations indicate that oil can charge both the downdip and updip reservoirs, but the updip reservoirs are usually favored. Only a limited amount of oil can charge a downdip reservoir. Different from the oil charge patterns, gas can only charge the updip sands.

Back doors can greatly affect hydrocarbon migration and entrapment. On the one hand, updip back doors act as routes for water escaping from reservoirs, in order to make room for a hydrocarbon charge. Updip back doors improve the efficiency of an oil charge. On the other hand, updip back doors also provide routes for hydrocarbon escape from the reservoirs, especially for gas. To commercially entrap gas, sealing faults are required. Generally, downdip back doors have little effect on hydrocarbon migration and entrapment, especially under geopressure. Without any updip back door, the segregation of oil and gas occurs during a hydrocarbon charge, which favors the retention of oil over gas. Otherwise, gas will usually be found over oil. The downdip back door can only cause a very limited downdip oil charge, even under hydrostatic pressure.

Simulations using growth fault models indicate that the chance for a hydrocarbon charge in reservoirs through growth faults is not consistent. Back doors can change the pattern of a hydrocarbon charge. Generally, both lower and updip sands are favored by hydrocarbons. Reservoir sands along high permeability charging faults are usually favored. Reservoirs along low permeability charging faults may also be bypassed. Provided that the dipping angles of reservoirs are very small, both updip and downdip back doors could facilitate oil penetration a barrier in order to charge reservoirs, no matter whether the reservoirs are updip or downdip.

CHAPTER VII

CONCLUSIONS

Faults are primary factors that controlling hydrocarbon migration and distribution in fault-compartmentalized reservoirs vertically separated by impermeable shale. On the one hand, hydrocarbons migrate along faults and charge stacked fault-bounded reservoirs. On the other hand, fluid (water, oil and/or gas) escapes from reservoirs through faults, including charging faults. The sealing capacity of a fault is determined by the difference between the displacement pressures of the faults and the displacement pressures of the adjacent reservoirs.

After having fixed the width of faults and the properties of reservoirs, it was found that hydrocarbon charges in stacked fault-bounded reservoirs are mainly affected by five factors: charge time, charging faults, back doors, pressure and geological structures. The charge time should be at least 10,000 years for commercial oil accumulation in those traps in which oil can charge in oil-water systems when the displacement pressure of the charging fault is 0.68 psi. The charge time required for commercial hydrocarbon accumulation in oil-gas-water systems can be reduced to only several thousand years since gas is less dense and viscous than oil or water.

The oil transportation ability of a charging fault was therefore defined in order to investigate how the properties of charging faults affect oil migration and entrapment in oil-water systems. The oil transportation ability of a charging fault was assessed through the oil charge efficiency by which oil can charge a single reservoir through the charging fault, and at the same that fluid (oil and/or water) is allowed to escape only through that same charging fault. The updip oil transportation ability of a charging fault was determined by the properties of the fault. The lower the displacement pressure of the fault, the higher its updip oil transportation ability. On the contrary, the downdip oil transportation ability of a fault is generally low and cannot result in any commercial downdip oil accumulation.

Back doors – faults other than charging faults in stacked, fault-bounded reservoirs – could facilitate water escape from reservoirs in order to improve hydrocarbon charge efficiency. Otherwise, water escaping from charging faults could cause a slower charge or even no charge at all. Generally, oil is sensitive to back doors, but gas isn't. Back doors can be divided into updip back doors and downdip back doors, according to

the geological relationship between the charging faults and the back doors. They have different effects on hydrocarbon migration and entrapment.

An updip back door generally improves an updip oil charge. This study investigates the role of an updip back door whose displacement pressure is 0.24, 0.68, 3.63, 7.38, 14.13, 28.76, or 55.03 psi. It was found that the lower the displacement pressure of the updip back door, the more efficient the updip oil charge before 3,000 years under hydrostatic pressure. However, trapping requires a high displacement pressure, or else oil will escape through the updip back door, thus resulting in a low oil column height. Simulations indicate that the updip back door whose displacement pressure is equal to or higher than 28.76 psi, actually acts as a sealing fault to oil migration under hydrostatic pressure in oil-water systems.

The effects of an updip back door on gas migration and entrapment are essential, since gas is less dense and viscous than oil. Commercially trapping gas in a fault-bounded reservoir requires a sealing updip bounding fault. Otherwise gas could easily escape from the reservoir through an updip back door, even though the displacement pressure of that updip back door is probably very high. Simulations show that commercial gas cannot be trapped by an updip back door whose displacement pressure is as high as 55.03 psi and whose permeability is only 0.1 md.

A downdip back door generally has little effect on a downdip hydrocarbon charge. Since little water can flow out of a downdip reservoir through a downdip back door, a very limited amount of oil can charge into the downdip reservoir. The downdip reservoir is usually bypassed by gas even though the downdip back door exists.

Since geopressure always acts with a buoyant force, geopressure enhances the updip oil transportation of a charging fault and the positive effects of an updip back door on an updip oil charge. Geopressure and updip back doors both result in a more efficient updip oil charge. A physical barrier is not necessarily a barrier to updip oil migration with the aid of geopressure and an updip back door. Geopressure impedes a downdip hydrocarbon charge. The percent charge of a downdip oil charge under geopressure is determined by the geopressure and the oil transportation of the updip charging fault.

Back doors also affect hydrocarbon migration pathways under both hydrostatic pressure and geopressure. Although many of the concluded results of the effects regarding back doors on oil or gas percent charges are applicable when predicting and explaining hydrocarbon migration pathways, things are not always so

simple. Stacked fault-bounded reservoirs can be bypassed by hydrocarbons, depending on the properties of both the charging faults and the back doors. This study investigates the effects of back doors on hydrocarbon migration pathways on two stacked reservoirs bounded by faults. Simulations have shown that oil charges both reservoirs under hydrostatic pressure when the difference in the properties of the downdip charging faults and the updip back doors is small. However, either the upper or the lower reservoirs could be bypassed when the difference is large. Moreover, hydrocarbon migration pathways under hydrostatic pressure are different from those under geopressure, even in the same geological structures. For example, when the displacement pressure of a charging fault is 3.63 psi, the upper reservoir is usually bypassed under hydrostatic pressure when the displacement pressure of the updip back door is equal to or less than 1.40 psi. The migration pathways could be different under geopressure.

Hydrocarbon migration and entrapment in complex geological structures are also very complex. Any one of the above controlling factors could change the patterns of hydrocarbon charge and distribution. The chances for hydrocarbons to charge reservoirs along growth faults are not equal. Generally, lower reservoirs and updip reservoirs are favored. Reservoirs along high-permeability charging faults are also favored. Reservoirs along charging faults with high displacement pressures are often bypassed. Oil can charge both downdip and updip reservoirs, but updip reservoirs are usually favored. Only a limited amount of oil usually charges downdip reservoirs. Different from the oil charge patterns, gas only charges updip reservoirs. Geopressure and updip back doors facilitate oil charges in updip fault-bounded reservoirs. Provided that the dipping angles of reservoirs are small, both updip and downdip back doors could facilitate oil penetration of a barrier in order to charge the reservoirs, no matter whether the reservoirs are updip or downdip.

Interreservoir migration among stacked fault-bounded reservoirs is an important mechanism for hydrocarbon accumulation and trap identification. Simulations suggest that gas is not sensitive to bounding faults in stacked faulted bounded reservoirs and sealing faults are required for commercial gas accumulation. Therefore, only oil interreservoir migration is studied here under hydrostatic pressure. Interreservoir migration without an oil supply is affected by the following factors: migration time and the properties of the bounding faults. In general, interreservoir migration driven only by a buoyancy force is a very slow process, even though the displacement pressures of the bounding faults might be very low.

Overall, hydrocarbon migration and entrapment in stacked fault-bounded reservoirs are complex, but also dynamic. Therefore, the numerical simulations were applied in this study. However, since the data regarding the properties of faults and fluids were sparse, necessary assumptions were made and simulation results have to be compared to observations in fields and be improved in the future.

REFERENCES CITED

Ahmed, U., Crary, S. F., and Coates, G. R., 1989, Permeability estimation: the various sources and their interrelationship: SPE paper 19604 presented at the 1989 SPE Annual Technical Conference and Exhibition, San Antonio, TX, 8-11 Oct., p. 649-662.

Alexander, L. L., and Handschy, J., 1998, Fluid flow in a faulted reservoir system: fault trap analysis for the Block 330 Field in Eugene Island, South Addition, offshore Louisiana: AAPG Bulletin, v. 82, p. 387-411.

Allan, U. S., 1989, Model for hydrocarbon migration and entrapment within faulted structures: AAPG Bulletin, v. 73, p. 803-811.

Allen, P. A. and Allen, J. R., 1990, Basin analysis: principles and applications: Boston, Blackwell Science Publications, 451p.

Antonellini, M., and Aydin, A., 1994, Effect of faulting on fluid flow in porous sandstones,: petrophyscial properties: AAPG Bulletin, v. 78, p. 355-377.

Berg, R. R., 1975, Capillary pressures in stratigraphic traps: AAPG Bulletin, v. 59, p. 939-956.

Berg, R. R. and Avery, A. H., 1995, Sealing properties of tertiary faults, Texas Gulf Coast: AAPG Bulletin, v. 79, p. 375-393.

Berg, R. R., 1996, Personal communication: Department of Geology and Geophysics, Texas A&M University.

Berg, R. R. and Gangi, A. F., 1999, Primary migration by oil-generation source rocks: application to the Austin Chalk, Texas: AAPG Bulletin, v. 83, p. 727-756.

Bishop, R. S., Gehman, H. M., Jr. and Young, A., 1983, Concepts for estimating hydrocarbon accumulation and dispersion: AAPG Bulletin, v. 67, p. 337-348.

Bouvier, J. D., Kaars-Sijpesteijn, C. H., Kluesner, D. F., Onyejekwe, C. C., and Vanderpal, R. C., 1989, Three-dimensional seismic interpretation and fault sealing investigation, Nun River field, Nigeria, AAPG Bulletin, v. 73, p. 1397-1414.

Davies, J. B. and Archambeau, C. B., 1997, Analysis of high-pressure fluid flow in fractures with application to Yucca Mountain, Nevada, slug test data: Tectonophysics, v. 277, p. 83-98.

Downey, M. W., 1984, Evaluating seals for hydrocarbon accumulations: AAPG Bulletin, v. 68, p. 1752-1763.

Eclipse® manual, 1998, GeoQuest Company, Houston, Texas.

England, W. A., Mackenzie, A. S., Mann, D. M. and Quigley, T. M., 1987, The movement and entrapment of petroleum fluids in the subsurface: J. Geol. Soc., London, v. 144, p. 327-347.

Ewing, T. E. and Fergeson, W. G., 1989, The downdip Yegua trend – an overview: Gulf Coast Association of Geological Societies Transactions, v. 39, p. 76-83.

Gibson, R. G., 1994, Fault-zone seals in siliciclastic strata of the Columbus Basin, offshore Trinidad: AAPG Bulletin, v. 78, p. 1372-1385.

Gussow, W. C., 1954, Differential entrapment of oil and gas: a fundamental principle: AAPG Bulletin, v. 5, p. 816-853.

Hart, B. S., Sibley, D. M. and Flemings P. B., 1997, Seismic stratigraphy, facies architecture, and reservoir character of a Pleistocene shelf-margin lowstand delta complex, Eugene Island Block 330 field, offshore Louisiana: AAPG Bulletin, v. 81, p. 380-397.

Hawkins, J. M., Luffel, M. L., and Harris, T. G., 1993, January, Capillary pressure model predicts distance to gas/water, oil/water contact: Oil and Gas Journal, p. 39-43.

Hintz, J. C., 2001, Trapping capacity of fault zones, downdip Yegua formation, Texas Gulf Coast basin: Master Thesis, Texas A&M University.

Holland, D.S., Nunan, W.E., Lammlein, D.R., and Woodhams, R.L., 1990, Eugene Island Block 330 field, offshore Louisiana, in E. A. Beaumont and N. H. Foster, eds., Structural traps III, tectonic fold and fault traps: Tulsa, Oklahoma, AAPG Treatise on Petroleum Geology, Atlas of Oil and Gas Fields, p. 103-143.

Hubbert, M.K., 1953, Entrapment of petroleum under hydrodynamic conditions: AAPG Bulletin, v. 37, p. 1954-2026.

Jev, B. I., Sijpesteijn, C. H., Peters, M. P. A. M., Watts, N. L., and Wilkie, J. T., 1993, Akaso field, Nigeria: use of integrated 3_D seismic, faulting slicing, clay smearing, and RFT pressure data on fault trapping and dynamic leakage: AAPG Bulletin, v. 77, p. 1389-1404.

Kim, J., 1999, Mineralogical and fabric changes during burial diagenesis of shale and their effects on petrophysical properties: Ph.D. Dissertation, Texas A&M University.

Kulander, C. S., 1998, Geological evolution and structural controls on hydrocarbon flow in the Ship Shoal Block 274/293 field, offshore Louisiana, Gulf of Mexico: Ph.D. Dissertation, Texas A&M University.

Kuo, L., 1997, Gas exsolution during fluid migration and its relation to overpressure and petroleum accumulation: Marine and Petroleum Geology, v. 14, p. 221-229.

MacPherson, L. A. and Berry, L. N., September-October, 1972, Prediction of fracture gradients from log derived elastic moduli: The Log Analyst, p. 12-19.

Mattax, C. C. and Dalton, R. L., 1990, Reservoir simulation: Monograph Volume 13, SPE Henry L. Doherty series, Richard, Texas, the Society of Petroleum Engineers Inc..

Matthai, S. K. and Roberts, S. G., The influence of fault permeability on single-phase fluid flow near fault-sand intersections: results from steady-state high-resolution models of pressure-driven fluid flow: AAPG Bulletin, v. 80, p. 1763-1779.

Nunn, J. A., 1996, Buoyancy-driven propagation of isolated fluid-filled fractures: implications for fluid transport in Gulf of Mexico geopressured sediments: J. Geophys. Res., v. 101, p. 2963-2970.

Roberts, S. J., Nunn, J. A., Cathles, L. and Cipriani, 1996, Explusion of abnormally pressure fluids along faults: J. Geophys. Res., v. 101, p. 28231-28252.

Schlomer, S. and Krooss, B. M., 1997, Experimental characterisation of the hydrocarbon sealing efficiency of cap rock: Marine and Petroleum Geology, v. 14, p. 565-580.

Schowalter, T. T., 1979, Mechanics of secondary hydrocarbon migration and entrapment: AAPG Bulletin, v. 63, p. 723-760.

Schumacher, D., 1993, Eugene Island Block 330 field, offshore Louisiana: geochemical evidence for active hydrocarbon recharging (abs.): 1993 AAPG Annual Convention Program, p. 179-179.

Skerlec, G.M., 1999, Evaluating top and fault seal: Treatise of Petroleum Geology/Handbook of Petroleum Geology: Exploring for Oil and Gas Traps, p. 10.3-10.94, Tulas, Oklahoma, American Association of Petroleum Geologists.

Smith, D. A., 1966, Theoretical considerations of sealing and non-sealing faults, AAPG Bulletin, v. 50, p. 363-374.

Smith, D. A., 1980, Sealing and nonsealing faults in Louisiana Gulf Coast salt basin: AAPG Bulletin, v. 64, p. 145-172.

Standing, M. B., 1975, Notes on relative permeability relationships. (Personal collection, J. Bai)

Thomeer, J. H., 1960, March, Introduction of a pore geometrical factor defined by the capillary pressure curve: Journal of Petroleum Technology, p. 73-77.

Thomeer, J. H., 1983, April, Air permeability as a function of three pore-network parameter: Journal of Petroleum Technology, p. 809-814.

Wagner, B. E., 1998, Pressure trends in lower Viosca Knoll and Mississippi Canyon, Gulf of Mexico deep water: implications for seal, column heights and hydrocarbon migration: Houston Geological Society Bulletin, v. 40, p. 8-11.

Wang, C. and Xie, X., 1998, Hydrofracturing and episodic fluid in shale-rich basins – a numerical study: AAPG Bulletin, v. 82, p. 1857-1869.

Watts, N. L., 1987, Theoretical aspects of cap-rock and fault seals for single- and two-phase hydrocarbon columns: Marine and Petroleum Geology, v. 4, p. 274-307.

Whelan, J.K., Kennicutt, M.C., Brooks, J.M., Schumacher, D. and Eglinton, L.B., 1994, Organic geochemical indicators of dynamical fluid flow processes in petroleum basins: Organic Geochemistry, v. 22, p. 587-615.

Wilhelm, O., 1945, Classification of petroleum reservoirs: AAPG Bulletin, v. 29, p. 1537-1580.

William, W. R. and Hubbert, M. K., 1959, Role of fluid pressure in mechanics of overthrust faulting: Geol. Soc. America Bulletin, v. 70, p. 115-206.

Yielding, G., Freeman, B., and Needham, D.T., 1997, Quantitative fault seal prediction: AAPG Bulletin, v. 81, p. 897-917.

APPENDIX A

In Eclipse® software water formation volume factor (B_w) at pressure P is calculated as

$$B_w(P) = \frac{B_w(P_{ref})}{1 + X + \frac{X^2}{2}} \tag{A-1}$$

where $B_w(P_{ref})$ is the water formation volume factor at reference pressure P_{ref}. X is related with pressure P and compressibility C_w.

$$X = C_w(P - P_{ref}) \tag{A-2}$$

APPENDIX B

In Eclipse® software the compressibility of rock C_f is defined as

$$C_f = \left(\frac{dV}{dP}\right)\Big/_V \tag{B-1}$$

where V is the rock volume at pressure P. The rock compressibility C at reference pressure P_{ref} is assumed to be 4×10^{-3}/psi in the study. The volume V at pressure P is calculated by

$$V(P) = V(P_{ref})(1 + X + \frac{X^2}{2}) \tag{B-2}$$

where $X = C_f(P - P_{ref})$.

VITA

NAME:	Jianyong Bai
ADDRESS:	109 South Yan'an Road
	Changji, Xinjiang, China 831100
EDUCATION:	B.E. (Engineering Mechanics), Xi'an Jiantong University, July 1991
	M.S. (Engineering Mechanics), Tsinghua University, July 1997
	Ph.D. (Geophysics), Texas A&M University, May 2003
EXPERIENCE:	Intern – Shell Exploration & Production Technology Company, Houston, Texas, 5/02 – 11/02
	Research Assistant – Department of Geology & Geophysics, Texas A&M University, 6/98 – 12/01
AWARDS AND HONORS:	SEG/ Jim & Ruth Harrison Scholarship — 2002 – 2003
	SEG/Phillips Petroleum scholarship #1 — 2001-2002
	Phi Kappa Phi honor member — Texas A&M Univ. — 2001, 2002, 2003
	SEG/Carl Savit scholarship — 2000 – 2001
	Chevron scholarship — Texas A&M Univ. — 1999 – 2000